# **SANDIA REPORT**

SAND2018-0329 Unlimited Release January 2018

# **Uncertainty Analysis of Consequence Management (CM) Data Products**

Brian D. Hunt, Aubrey C. Eckert-Gallup, Lainy D. Cochran, Terry D. Kraus, Sean D. Fournier, Mark B. Allen, Richard R. Schetnan, Matthew D. Simpson, Colin E. Okada, Avery A. Bingham

Prepared by Sandia National Laboratories Albuquerque, New Mexico 87185 and Livermore, California 94550

Sandia National Laboratories is a multimission laboratory managed and operated by National Technology and Engineering Solutions of Sandia, LLC, a wholly owned subsidiary of Honeywell International, Inc., for the U.S. Department of Energy's National Nuclear Security Administration under contract DE-NA0003525.



Issued by Sandia National Laboratories, operated for the United States Department of Energy by National Technology and Engineering Solutions of Sandia, LLC.

**NOTICE:** This report was prepared as an account of work sponsored by an agency of the United States Government. Neither the United States Government, nor any agency thereof, nor any of their employees, nor any of their contractors, subcontractors, or their employees, make any warranty, express or implied, or assume any legal liability or responsibility for the accuracy, completeness, or usefulness of any information, apparatus, product, or process disclosed, or represent that its use would not infringe privately owned rights. Reference herein to any specific commercial product, process, or service by trade name, trademark, manufacturer, or otherwise, does not necessarily constitute or imply its endorsement, recommendation, or favoring by the United States Government, any agency thereof, or any of their contractors or subcontractors. The views and opinions expressed herein do not necessarily state or reflect those of the United States Government, any agency thereof, or any of their contractors.

Printed in the United States of America. This report has been reproduced directly from the best available copy.

Available to DOE and DOE contractors from

U.S. Department of Energy Office of Scientific and Technical Information P.O. Box 62 Oak Ridge, TN 37831

Telephone: (865) 576-8401 Facsimile: (865) 576-5728 E-Mail: reports@osti.gov

Online ordering: <a href="http://www.osti.gov/scitech">http://www.osti.gov/scitech</a>

Available to the public from

U.S. Department of Commerce National Technical Information Service 5301 Shawnee Rd Alexandria, VA 22312

Telephone: (800) 553-6847 Facsimile: (703) 605-6900 E-Mail: orders@ntis.gov

Online order: <a href="https://classic.ntis.gov/help/order-methods/">https://classic.ntis.gov/help/order-methods/</a>



SAND2018-0329 January 2018 Unlimited Release

# **Uncertainty Analysis of Consequence Management (CM) Data Products**

Brian D. Hunt<sup>1</sup>, Aubrey C. Eckert-Gallup<sup>2</sup>, Lainy D. Cochran<sup>1</sup>, Terry D. Kraus<sup>1</sup>, Sean D. Fournier<sup>3</sup>, Mark B. Allen<sup>3</sup>, Richard R. Schetnan<sup>4</sup>

Departments 6631<sup>1</sup>, 8853<sup>2</sup>, 631<sup>3</sup>, and 10731<sup>4</sup> Sandia National Laboratories P.O. Box 5800 Albuquerque, New Mexico 87185-0748

# Matthew D. Simpson

Lawrence Livermore National Laboratory National Atmospheric Release Advisory Center P.O. Box 808, L-103 Livermore, CA 94551

# Colin E. Okada and Avery A. Bingham

National Security Technologies, Remote Sensing Laboratory
Contractor to US Department of Energy
Nellis AFB, Bldg. 2211
4600 North Hollywood Blvd
Las Vegas, NV 89191

#### Abstract

The goal of this project is to develop and execute methods for characterizing uncertainty in data products that are developed and distributed by the DOE Consequence Management (CM) Program. A global approach to this problem is necessary because multiple sources of error and uncertainty from across the CM skill sets contribute to the ultimate production of CM data products. This report presents the methods used to develop a probabilistic framework to characterize this uncertainty and provides results for an uncertainty analysis for a study scenario analyzed using this framework.

#### **ACKNOWLEDGMENTS**

The authors would like to acknowledge the contributions of Dustin Whitener (SNL), John Fulton (SNL), and John "Adam" Stephens (SNL) to the effort to update Turbo FRMAC<sup>©</sup> to work with Dakota and the technical input and review of Keith Eckerman (ORNL), Nathan Bixler (SNL), Nevin Martin (SNL), and Douglas Osborn (SNL). The authors thank Arthur Shanks (SNL), Jim Phelan (SNL), and RaJah Mena (RSL) for the support that they provided over the duration of this project.

This work was funded by the Department of Energy (DOE), National Nuclear Security Administration (NNSA), NA-84 Technology Integration Program.

# **TABLE OF CONTENTS**

1.	Intro	duction		25			
2.	Study	Scenario Scenario		27			
3.	Unce	Uncertainty Quantification Methods					
	3.1.	3.1. Introduction to Uncertainty Quantification & Methods					
	3.2.	Uncerta	inty Propagation	31			
		3.2.1.	Sampling Methods & Software	32			
		3.2.2.	Propagating Uncertainty in Turbo FRMAC <sup>©</sup>	32			
		3.2.3.	Turbo FRMAC <sup>©</sup> Software Updates	34			
	3.3.	Statistic	al Post-processing Methods	34			
		3.3.1.	Uncertainty Analysis Methods & Results	35			
		3.3.2.	Sensitivity Analysis Methods & Results	35			
		3.3.3.	Sampling Confidence Intervals (CIs)	38			
4.	Sourc	Sources of Uncertainty & Input Distributions					
	4.1.	Public P	Protection DRL Input Distributions	41			
		4.1.1.	Deposition or Integrated Air Activity	41			
		4.1.2.	Deposition Velocity	41			
		4.1.3.	Breathing Rates	42			
		4.1.4.	Deposition External Dose Coefficient	45			
		4.1.5.	Ground Roughness Factor	46			
		4.1.6.	Inhalation Dose Coefficient	48			
		4.1.7.	Resuspension Factor	49			
		4.1.8.	Protective Action Guide	50			
		4.1.9.	Plume External Dose Coefficient	50			
		4.1.10.	Exposure to Dose Conversion Factor	51			
		4.1.11.	Weathering Factor	51			
		4.1.12.	Yield	53			
	4.2.	Data Co	ollection Sources of Uncertainty	54			
		4.2.1.	Laboratory Analysis	54			
		4.2.2.	In Situ Deposition Measurements	59			
		4.2.3.	AMS Measurements	65			
	4.3.	NARAC	C Atmospheric Dispersion Sources of Uncertainty	69			

		4.3.1.	Benchmark Data	69
		4.3.2.	Quantifying NARAC Concentration Uncertainty	71
		4.3.3.	Implementation of NARAC Uncertainty for CM Probabilistic	
			nent	
	4.4.	Summa	ry of Assigned Input Distributions	74
5.	Proba	abilistic A	nalysis Results	75
	5.1.	Laborate	ory Analysis	75
		5.1.1.	Uncertainty Analysis Results	76
		5.1.2.	Sensitivity Analysis Results	81
		5.1.3.	Sampling Confidence intervals	92
	5.2.	NARAC	Z	92
		5.2.1.	Uncertainty Analysis Results	92
		5.2.2.	Sensitivity Analysis Results	98
		5.2.3.	Sampling Confidence Intervals	108
	5.3.	Compar	rison of Uncertainty Analysis Results	108
		5.3.1.	DRL Result Comparisons	108
		5.3.2.	DP Result Comparisons	110
6.	Sumr	nary		115
	6.1.	Summa	ry of Overall Uncertainty Results	115
	6.2.	Incorpor	rating Uncertainty Results in Data Products	115
	6.3.	Implicat	tions & Future Work	119
7.	Refer	ences		121
APPl	ENDIX	A: Prob	pabilistic Analysis Results for In Situ Deposition and AMS	125
	A.1.	In Situ I	Deposition	125
		A.1.1.	Uncertainty Analysis Results	125
		A.1.2.	Sensitivity Analysis Results	126
		A.1.3.	Sampling Confidence Intervals	130
	A.2.	AMS		130
		A.2.1.	Uncertainty Analysis Results	130
		A.2.2.	Sensitivity Analysis Results	
		A.2.3.	Sampling Confidence Intervals	

# **LIST OF FIGURES**

_	. Comparison of cumulative probabilities for the Cs-137 Deposition DRL for NARAC, Laboratory Analysis, In Situ Deposition, and AMS
-	2. Comparison of cumulative probabilities for the Cs-137 Total DP for NARAC, Laboratory Analysis, In Situ Deposition, and AMS
Figure 3.2-1.	Typical Turbo FRMAC <sup>©</sup> simulation
Figure 3.2-2.	Turbo FRMAC <sup>©</sup> execution under probabilistic framework
Figure 3.3-1.	Example of scatter plots for the Dose Rate DRL for Laboratory Analysis and the first four inputs shown in Table 3.3-2.
Figure 4.1-1.	Empirical and parameterized probability densities for deposition velocity 42
Figure 4.1-2.	Empirical and parameterized probability densities for breathing rate, activity averaged, adult male
Figure 4.1-3.	Empirical and parameterized probability densities for breathing rate, light exercise, adult male
Figure 4.1-4.	Empirical and parameterized probability densities for the deposition external dose coefficient multiplier
Figure 4.1-5.	Empirical and parameterized probability densities for the ground roughness factor.
Figure 4.1-6.	Empirical and parameterized probability densities for the inhalation dose coefficient multiplier
	Empirical and parameterized probability densities for the resuspension coefficient multiplier
Figure 4.1-8.	Empirical and parameterized probability densities for the plume external dose coefficient multiplier
	Empirical and parameterized probability densities for the weathering coefficient multiplier
	Empirical and parameterized probability densities for activity per area for laboratory measurements
Figure 4.2-2.	In situ measurement geometry
	Distribution of the efficiency for a uniform surface deposition of 662 keV gamma rays for a DetectiveEX-100
Figure 4.2-4.	Empirical and parameterized probability densities for activity per area for in situ deposition measurements
-	Empirical and parameterized probability densities for activity per area for AMS measurements.
Figure 4.3-1.	NARAC r value probability function for the Prairie Grass Experiment71

Figure 4.3-2.	Empirical and parameterized probability densities for the air concentration multiplier
Figure 5.1-1.	Cumulative probability with mean and percentiles of interest for the Dose Rate DRL for Laboratory Analysis
Figure 5.1-2.	Cumulative probability with mean and percentiles of interest for the Cs-137 Deposition DRL for Laboratory Analysis
Figure 5.1-3.	Cumulative probability with mean and percentiles of interest for the Cs-137 Integrated Air DRL for Laboratory Analysis
Figure 5.1-4.	Cumulative probability with mean and percentiles of interest for the Cs-137 Plume Inhalation DP for Laboratory Analysis
Figure 5.1-5.	Cumulative probability with mean and percentiles of interest for the Cs-137 Plume Submersion DP for Laboratory Analysis
Figure 5.1-6.	Cumulative probability with mean and percentiles of interest for the Cs-137 Resuspension Inhalation DP Laboratory Analysis
Figure 5.1-7.	Cumulative probability with mean and percentiles of interest for the Cs-137 Groundshine DP Laboratory Analysis
	Cumulative probability with mean and percentiles of interest for the Cs-137 Total DP Laboratory Analysis
Figure 5.1-9.	Scatter plots for the Dose Rate DRL for Laboratory Analysis and the first four inputs shown in Table 5.1-3
Figure 5.1-10	O. Scatter plots for the Cs-137 Deposition DRL for Laboratory Analysis and the first four inputs shown in Table 5.1-4
Figure 5.1-11	1. Scatter plots for the Cs-137 Integrated Air DRL for Laboratory Analysis and the first four inputs shown in Table 5.1-5
Figure 5.1-12	2. Scatter plots for the Cs-137 Plume Inhalation DP for Laboratory Analysis and the first four inputs shown in Table 5.1-6
Figure 5.1-13	3. Scatter plots for the Cs-137 Plume Submersion DP for Laboratory Analysis and the first three inputs shown in Table 5.1-7
Figure 5.1-14	4. Scatter plots for the Cs-137 Resuspension Inhalation DP for Laboratory Analysis and the first four inputs shown in Table 5.1-8
	5. Scatter plots for the Cs-137 Groundshine DP for Laboratory Analysis and the first four inputs shown in Table 5.1-9
Figure 5.1-16	5. Scatter plots for the Cs-137 Total DP for Laboratory Analysis and the first four inputs shown in Table 5.1-10
Figure 5.2-1.	Cumulative probability with mean and percentiles of interest for the Dose Rate DRL results for NARAC
Figure 5.2-2.	Cumulative probability with mean and percentiles of interest for the Cs-137 Deposition DRL for NARAC

Figure 5.2-3. Cumulative probability with mean and percentiles of interest for the Cs-137  Integrated Air DRL for NARAC
Figure 5.2-4. Cumulative probability with mean and percentiles of interest for the Cs-137 Plume Inhalation DP for NARAC
Figure 5.2-5. Cumulative probability with mean and percentiles of interest for the Cs-137 Plume Submersion DP for NARAC
Figure 5.2-6. Cumulative probability with mean and percentiles of interest for the Cs-137 Resuspension Inhalation DP for NARAC
Figure 5.2-7. Cumulative probability with mean and percentiles of interest for the Cs-137 Groundshine DP for NARAC.
Figure 5.2-8. Cumulative probability with mean and percentiles of interest for the Cs-137 Total DP for NARAC
Figure 5.2-9. Scatter plots for the Dose Rate DRL for NARAC and the first four inputs shown in Table 5.2-3.
Figure 5.2-10. Scatter plots for the Cs-137 Deposition DRL for NARAC and the first four inputs shown in Table 5.2-4.
Figure 5.2-11. Scatter plots for the Cs-137 Integrated Air DRL for NARAC and the first four inputs shown in Table 5.2-5.
Figure 5.2-12. Scatter plots for the Cs-137 Plume Inhalation DP for NARAC and the first three inputs shown in Table 5.2-6
Figure 5.2-13. Scatter plots for the Cs-137 Plume Submersion DP for NARAC and the first two inputs shown in Table 5.2-7.
Figure 5.2-14. Scatter plots for the Cs-137 Resuspension Inhalation DP for NARAC and the firs four inputs shown in Table 5.2-8
Figure 5.2-15. Scatter plots for the Cs-137 Groundshine DP for NARAC and the first four inputs shown in Table 5.2-9.
Figure 5.2-16. Scatter plots for the Cs-137 Total DP for NARAC and the first four inputs shown in Table 5.2-10
Figure 5.3-1. Comparison of cumulative probabilities for the Dose Rate DRL for NARAC, Laboratory Analysis, In Situ Deposition, and AMS
Figure 5.3-2. Comparison of cumulative probabilities for the Cs-137 Deposition DRL for NARAC, Laboratory Analysis, In Situ Deposition, and AMS
Figure 5.3-3. Comparison of cumulative probabilities for the Cs-137 Integrated Air DRL for NARAC, Laboratory Analysis, In Situ Deposition, and AMS
Figure 5.3-4. Comparison of cumulative probabilities for the Cs-137 Plume Inhalation DP for NARAC, Laboratory Analysis, In Situ Deposition, and AMS
Figure 5.3-5. Comparison of cumulative probabilities for the Cs-137 Plume Submersion DP for NARAC, Laboratory Analysis, In Situ Deposition, and AMS

Figure 5.3-6.	Comparison of cumulative probabilities for the Cs-137 Resuspension Inhalation D for NARAC, Laboratory Analysis, In Situ Deposition, and AMS	
Figure 5.3-7.	Comparison of cumulative probabilities for the Cs-137 Groundshine DP for NARAC, Laboratory Analysis, In Situ Deposition, and AMS	2
Figure 5.3-8.	Comparison of cumulative probabilities for the Cs-137 Total DP for NARAC, Laboratory Analysis, In Situ Deposition, and AMS	3
Figure 6.2-1.	Data product displaying the Cs-137 Deposition DRL distribution from the NARAG simulations.	
Figure 6.2-2.	Data product displaying the Cs-137 Deposition DRL mean result from the NARAG simulations and the default DRL	
	LIST OF TABLES	
Table ES - 1.	. Summary of input distributions for Public Protection DRL calculation	6
Table ES - 2.	. Mean DRL uncertainty results for Laboratory Analysis and NARAC compared to default DRL results	
Table ES - 3	. Mean DP uncertainty results for Laboratory Analysis and NARAC compared to default DP results	8
Table 2-1. Pu	ablic Protection DRL calculation default inputs	28
Table 2-2. Pu	ublic Protection DRL calculation default results	29
Table 3.3-1.	Example of DRL uncertainty results for Laboratory Analysis simulations 3	35
Table 3.3-2.	Example of sensitivity analysis results for the Dose Rate DRL for Laboratory  Analysis	37
Table 4.1-1.	FRMAC Assessment default activity times and activity-specific breathing rates for adult male	
Table 4.2-1.	Laboratory Analysis sources of uncertainty5	58
Table 4.2-2.	Estimated count rate in the aerial detectors flying over an area that is uniformly contaminated at $330  \mu \text{Ci/m}^2$	56
Table 4.2-3.	Uncertainty in estimated count rate in the aerial detectors flying over an area that is uniformly contaminated at 330 µCi/m²	
Table 4.3-1.	Distribution of NARAC observed to predicted concentration ratios for the Prairie Grass and Diablo Canyon tracer gas experiments	'O
Table 4.4-1.	Summary of input distributions for Public Protection DRL Calculation	′4
Table 5.1-1.	DRL uncertainty results for Laboratory Analysis simulations	'6
Table 5.1-2.	DP uncertainty results for Laboratory Analysis simulations	18

Table 5.1-3. Sensitivity analysis results for the Dose Rate DRL for Laboratory Analysis 83
Table 5.1-4. Sensitivity analysis results for the Cs-137 Deposition DRL for Laboratory Analysis.
Table 5.1-5. Sensitivity analysis results for the Cs-137 Integrated Air DRL for Laboratory Analysis
Table 5.1-6. Sensitivity analysis results for the Cs-137 Plume Inhalation DP for Laboratory Analysis
Table 5.1-7. Sensitivity analysis results for the Cs-137 Plume Submersion DP for Laboratory Analysis
Table 5.1-8. Sensitivity analysis results for the Cs-137 Resuspension Inhalation DP for Laboratory Analysis
Table 5.1-9. Sensitivity analysis results for the Cs-137 Groundshine DP for Laboratory Analysis.
Table 5.1-10. Sensitivity analysis results for the Cs-137 Total DP for Laboratory Analysis 91
Table 5.1-11. Sampling confidence intervals for Laboratory Analysis simulations
Table 5.2-1. DRL uncertainty results for NARAC simulations
Table 5.2-2. DP uncertainty results for NARAC simulations
Table 5.2-3. Sensitivity analysis results for the Dose Rate DRL for NARAC
Table 5.2-4. Sensitivity analysis results for the Cs-137 Deposition DRL for NARAC
Table 5.2-5. Sensitivity analysis results for the Cs-137 Integrated Air DRL for NARAC 101
Table 5.2-6. Sensitivity analysis results for the Cs-137 Plume Inhalation DP for NARAC 103
Table 5.2-7. Sensitivity analysis results for the Cs-137 Plume Submersion DP for NARAC 104
Table 5.2-8. Sensitivity analysis results for the Cs-137 Resuspension Inhalation DP for NARAC.
Table 5.2-9. Sensitivity analysis results for the Cs-137 Groundshine DP for NARAC 106
Table 5.2-10. Sensitivity analysis results for the Cs-137 Total DP for NARAC
Table 5.2-11. Sampling confidence intervals for NARAC simulations
Table A.1- 1. DRL uncertainty results for In Situ Deposition simulations
Table A.1- 2. DP uncertainty results for In Situ Deposition simulations
Table A.1- 3. Sensitivity analysis results for the Dose Rate DRL for In Situ Deposition 126
Table A.1-4. Sensitivity analysis results for the Cs-137 Deposition for In Situ Deposition 126
Table A.1- 5. Sensitivity analysis results for the Cs-137 Integrated Air DRL for In Situ Deposition
Table A.1- 6. Sensitivity analysis results for the Cs-137 Plume Inhalation DP for In Situ Deposition

Table A.1- 7. Sensitivity analysis results for the Cs-137 Plume Submersion DP for In Situ  Deposition.	128
Table A.1- 8. Sensitivity analysis results for the Cs-137 Resuspension Inhalation DP for In Supersition.	
Table A.1- 9. Sensitivity analysis results for the Cs-137 Groundshine DP for In Situ Deposit	
Table A.1- 10. Sensitivity analysis results for the Cs-137 Total DP for In Situ Deposition	
Table A.1- 11. Sampling confidence intervals for In Situ Deposition simulations	130
Table A.2- 1. DRL uncertainty results for AMS simulations.	130
Table A.2- 2. DP uncertainty results for AMS simulations.	130
Table A.2- 3. Sensitivity analysis results for the Dose Rate DRL for AMS	131
Table A.2- 4. Sensitivity analysis results for the Cs-137 Deposition DRL for AMS	131
Table A.2- 5. Sensitivity analysis results for the Cs-137 Integrated Air DRL for AMS	132
Table A.2- 6. Sensitivity analysis results for the Cs-137 Plume Inhalation DP for AMS	132
Table A.2-7. Sensitivity analysis results for the Cs-137 Plume Submersion DP for AMS	133
Table A.2- 8. Sensitivity analysis results for the Cs-137 Resuspension Inhalation DP for AM	
Table A.2- 9. Sensitivity analysis results for the Cs-137 Groundshine DP for AMS	134
Table A.2- 10. Sensitivity analysis results for the Cs-137 Total DP for AMS	134
Table A.2- 11. Sampling confidence intervals for AMS simulations	135

#### **EXECUTIVE SUMMARY**

#### Background

This document describes the methods and results of a project performed under the DOE NNSA NA-84 Technology Integration Program to develop and execute methods for characterizing uncertainty in data products that are developed and distributed by the DOE Consequence Management (CM) Program. The sources of error and uncertainty that contribute to overall uncertainty in CM data products span the entire process used to develop these products. Thus, this project required collaboration with subject matter experts across the range of CM skill sets to quantify the uncertainty in the inputs from each area of the CM process. Probabilistic methods were applied to understand how individual uncertainties contribute to the aggregated uncertainty in the values used to create data products. The ultimate goal of this project is to quantify the confidence level of data products to ensure that appropriate public and worker protections decisions are supported by defensible analysis.

# **Purpose and Scope**

The goal of this analysis is to characterize uncertainty in the CM data product development process. This process does not require the characterization of uncertainty inherent to the situation under analysis; sources of uncertainty such as the type of release, location of release, weather, etc., were held constant for this project in order to allow for the examination of the impact of sources of uncertainty within the analysis process itself. A demonstration scenario was selected for this analysis with the following characteristics:

- Detonation of a Cesium-137 radiological dispersal device on level terrain within a stable wind class
- Idealized particle size distribution (particles created by the detonation and atmospherically dispersed are all 1 µm diameter)
- Source term of sufficient quantity to create an activity per area of 330 μCi/m² at a hypothetical location downwind

The scope of this project is limited to the analysis of the uncertainty associated with Public Protection Derived Response Levels (DRLs), which are used to evaluate the radiological impacts to members of the public from exposure to radioactive material. A DRL is a level of radioactivity in the environment that would be expected to produce a dose equal to the corresponding Protective Action Guide (PAG), as defined in the 2017 EPA PAG Manual. The data products for which Public Protection DRLs are calculated are used to help decision makers determine where protective actions (e.g., sheltering, evacuation, or relocation of the public) may be warranted. The DRL calculation for this analysis was for the Early Phase (Total Dose) Time Phase and used all Federal Radiological Monitoring and Assessment Center (FRMAC) defaults, as specified in the FRMAC Assessment Manual, Vol. 1, and the ICRP Recommended lung clearance type.

In order to calculate DRLs, Dose Parameters (DP) must also be calculated. A DP represents the integrated dose to a receptor from a particular dose pathway. The four primary pathways considered in FRMAC Assessments for the Early Phase (Total Dose) Time Phase are Plume Inhalation, Plume Submersion, Resuspension Inhalation, and Groundshine. The DPs for these

pathways are summed to get a Total DP, which is then used to calculate DRLs. The probabilistic analysis results for this project include both DRL and DP uncertainties because the uncertainties associated with the different dose pathways for a given scenario are important for understanding overall DRL uncertainty.

# **Uncertainty Quantification Approach**

A probabilistic framework was developed to propagate uncertainty in simulation inputs through the calculations performed in Turbo FRMAC<sup>®</sup> to characterize uncertainty in the data products that result from simulation outputs. As stated above, this framework was developed for a single release scenario and its resulting data products and serves as a proof of concept that could be applied to additional release scenarios and data products in the future.

The meaning of the term uncertainty in the context of this report is defined as follows. The true value of a model result (i.e., the true DRL value) is assumed to be fixed but unknown. The variation in the observation of this result (i.e., the approximate DRL calculated from a given Turbo FRMAC<sup>©</sup> simulation) relative to this fixed value is termed as the uncertainty in the model result. The collection of many Turbo FRMAC<sup>©</sup> simulations with varying inputs calculated using the principles of Monte Carlo Analysis can be used to quantify this uncertainty.

The project does not seek to quantify model uncertainty; the same models that are currently available in Turbo FRMAC<sup>©</sup> and were employed for the scenario of interest were used for every simulation. The current practice for the calculation of quantities such as DRLs for data products is to use a set of constant default input parameter values. These input parameters, though supported by standard-practice, literature, and data, are inherently approximations. In addition, parameters and inputs derived from data collection during an event are uncertain due to a variety of factors including those related to the measurement device and methods, field contamination, etc. The scope of this project seeks to identify and characterize the relationship between the uncertainty in these inputs to the overall uncertainty in CM data products.

A Monte Carlo analysis was used to characterize uncertainty in data products for the purposes of this project. The process of executing a Monte Carlo analysis for the purposes of this project is described as follows. First, the uncertainty in Turbo FRMAC<sup>©</sup> inputs used in the calculation of DRLs for the study scenario was characterized using probability distributions. These distributions were then sampled many times. A single deterministic Turbo FRMAC<sup>©</sup> simulation was run for each sample, propagating uncertainty through the model. The final collection of simulation results was then analyzed to characterize overall uncertainty (uncertainty analysis) and to determine the contribution of each variable to the overall uncertainty (sensitivity analysis). The methods used to execute each of these steps, including the tools used and details regarding updates to Turbo FRMAC<sup>©</sup> required for this analysis, are described in detail in the body of the document.

# Sources of Uncertainty & Input Distributions

The first step in characterizing the overall uncertainty in CM data products is to assess the uncertainty in the inputs that are used in to calculate DRLs for these data products. These inputs are assigned a probability distribution that describes the uncertainty that might be expected for a given parameter and that is based on published data and/or expert opinion. Table ES - 1 lists the Public Protection DRL inputs and the probability distributions assigned for this analysis. In

determining the distributions for the Public Protection DRL inputs, the original reference for each input was examined for uncertainty information. Additional references were used when the original references did not provide the needed uncertainty information.

DRL calculations are based on measured or projected concentrations of radionuclides in the environment. Measured values can be provided through multiple sources, including analytical laboratory results (hereafter termed Laboratory Analysis) or field measurements obtained either through aerial measuring systems (AMS) or ground-based monitoring teams (In Situ Deposition). Projections are usually obtained from atmospheric modelling calculations performed using plume projections from the National Atmospheric Release Advisory Center (NARAC). In order to characterize the uncertainty in data products due to varying sources of activity information, a probabilistic analysis was completed for each activity source (Laboratory Analysis, In Situ Deposition, AMS, and NARAC). The probabilistic runs for Laboratory Analysis, In Situ Deposition, and AMS used a mixture based on activity per area with the same parameter distributions type (Normal) and with the same mean value but with a different standard deviation (SD) based on the uncertainty in each activity source. The runs for NARAC used a distribution for integrated air activity instead of activity per area.

Table ES - 1. Summary of input distributions for Public Protection DRL calculation.

Input	Default Value	Distribution Type	Mean	SD	Mode	Lower Bound	Upper Bound	Units
Air Concentration Uncertainty Multiplier – NARAC*	1	Lognormal <sup>+</sup>	0.59	3.99				
Activity per Area – In Situ	330	Normal	330	3.74				μCi/m²
Activity per Area – AMS	330	Normal	330	9.29				μCi/m²
Activity per Area – Laboratory Analysis	330	Normal	330	17				μCi/m²
Deposition Velocity	3.00E-3	Triangular			3.00E-3	3.00E-4	3.00E-2	m/s
Breathing Rate – Light Exercise, Adult Male	1.50	Normal	1.75	0.42		0.54	3.00	m <sup>3</sup> /hr
Breathing Rate – Activity-Averaged, Adult Male	0.92	Triangular			0.92	0.54	1.50	m <sup>3</sup> /hr
Ground Roughness Factor	0.82	Normal	0.82	0.082		0	1	
Resuspension Coefficient  Multiplier <sup>‡</sup>	1	Lognormal <sup>+</sup>	1	4.2				
Weathering Coefficient Multiplier <sup>‡</sup>	1	Lognormal <sup>+</sup>	1	1.2				
Deposition External Dose Coefficient Multiplier	1	Triangular			0.8	0.5	1.5	
Inhalation Dose Coefficient Multiplier§	1	Lognormal <sup>+</sup>	1	1.5				
Plume External Dose Coefficient Multiplier	1	Triangular			0.8	0.5	1.5	

<sup>\*</sup> This uncertainty multiplier is multiplied by a user-defined air concentration value to sample air concentration with uncertainty. This distribution is calculated from the comparison of NARAC predictions to experimental data.

<sup>+</sup> The means and standard deviations (SD) listed for lognormal distributions on this table are the geometric mean and geometric standard deviation, respectively. The lognormal distribution is defined by parameters  $\mu$ , the mean of the natural logarithm of the data, and  $\sigma$ , the standard deviation of the natural logarithm of the data. Then, the geometric mean (*GM*) is given by  $GM = e^{\mu}$  and the geometric standard deviation (*GSD*) is given by  $GSD = e^{\sigma}$ .

<sup>‡</sup> These multipliers are to be applied only to the coefficients outside the exponentials in the Resuspension and Weathering Factors

<sup>§</sup> This multiplier is specifically for Cs-137, Type F, Effective (Whole Body). Ba-137m is present at equilibrium with Cs-137 at the start of the time phase. The uncertainty in the Ba-137m inhalation dose coefficient is neglected because its ingrowth from Cs-137 over the dose commitment period dominates the delivered dose. The Cs-137 inhalation dose coefficient accounts for dose and uncertainty from the ingrowth of Ba-137m. (per communication with Keith Eckerman on May 10, 2017)

#### Probabilistic Analysis Results

The probabilistic analysis completed for each source of activity (NARAC, Laboratory Analysis, In Situ Deposition, and AMS) used 10,000 Turbo FRMAC® simulations to generate a set of results for each output of interest. These results were analyzed to characterize the uncertainty in each output, to determine the relationship between the uncertainty in each input to the uncertainty in the output, and to confirm that the selected sample size adequately captures the mean value for each output. The primary DRL outputs of the analysis are the Dose Rate DRL, Cs-137 Deposition DRL, and Cs-137 Integrated Air DRL. The DP outputs of this analysis are the Plume Inhalation DP, Plume Submersion DP, Resuspension Inhalation DP, Groundshine DP, and Total DP. The Exposure Rate DRL and Beta DRL outputs were included in the simulations but are not reported in the results as they are essentially the same as the Dose Rate DRL and Cs-137 Deposition DRL, respectively. The Alpha DRL output was included in the simulations as well but is not reported because it was zero for this scenario.

Table ES - 2 and Table ES - 3 contain the mean DRL and DP results, respectively, calculated for the Laboratory Analysis and NARAC activity sources from the 10,000 simulation results for each of these input sets. The tables also show the default results which represent the normal operating defaults for Turbo FRMAC<sup>©</sup> for the scenario of interest before any uncertainty is applied to the inputs. The results for the Laboratory Analysis, In Situ, and AMS simulations are nearly the same, although slight differences can be seen in the DP outputs for these varying sources of deposition data. This is expected because the only difference between these simulations is the SD on the distribution for activity per area. For the sake of brevity, Laboratory Analysis was chosen to represent the results for this group because the results are similar enough that the same conclusions can be drawn for each deposition data source. The Laboratory Analysis results are displayed in Table ES - 2 and Table ES - 3 because the activity per area distribution for Laboratory Analysis has the largest SD of the three similar sources. Figure ES - 1 and Figure ES - 2 show cumulative distribution functions for the Cs-137 Deposition DRL and Total DP, respectively.

Table ES - 2. Mean DRL uncertainty results for Laboratory Analysis and NARAC compared to default DRL results.

Output Name	Default	Laboratory Analysis	NARAC
Dose Rate DRL [mrem/hr]	1.98	3.869	3.868
Cs-137 Deposition DRL [μCi/m²]	3.31E2	712.550	712.554
Cs-137 Integrated Air DRL [μCi-s/m³]	1.10E5	75856.595	75875.319

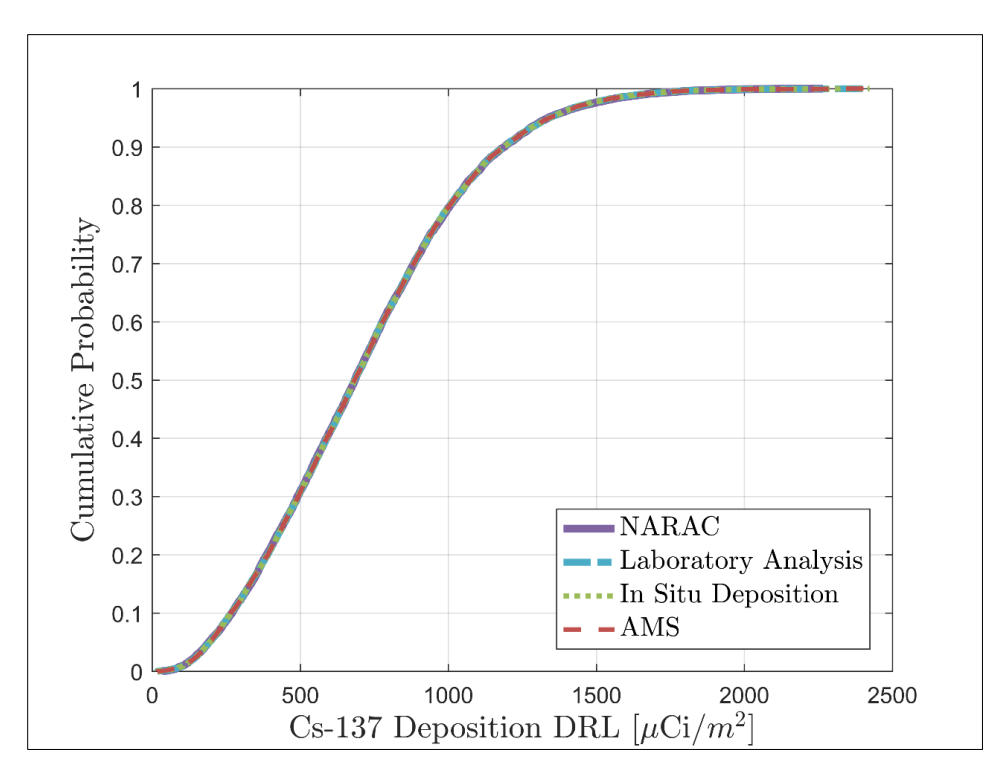


Figure ES - 1. Comparison of cumulative probabilities for the Cs-137 Deposition DRL for NARAC, Laboratory Analysis, In Situ Deposition, and AMS.

Table ES - 3. Mean DP uncertainty results for Laboratory Analysis and NARAC compared to default DP results.

Output Name	Default	Laboratory Analysis	NARAC
Cs-137 Plume Inhalation DP [mrem]	7.93E2	468.811	1545.6
Cs-137 Plume Submersion DP [mrem]	10.4	4.501	14.704
Cs-137 Resuspension Inhalation DP [mrem]	4.42	14.128	78.834
Cs-137 Groundshine DP [mrem]	1.89E2	179.447	1023.456
Cs-137 Total DP [mrem]	9.97E2	666.886	2662.594

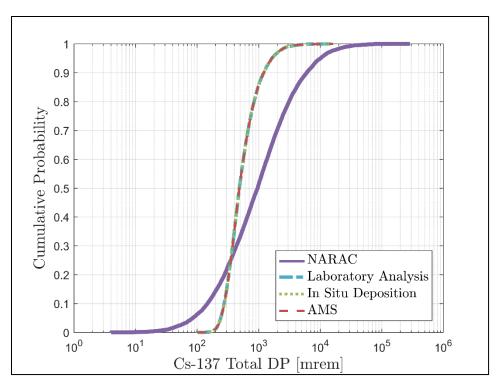


Figure ES - 2. Comparison of cumulative probabilities for the Cs-137 Total DP for NARAC, Laboratory Analysis, In Situ Deposition, and AMS.

The DRL results are visually the same for all four of the activity sources in Figure ES - 1 because the only input distribution that distinguishes the four sets of simulations from each other is the activity per area or air concentration multiplier distributions, and the contribution to uncertainty from these distributions is effectively cancelled out in the DRL ratio because the mixture consists of a single radionuclide. Table ES - 2 shows a slight numerical difference in the air concentration-based NARAC results relative to the deposition-based Laboratory Analysis results due to the aggregated uncertainty in the Total DP distribution, which is difference in the NARAC simulations and the other three deposition-based simulations. This difference in Total DP is distinguishable and can be seen in Figure ES - 2.

The DP results are essentially the same for Laboratory Analysis, In Situ Deposition, and AMS because the only difference between these simulations is the SD on the distribution for activity per area, and the sensitivity results showed that activity per area is not an important contributor to DP uncertainty for this analysis. This is shown in by the overlapping lines in Figure ES - 2. Figure ES - 2 also shows that the NARAC DP results have a greater distribution spread than the other simulations, using the Total DP as an example. This greater spread is caused by the distribution for the air concentration multiplier, which is wider than the distribution for activity per area.

The sensitivity analysis showed that the uncertainty in the NARAC-modeled air concentration is the most important contributor to DP uncertainty when the dose projection uses integrated air activity to define the radionuclide mixture. The uncertainty in deposition velocity is the most important contributor to DP uncertainty when the dose projection uses activity per area data to

define the radionuclide mixture. These results can be used to motivate additional studies to better characterize these inputs and in turn reduce the overall uncertainty in the DP and DRL results.

It is important to note that the mixture for this analysis consisted of a single radionuclide at a concentration equal to the DRL. A radionuclide with different decay characteristics (e.g., half-life, radiations emitted) will likely yield different results, as will a mixture of multiple radionuclides. Also, an analysis using only the ground pathways (resuspension inhalation and groundshine) will likely yield very different results from this analysis, in which the inputs to the plume DPs dominated the overall uncertainty.

The goal of this project was to develop the methods that could be used to execute a probabilistic analysis for the values used to generate CM data products; this project does not seek to provide specific and final information regarding the uncertainty in data products as a whole. Therefore, the results presented in this report should be considered examples derived from a proof of concept of simulation methods and should not be explicitly applied or used to draw conclusions about the full range of potential uncertainties in data products. As the scope of this project was focused on the development of methods for characterizing uncertainty in data products, the discussion provided in this report could be expanded further as results are generated for other analyses in future work.

# Insights & Future Work

The results of the probabilistic analysis used to characterize uncertainty in CM data products show that this uncertainty could be large. However, the mean result for the Deposition DRL, which is the most frequently used DRL for public protection data products, is larger than the same result calculated using the default values for all inputs. This demonstrates that, for the given study scenario, the default DRL is conservative in comparison to the best estimate of the DRL derived from this uncertainty analysis. The sensitivity analysis results point to input variables whose uncertainty impacts uncertainty in simulation results the most. These important variables could be targeted for further study in order to reduce the uncertainty in the data products for which they are used as simulation inputs. It is critical to note that these results have only been generated for a limited study scenario; implications of these findings for a wider range of CM scenarios and data products is an important area of future work. The application of the methods and tools developed and used to perform this analysis will be expanded in an extension of this project. As the scenarios studied increase in complexity, the statistical methods and tools used to both generate simulation inputs and to perform uncertainty and sensitivity analysis may need to be adapted to adequately analyze results.

The potential for implementation of uncertainty quantification calculations in a real-world response must be studied further. The current implementation of these calculations in Turbo FRMAC® executes the simulation for each sample one after the other; parallelization of these calculations would help to increase the calculation speed for a probabilistic analysis of a given scenario. However, the bulk of the effort required to run a comprehensive probabilistic analysis is in the definition of the input distributions that will be used to generate input samples. These input distributions may need to be changed based on the release scenario, information and data collected in the field as a response is happening, etc. As additional scenarios are analyzed using the probabilistic framework described in this report, it may be possible to streamline the definition of input distributions by generating a database of distributions for the most likely

scenarios. This may make uncertainty quantification for real-world responses more feasible in the future. The ultimate use of and audience for uncertainty analysis results in a real-world response will require further discussion. This will require further development of map products and a consideration of how such products might be interpreted by decision makers.

# **NOMENCLATURE**

Abbreviation	Definition
AGL	Above ground level
AMS	Aerial Measurement Systems
Ba-137m	Metastable barium-137
CDF	Cumulative distribution function
CI	Confidence interval
CM	Consequence Management
Cs-137	Cesium-137
DOE	Department of Energy
DP	Dose parameter
DRL	Derived response level
EFH	Exposure Factors Handbook
EPA	Environmental Protection Agency
FAL	Fly Away Laboratory
FRMAC	Federal Radiological Monitoring and Assessment Center
GM	Geometric mean
GPS	Global positioning system
GSD	Geometric standard deviation
HE	High explosive
ICRP	International Commission on Radiological Protection
LHS	Latin Hypercube Sampling
MACCS	MELCOR Accident Consequence Code System
NARAC	National Atmospheric Release Advisory Center
NIST	National Institute of Standards and Technology
NRC	Nuclear Regulatory Commission
ORNL	Oak Ridge National Laboratory
PAG	Protective action guide
PSD	Particle size distribution
$\mathbb{R}^2$	Value indicating the amount of output variance explained by a given regression model
R <sup>2</sup> Individual	Value indicating the increase in the overall R <sup>2</sup> as each input is added to the regression model
RA	Radar altimeter
RASCAL	Radiological Assessment System for Consequence AnaLysis

Abbreviation	Definition			
RDD	Radiological dispersal device			
ROI	Region of interest			
RSL	Remote Sensing Laboratory			
SD	Standard deviation			
SNL	Sandia National Laboratories			
SOARCA	State-of-the-Art Reactor Consequence Analysis			
SRRC	Standardized rank regression coefficient			
TPU	Total propagated uncertainty			

#### 1. INTRODUCTION

This document describes the methods and results of a project performed under the DOE NNSA NA-84 Technology Integration Program to develop and execute methods for characterizing uncertainty in data products that are developed and distributed by the DOE Consequence Management (CM) Program. A global approach to this problem is necessary because multiple sources of error and uncertainty contribute to the ultimate production of data products. Therefore, this project required collaboration with subject matter experts across a wide range of CM skill sets in order to quantify the uncertainty from each area of the CM process and to understand how variations in these uncertainty sources contribute to the aggregated uncertainty present in data products. The ultimate goal of this project is to quantify the confidence level of data products to ensure that appropriate public and worker protections decisions are supported by defensible analysis.

The scope of this project is limited to the analysis of the uncertainty associated with Public Protection Derived Response Levels (DRLs), which are used to evaluate the radiological impacts to members of the public from exposure to radioactive material. A DRL is a level of radioactivity in the environment that would be expected to produce a dose equal to the corresponding Protective Action Guide (PAG), as defined in the 2017 EPA PAG Manual [1]. The data products for which Public Protection DRLs are calculated are used to help decision makers determine where protective actions (e.g., sheltering, evacuation, or relocation of the public) may be warranted.

Assessment Scientists use the Turbo FRMAC<sup>®</sup> software [2] to estimate the projected dose following a radiological release to the environment. This projected dose is then used to create a data product (typically a map) which is used by decision makers to make appropriate protective action decisions. These calculations performed by Turbo FRMAC<sup>®</sup> rely on data which may be collected from one of several methods: analytical results from laboratories, results from Aerial Measurement Systems (AMS), or field measurements made by ground-based monitoring teams. Source term data can also be generated using computer models (e.g., RASCAL). The results of the Assessment calculations are then used to create contours on a data grid developed using National Atmospheric Release Advisory Center (NARAC) atmospheric dispersion predictions.

A probabilistic framework was developed to characterize the CM process and the interrelated nature of error and uncertainty propagation that contributes to the overall uncertainty in data products. This framework was developed for an idealized single release scenario and resulting data product that serves as a proof of concept that could be applied to additional, more complex release scenarios and data products in the future. The results of probabilistic runs for a study scenario were analyzed using statistical methods to characterize their uncertainty and to quantify the importance of uncertainty in simulation inputs to the uncertainty in simulation outputs. The goal of this project is to develop the methods that could be used to execute a probabilistic analysis for data products; this project does not seek to provide specific and final information regarding the uncertainty in data products as a whole. Therefore, the results presented in this report should be considered examples derived from a proof of concept of simulation methods and should not be explicitly applied or used to draw conclusions about the full range of potential uncertainties in data products.

This report is organized as follows. Chapter 2 describes the study scenario that was selected to pilot the methods and derive simulation results. Chapter 3 presents the uncertainty quantification methods that were applied to develop a probabilistic framework and describes the methods that were used in the statistical post-processing of simulation outputs. Chapter 4 details the distributions that were selected for each simulation inputs and provides a referential basis for each of these distribution selections. Chapter 5 provides the results of the probabilistic analysis conducted for the study scenario. Chapter 6 summarizes the methods and results presented in the report and provides information about future areas of study.

#### 2. STUDY SCENARIO

The goal of this analysis is to characterize uncertainty in the CM data product development process. This does not require the characterization of uncertainty inherent to the situation under analysis; sources of uncertainty such as the type of release, location of release, weather, etc., were held constant for this project in order to allow for the examination of the impact of sources of uncertainty within the analysis process itself. A demonstration scenario was selected for this analysis with the following characteristics:

- Detonation of a Cs-137 radiological dispersal device (RDD) on level terrain within a stable wind class
- Idealized particle size distribution (particles created by the detonation and atmospherically dispersed are all 1 µm diameter)
- Source term of sufficient quantity to create an activity per area of 330 μCi/m² at a hypothetical location downwind. This concentration was assumed because it is equivalent to the default, Early Phase (Total Dose) Deposition DRL for Cs-137

The DRL calculation for this analysis is for the Early Phase (Total Dose) Time Phase and uses all Federal Radiological Monitoring and Assessment Center (FRMAC) defaults, as specified in the FRMAC Assessment Manual, Vol. 1 [3], and the ICRP Recommended lung clearance type.

In order to calculate DRLs, Dose Parameters (DP) must also be calculated. A DP represents the integrated dose to a receptor from a particular dose pathway. The four primary pathways considered in FRMAC Assessments for the Early Phase (Total Dose) Time Phase are Plume Inhalation, Plume Submersion, Resuspension Inhalation, and Groundshine. The DPs for these pathways are summed to get a Total DP, which is then used to calculate DRLs. The probabilistic analysis results for this project include both DRL and DP uncertainties because the uncertainties associated with the different dose pathways for a given scenario are important for understanding overall DRL uncertainty. For details on how DRLs and Dose Parameters (DP) are calculated, refer to Section 1 of the FRMAC Assessment Manual, Vol. 1.

The default values for the DRL calculation inputs are listed in Table 2-1. Table 2-2 contains the results of interest obtained using the inputs in Table 2-1. The results in Table 2-2 are the values for each output derived from a single Turbo FRMAC<sup>©</sup> simulation using the default values for each input. These are the results that are currently used to generate data products and will be referred to throughout the remainder of this report as "default" results. Note, the dose parameters (DP) included in Table 2-2 are "rolled up," i.e., they include the dose contribution from Ba-137m (Cs-137 daughter).

Table 2-1. Public Protection DRL calculation default inputs.

Term	Definition	Value	Units
Ã	Integrated air activity of Cs-137 (assumed for this analysis) (See Section 4.1.1)	1.10E5	μCi-s/m³
$BR_{AA}$	Activity-Averaged Breathing Rate, the average volume of air breathed per unit time by an adult male (ICRP94, Table B.16B) (See Section 4.1.3.1)	0.92	m³/hr
$BR_{LE}$	Light-Exercise Breathing Rate, the volume of air breathed per unit time by an adult male during light exercise (ICRP94, Table 6) (See Section 4.1.3.2)	1.50	m³/hr
Dp_ExDC	Deposition External Dose Coefficient, the external dose rate to the whole body from Cs-137 per unit activity deposited on the ground (See Section 4.1.4)	4.17E-5	$\frac{\text{mrem-m}^2}{\mu\text{Ci-hr}}$
Dp	Deposition, the areal activity of Cs-137 (assumed for this analysis), also referred to as "activity per area" (See Section 4.1.1)	330	μCi/m²
GRF	Ground Roughness Factor, a constant that compensates for the fact that the external exposure is not coming from an infinite flat plane (See Section 4.1.5)	0.82	unitless
InhDC	Inhalation Dose Coefficient, the committed effective dose coefficient for inhalation of Cs-137, Lung Clearance Type F (See Section 4.1.6)	17.3	mrem/μCi
K	Resuspension Factor, the fraction of radioactive material transferred from the surface to the breathing zone at given time <i>t</i> after initial deposition (See Section 4.1.7)	Maxwell/ Anspaugh method	m <sup>-1</sup>
PAG	Protective Action Guide for the Early Phase (Total Dose) time phase (See Section 4.1.8)	1000	mrem
Pl_ExDC	Plume External Dose Coefficient, the external dose rate to the whole body from submersion in Cs-137 in the plume (See Section 4.1.9)	1.25E-3	$\frac{\text{mrem-m}^3}{\mu\text{Ci-hr}}$
$V_d$	Deposition Velocity, the rate at which airborne material is deposited on the ground (See Section 4.1.2)	3.00E-3	m/s
WF	Weathering Factor, the adjustment for the decrease that occurs over time as the deposited material is removed by a physical process (e.g., migration into the soil column or wind) (See Section 4.1.11)	Anspaugh 2002 model	unitless
$XDCF_C$	Exposure to Dose Conversion Factor (chronic), the constant used to convert external exposure (mR) to deep tissue (1 cm) dose (mrem) (see Section 4.1.10)	1.0	mrem/mR
$Y_{\alpha}$	Yield, the alpha activity per total (nuclear transformation) activity of Cs-137 (See Section 4.1.12)	0	unitless
$Y_{eta}$	Yield, the beta activity per total (nuclear transformation) activity of Cs-137 (See Section 4.1.12)	1.0	unitless

Table 2-2. Public Protection DRL calculation default results.

Term	Value	Units	
Dose Rate DRL	1.98	mrem/hr	
Cs-137 Deposition DRL	3.31E2	μCi/m²	
Cs-137 Integrated Air DRL	1.10E5	μCi-s/m <sup>3</sup>	
Cs-137 Plume Inhalation DP	7.93E2	mrem	
Cs-137 Plume Submersion DP	10.4	mrem	
Cs-137 Resuspension Inhalation DP	4.42	mrem	
Cs-137 Groundshine DP	1.89E2	mrem	
Cs-137 Total DP	9.97E2	mrem	

#### 3. UNCERTAINTY QUANTIFICATION METHODS

# 3.1. Introduction to Uncertainty Quantification & Methods

The goal of this project is to develop and execute methods for characterizing uncertainty in data products that are developed and distributed by CM. In order to accomplish this goal, the concepts of error and uncertainty in the context of this project must first be defined. For the purposes of this project, the inherent error in a given measurement, or variation of a measurement from the exact value being measured, can also be termed as uncertainty in the fixed value of the measurement. Thus, for the purposes of this project, the terms error and uncertainty are used interchangeably and will be referred to as uncertainty throughout this chapter.

The development of data products employs mathematical models to calculate results related to the release of nuclear material in a given environment. These models are based on data and known physical principals, but cannot provide exact descriptions of all potential release scenarios due to limitations in the amount of data available, limitations in the level of understanding of processes following a release, and inherent randomness in physical parameters and processes. This means that the models employed are necessarily approximations of reality and their results contain a certain level of uncertainty.

The scope of this project seeks to identify the uncertainty in data products resulting from the uncertainties in model input parameters. The project does not seek to quantify model uncertainty; the same models that are currently available in Turbo FRMAC<sup>©</sup> and are employed for the scenario of interest are used for every simulation. The current practice for the calculation of quantities such as DRLs for data products is to use a set of constant default input parameter values. These input parameters, though supported by standard-practice, literature, and data, are inherently approximations. In addition, parameters and inputs derived from data collection during an event are uncertain due to a variety of factors including those related to the measurement device and methods, field contamination, etc.

A Monte Carlo analysis was used to characterize uncertainty in data products for the purposes of this project. Monte Carlo type analyses are often employed to characterize uncertainty in simulation results [4], [5]. The process of executing a Monte Carlo analysis is fairly straightforward [5]. First, the uncertainty in model inputs is characterized using probability distributions. These distributions are then sampled many times. A single deterministic simulation is run for each sample, propagating uncertainty through the model (Section 3.2). The final collection of simulation results is then analyzed to characterize overall uncertainty and contribution of each variable to the overall uncertainty (Section 3.3). The following sections describe each of these steps and how they have been implemented for this project in detail.

#### 3.2. Uncertainty Propagation

The first step in a Monte Carlo analysis is to define a probability distribution for each uncertain input. These distributions are selected based on published data and/or expert opinion and describe the uncertainty that might be expected for a given parameter. The basis for and selection of distributions for the uncertain inputs considered in this project is described in detail in Chapter 4. Following the selection of distributions, a sampling method must be selected and used to sample each of the input distributions. Sampling methods and the software used to implement these methods for the purposes of this project are described in Section 3.2.1. The sampled inputs

must be propagated through the model of interest, in this case Turbo FRMAC<sup>©</sup>, to produce a simulation result for each sample. The details of this propagation and its implementation are given in Section 3.2.2. Finally, Turbo FRMAC<sup>©</sup> was modified to read in sampled input values and run many simulations to generate outputs for each sample. These software updates are described in Section 3.2.3.

### 3.2.1. Sampling Methods & Software

The probability distributions selected for all uncertain inputs in a Monte Carlo analysis must be sampled a sufficient number of times in order to produce a collection of inputs that will be simulated using the model of interest. There are many methods that may be employed for sampling from these distributions [5]. Simple random sampling (SRS) is the most basic method for generating samples and simply involves taking a random sample from the distribution for each input [6]. Latin Hypercube Sampling (LHS) stratifies the distribution for each uncertain input, samples from each strata, and randomly combines the sample from the strata for each input with similar stratified samples from the remaining inputs [5], [6], [7], [8], [9], [10]. LHS is commonly used for obtaining result convergence with fewer samples and is most effectively applied in models that are computationally demanding. Because of these benefits, LHS was used for the purposes of this project.

The Dakota toolkit was selected as the sampling engine for this project and was used to generate samples using LHS from input distributions for each simulation [11]. The Dakota software was developed at Sandia National Laboratories (SNL) and provides an interface between simulation codes and iterative analysis methods. The uncertainty quantification package within Dakota is capable of sampling from distributions using many different methods, including LHS. The interface between the Dakota software and the simulation code Turbo FRMAC<sup>©</sup> is described in the following section.

# 3.2.2. Propagating Uncertainty in Turbo FRMAC®

Figure 3.2-1 shows a typical Turbo FRMAC<sup>©</sup> run with constant/fixed inputs. Each Turbo FRMAC<sup>©</sup> realization uses a single value for each input that is used to calculate the final result.

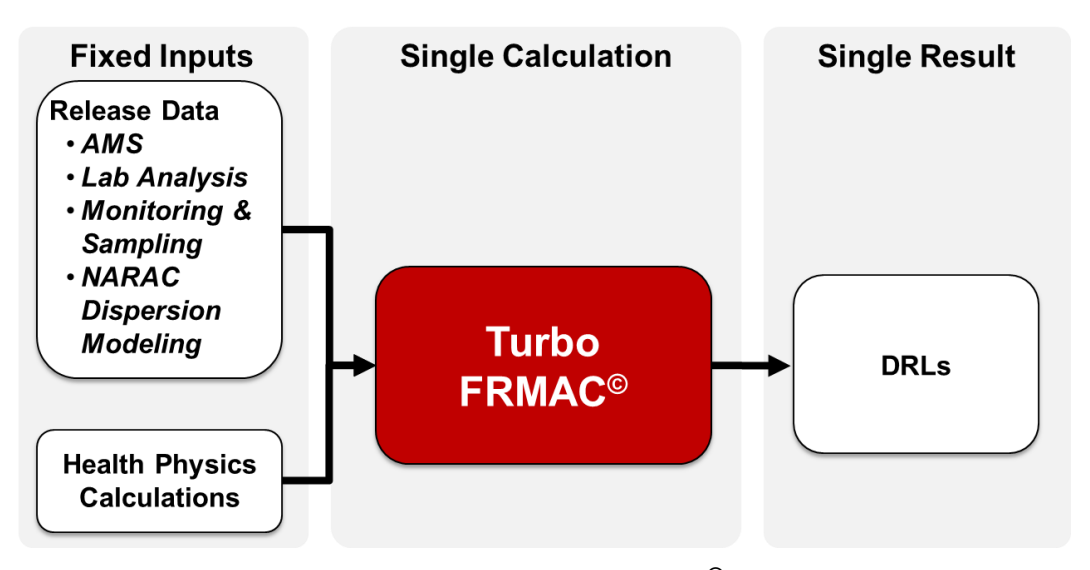


Figure 3.2-1. Typical Turbo FRMAC<sup>®</sup> simulation.

The application of Monte Carlo analysis techniques requires the process shown in Figure 3.2-1 to be executed many times using samples of input distributions defined for each of the inputs used to calculate the final result. This requires the development of a probabilistic framework that samples inputs, passes the inputs to the simulation code, and collects the results. This process is shown in Figure 3.2-2.

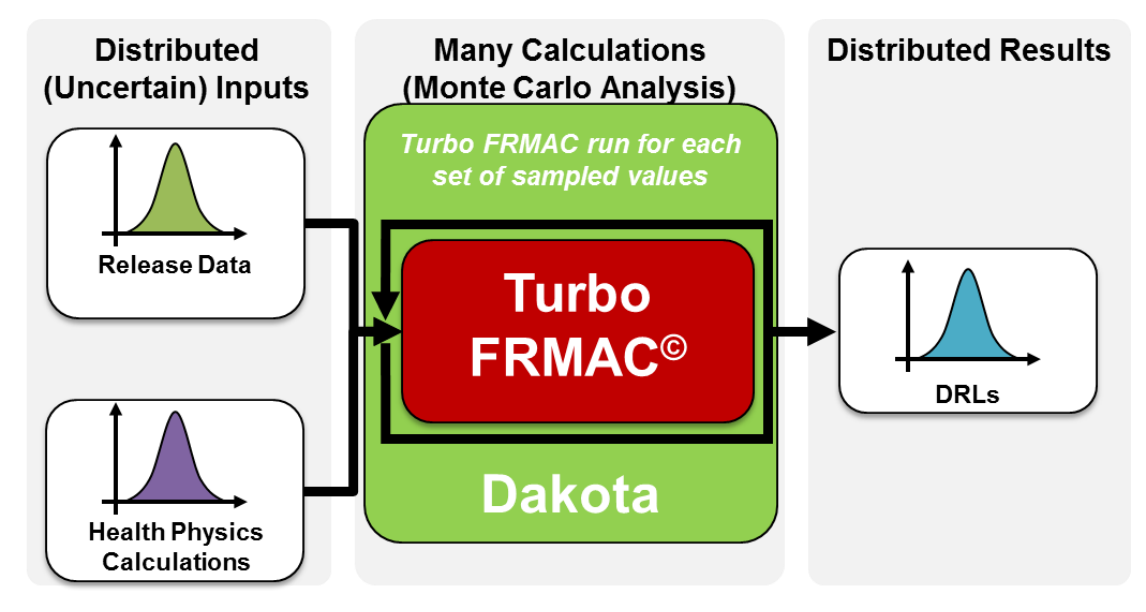


Figure 3.2-2. Turbo FRMAC<sup>©</sup> execution under probabilistic framework.

Although the Dakota toolkit is designed to be used as a wrapper code that runs a driver program, the program structure of Turbo FRMAC<sup>©</sup> did not easily lend itself to this implementation. Instead of running Dakota as a wrapper for a driver program, Dakota was run as a pre-processor to Turbo FRMAC<sup>©</sup>. In this step, Dakota samples the distributions for each of the inputs that will

be used to generate results for the study scenario and creates an input file. Turbo FRMAC<sup>©</sup> was modified to read in this input file and execute a realization for each sample. These updates are described in the following section.

# 3.2.3. Turbo FRMAC<sup>©</sup> Software Updates

The Dakota Error Analysis Tool was added to a development version of Turbo FRMAC<sup>©</sup>. This tool enables users to run batches of Public Protection DRL calculations from inputs specified in a structured data input file and sends the calculation results to a structured data output file that can then be used as input to other software and processes. To provide users with this capability, a simple user interface was developed that allows users to select an input file, choose a file location where the output will be saved, launch the calculations, monitor the progress of those calculations, and if needed, cancel the calculations. The user interface also alerts users to any errors that the software encounters during processing and notifies users when processing is complete. The Dakota Error Analysis Tool user interface is integrated into Turbo FRMAC<sup>©</sup> itself, making it accessible to users as a separate tool within Turbo FRMAC<sup>©</sup>.

To provide the batch processing of Public Protection DRL calculations, the Turbo FRMAC<sup>©</sup> software development team implemented methods to parse the calculation input distribution data from an input file, which would otherwise come from direct user input via the Turbo FRMAC<sup>©</sup> user interface. Methods were also developed to automatically instantiate new Turbo FRMAC<sup>©</sup> DRL calculations with a default radionuclide mixture and to configure those calculations with the parameters from the input files. The Dakota Error Analysis Tool was designed to automatically run the calculations, format the calculation results as structured data, and write that structured data to an output file with minimal user intervention.

The results of a Turbo FRMAC<sup>©</sup> execution under a run using the Dakota Error Analysis Tool provide a mapping from sampled inputs to simulation outputs. The uncertainty in these simulation outputs and the sensitivity of this uncertainty to uncertainty in simulation inputs can be characterized using the statistical methods described in Section 3.3.

# 3.3. Statistical Post-processing Methods

Following a probabilistic run of Turbo FRMAC<sup>©</sup> for a scenario of interest, the results must be analyzed to generate statistical information regarding result uncertainty and the sensitivity of this uncertainty to uncertainty in simulation inputs. A post-processing code was developed in the open-source statistical software "R" to accomplish this [12]. This code calculates summary statistics that describe the distributions of results and characterize the uncertainty in each output of interest, as is described in Section 0. This code also applies a linear rank regression analysis to the inputs and outputs of interest to determine and quantify the sensitivity of the uncertainty in the result outputs to the uncertainty in the simulation inputs, as is presented in Section 3.3.2. The examples presented in these sections are used to explain the applied statistical methods. Results presented in these sections will be presented in Chapter 5 along with additional explanations and analysis.

# 3.3.1. Uncertainty Analysis Methods & Results

The collection of results from a given Turbo FRMAC<sup>©</sup> representation for a single output of interest represents an estimate of the true distribution of this output. Thus, the simulation results represent an estimate of the uncertainty in this output, for example the Dose Rate DRL, given the uncertainty in the inputs. Uncertainty analysis results can be quantified by calculating percentiles of the output of interest over all of the samples for a simulation.

Calculating empirical quantiles is a straightforward process under the sampling scheme that was selected for this project. If the number of samples is equal to 100, then the 5<sup>th</sup>, 50<sup>th</sup>, and 95<sup>th</sup> percentiles are simply the 5<sup>th</sup>, 50<sup>th</sup>, and 95<sup>th</sup> largest values of the output of interest. This calculation can easily be scaled to various sample sizes. The mean is also calculated for each output of interest.

The uncertainty analysis results are presented for each simulation in tables that show these summary statistics along with the default value for the output that is calculated using a single simulation of Turbo FRMAC $^{\odot}$  with fixed, default values. This default value represents the normal operating defaults for Turbo FRMAC $^{\odot}$  for the scenario of interest before any uncertainty is applied to the inputs. An example of the display of uncertainty analysis results in this report is shown in Table 3.3-1 below.

Table 3.3-1. Example of DRL uncertainty results for Laboratory Analysis simulations.

Output Name	Default	Mean	5th	50th	95th
Dose Rate DRL [mrem/hr]	1.98	3.869	0.989	3.779	7.066
Cs-137 Deposition DRL [μCi/m²]	3.31E2	712.550	194.564	683.833	1342.506
Cs-137 Integrated Air DRL [μCi-s/m³]	1.10E5	75856.595	35836.703	68270.251	140970.833

This table is a replicate of Table 5.1-1. Section 5.1.1 provides an interpretation of these results in the context of the study scenario. The results in the uncertainty analysis results tables are shown out to three decimal places as this is the point at which some differences can be observed for simulations that have very similar results (Laboratory Analysis, In Situ Deposition, and AMS). While the precision of these results will be limited to fewer significant digits in practice, the inclusion of a larger number of digits allows for more insight into the comparison of results for the purposes of this report.

# 3.3.2. Sensitivity Analysis Methods & Results

The goal of sensitivity analysis is to characterize the relationship between the uncertainty in model inputs and the uncertainty in model outputs. Sensitivity analysis can be used to identify the amount of uncertainty in the outputs that can be attributed to each of the inputs for a probabilistic analysis. This allows the inputs that have the most significant impact on model results to be identified in a quantitative fashion. These inputs can then be targeted for future review if a reduction in output uncertainty is required.

The application of a sensitivity analysis begins with the selection of a regression model to quantify the relationship between simulation inputs and outputs. A linear rank regression model was selected for this project. The application of additional regression models to the results of this study, including models that explore additional complexities such as conjoint parameter interactions, is an area of future work. However, the sensitivity analysis results presented in this report show that the selected linear rank regression model was an appropriate choice for all outputs.

Linear rank regression is able to identify both linear and non-linear monotonic relationships between the input parameters and each output of interest [13]. Rank regression regresses upon the ranks or indices of the numerical inputs when they are sorted from smallest to largest. The numerical value of the input is replaced by its rank for use in the regression model. The model is fit to the rank of the input data using a stepwise process in which input parameters are added to and removed from the model as fitting iterates until a final solution is determined [14].

The quantitative metrics that are output from the application of a linear rank regression model provide information on model fit as well as the impact of individual inputs and the strength of their relationship with the output of interest. An example of these regression outputs is presented in Table 3.3-2 below. The R<sup>2</sup> for the model, shown in the first row of the table, quantifies the portion of the variance in the model response, i.e., Dose Rate DRL, that is captured by the linear rank regression model using the inputs sampled for the simulation. Generally, the closer that this R<sup>2</sup> value is to 1, the better the fit of the regression model. The "R<sup>2</sup> Individual" column in this table denotes the increase in the overall R<sup>2</sup> value as each input is added to the regression model. This value can be used to quantitatively assess how much of the variance in the model response can be attributed to each input individually. The sum of the "R<sup>2</sup> Individual" column is equivalent to the overall R<sup>2</sup> value that is given in the top row of each table. The standardized rank regression coefficient (SRRC) column represents the strength of the influence of each input and can be notionally interpreted as the slope of the line fitted to the ranks of each input and the output of interest. A positive SRRC value indicates that as an input increases, the output of interest also increases. Conversely, a negative SRRC value indicates that as an input decreases, the output of interest increases.

The rows of the tables used to present the sensitivity analysis results in this report are ordered in terms of variable importance to the outputs of interest with the most important variable appearing in the first row of each table. In this context, importance means that the variable has the strongest relationship with the output of interest and explains the greatest amount of output variance.

Table 3.3-2. Example of sensitivity analysis results for the Dose Rate DRL for Laboratory Analysis.

Dose Rate DRL, R <sup>2</sup> = 0.936					
Variable Name	R <sup>2</sup> Individual	SRRC			
Deposition Velocity	0.574	0.758			
Inhalation Dose Coefficient Multiplier	0.186	-0.429			
Breathing Rate, Light Exercise, Adult Male	0.063	-0.249			
Deposition External Dose Coefficient Multiplier	0.061	0.249			
Weathering Coefficient Multiplier	0.037	0.192			
Ground Roughness Factor	0.011	0.105			
Resuspension Coefficient Multiplier	0.004	-0.062			
Activity per Area	0.000	0.000			
Plume External Dose Coefficient Multiplier	0.000	0.000			
Breathing Rate, Activity Averaged, Adult Male	0.000	-0.010			

Table 3.3-2 is a replicate of Table 5.1-3. Section 5.1.2 provides an interpretation of these results in the context of the study scenario.

The equations for the four pathway DP results do not include some of the uncertain input variables that were used for each simulation. However, these inputs were included in the regression model to ensure a complete coverage of the uncertain input space. Inputs that are not included in result equations are shown in italics in the sensitivity analysis result tables for these DP outputs.

Scatter plots are often used to corroborate the results of sensitivity analyses. These plots can be used to confirm that the relationships between inputs and outputs are correctly quantified by the selected regression model. They can also be used to identify areas of the input space that may have been under-sampled and could be targeted for additional analysis. Examples of scatter plots for the first four important variables given in Table 3.3-2 are shown in Figure 3.3-1 below.

The scatter plot in the upper left of Figure 3.3-1 shows that deposition velocity has a strong, positive relationship with the Dose Rate DRL. The inhalation dose coefficient multiplier in the upper right is shown to have a slightly less strong, negative relationship with the Dose Rate DRL. The remaining two inputs shown in the bottom of the figure have relatively slight relationships with the Dose Rate DRL. These scatter plots therefore confirm the quantitative results shown in Table 3.3-2. Scatter plots like these are shown for each presentation of sensitivity analysis results in Chapter 5.

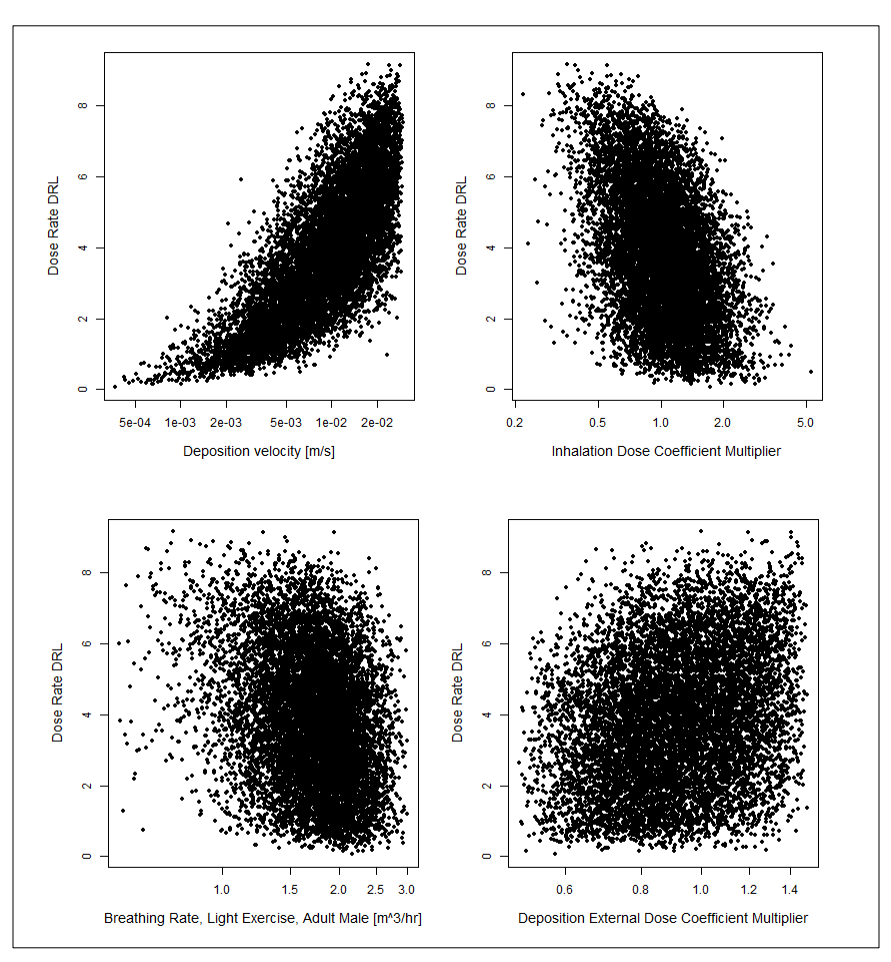


Figure 3.3-1. Example of scatter plots for the Dose Rate DRL for Laboratory Analysis and the first four inputs shown in Table 3.3-2.

Figure 3.3-1 is a replicate of Figure 5.1-9. Section 5.1.2 provides an interpretation of these results in the context of the study scenario.

# 3.3.3. Sampling Confidence Intervals (CIs)

The finite number of samples used to characterize the uncertainty in data products for the purposes of this report must also be taken into consideration; the characterization of uncertainty could only be exact if an infinite number of samples were used. Thus, the sampling uncertainty, or uncertainty due to a finite sample size, must be quantified to determine whether results can be considered to be stable or whether additional samples are needed to provide a precise estimate of uncertainty. A nonparametric bootstrap approach was used to quantify sampling uncertainty about the mean for each of the outputs under consideration in this analysis. The application of this method to the mean of each of the outputs is a 95% sampling confidence interval (CI) that can be interpreted as follows: 'there is a 95% confidence that the true mean falls in this interval.' The width of this CI can be used to determine whether more samples are needed to adequately capture the mean.

The use of the bootstrap procedure is a common method for providing estimates of sampling uncertainty [15]. For example, consider a set of observed data of size n. In the context of this report, this means that Turbo FRMAC<sup>©</sup> is run n times to produce a value for each output of interest. The steps taken to calculate the sampling CI are given as follows:

- 1. Take a random sample with replacement of size *n* from your observed data set. Sampling with replacement means that after a sample is taken from the original observed data set, it is replaced such that it could be sampled again.
- 2. Use the new sample to estimate the mean of the output of interest.
- 3. Repeat steps 1-2 many times to generate a set of estimates for the mean of the output of interest. The number of times that these steps are repeated depends upon how precise the CIs need to be. For the purposes of this report, a bootstrap sample size of 1000 was used.
- 4. Use the set of estimates of the mean to calculate sampling CIs about the mean. The percentile method was used to construct the sampling CIs in this report [15]. The lower bound of the 95% CI is then given by the 2.5<sup>th</sup> percentile of the distribution of the mean given by the set of bootstrap estimates. The upper bound of the 95% CI is the 97.5<sup>th</sup> percentile of the same distribution.

Sampling CIs were calculated for each output of interest following a probabilistic simulation completed for each activity source. The resulting CIs for this analysis are tabulated in Section 5, Probabilistic Analysis Results.

#### 4. SOURCES OF UNCERTAINTY & INPUT DISTRIBUTIONS

The following sections describe the probability distributions defined for the sources of error and uncertainty identified in each portion of the CM analysis process. Calculation inputs that contribute to uncertainty in the health physics calculations of Public Protection DRLs are described and assigned probability distributions in Section 4.1. Probability distributions for sources of uncertainty in data collection are given in Section 4.2. The distributions developed to characterize possible sources of uncertainty in NARAC atmospheric dispersion predictions are given in Section 4.3.

# 4.1. Public Protection DRL Input Distributions

In determining the distributions for the Public Protection DRL inputs, the original reference for each input was examined for uncertainty information. Additional references were used when the original references did not provide the needed uncertainty information. The RESRAD probabilistic analyses and U.S. Nuclear Regulatory Commission (NRC) State-of-the-Art Reactor Consequence Analysis (SOARCA) uncertainty analyses were also examined as potential sources of uncertainty information because those analyses have many inputs that are the same as or similar to those used in the FRMAC Assessment methods.

For details on the inputs described in the following sections, refer to Method 1.1 in the FRMAC Assessment Manual, Vol. 1 [3].

# 4.1.1. Deposition or Integrated Air Activity

Sections 4.2 and 4.3 include uncertainty information for deposition (also referred to as "activity per area") and integrated air activity, respectively. In a typical response, mixture information is initially provided by atmospheric modeling (NARAC) and eventually informed by field and laboratory measurements. For purposes of this analysis, mixtures and associated uncertainties from NARAC, in situ deposition measurements, AMS measurements, and laboratory analysis were treated as separate mixture inputs.

## 4.1.2. Deposition Velocity

Deposition velocity is the rate at which airborne material is deposited onto the ground. Turbo FRMAC<sup>©</sup> uses deposition velocity to convert between integrated air activity and activity per area. All deposition is assumed to be dry particulates. Wet deposition is not considered in FRMAC Assessment methods.

The FRMAC default deposition velocity for particulates is 0.3 cm/s. NUREG/CR-4551 Vol. 2 Rev. 1 Part 7 [16] provides a deposition velocity uncertainty for the NRC assessment of risks from severe accidents for five U.S. nuclear power plants (NUREG-1150 [17]). The recommended dry deposition velocity range was 0.03 cm/s to 3.0 cm/s with a most likely value of 0.3 cm/s, in agreement with the FRMAC default. The range accounts for uncertainty in particle diameter, wind speed, atmospheric stability, surface roughness, and aerosol density, and is intended to be applicable for a residential suburb (i.e., roads, lawns, and trees). A triangular distribution with this range and a mode of 0.3 cm/s was used for this analysis. This distribution is shown in Figure 4.1-1.

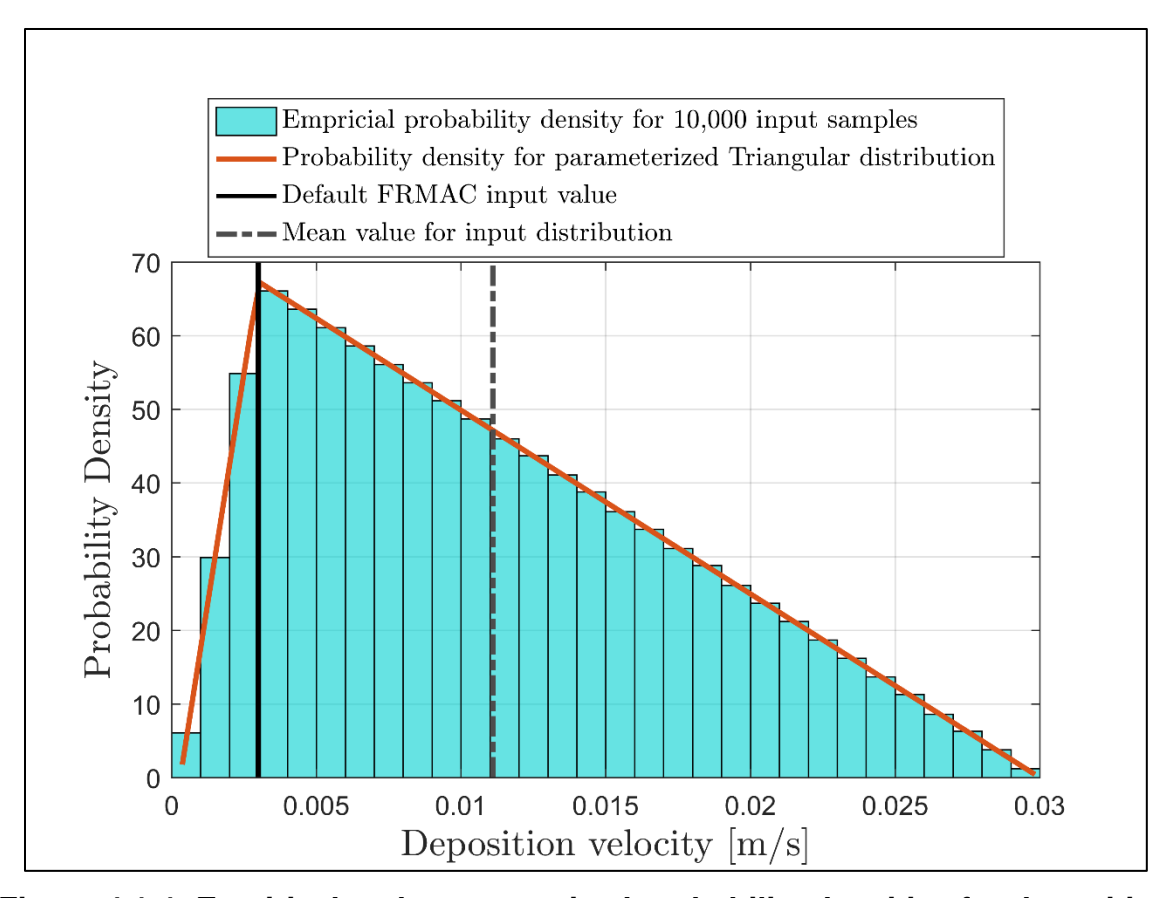


Figure 4.1-1. Empirical and parameterized probability densities for deposition velocity.

# 4.1.3. Breathing Rates

This initial analysis is limited to the Adult Whole Body age group and organ (FRMAC default assumption) and thus concerns adult, activity-specific breathing rates and activity times. The activity-specific breathing rates shown in Table 4.1-1 are from ICRP 66 Table B.15 [18]. A light-exercise breathing rate of 1.5 m³/hr is used for in-plume inhalation. An activity-averaged breathing rate of 0.92 m³/hr is used for inhalation of resuspended material. The activity times used to calculate activity-averaged breathing rate are shown in Table 4.1-1.

Table 4.1-1. FRMAC Assessment default activity times and activity-specific breathing rates for adult male.

Activity	Time (hr)	Breathing Rate (m³/hr)
Sleeping	8.50	0.45
Sitting	5.50	0.54
Light Exercise	9.75	1.50
Heavy Exercise	0.25	3.00
Total	24	

For this analysis, a distribution was needed for the light-exercise breathing rate by itself, and for either each activity-specific breathing rate or the overall activity-averaged breathing rate. The time budgeted for each activity was assumed to be fixed and not assigned an uncertainty.

The discrete values for respiratory frequency, tidal volume, and minute ventilation provided in ICRP 66, Table B.15 as a function of age, gender, and activity level do not include any information about associated error and it is difficult to determine the exact source of these values in the provided references. ICRP 66 does provide transformations for exercise that relate vital capacity to tidal volume at a respiratory frequency of 30 min<sup>-1</sup> and at maximal value. It also includes relationships between tidal volume at a respiratory frequency of 30 min<sup>-1</sup> and minute ventilation (i.e., breathing rate). This analysis of FRMAC methods needs to be able to distinguish between light and heavy exercise, and the relationships based on a fixed respiratory frequency of 30 min<sup>-1</sup> given in ICRP 66 do not allow for this distinction.

# 4.1.3.1. Activity-Averaged Breathing Rate

The developers of RESRAD provide triangular distributions for "residential" and "building occupancy" inhalation rates [19]. These distributions account for variation in activity level, gender, and age. The RESRAD approach was used to develop the overall activity-averaged breathing rate for this analysis, rather than applying distributions to each activity-specific breathing rate. For example, the RESRAD residential breathing rate distribution uses an activity-averaged breathing rate of 23 m³/d (0.96 m³/hr) as the mode, a sedentary breathing rate of 0.5 m³/hr as the minimum, and a moderate activity breathing rate of 1.5 m³/hr as the maximum. An activity-averaged breathing rate distribution similar to the RESRAD residential breathing rate distribution was developed for this analysis using the FRMAC default activity-specific breathing rates for sitting (0.54 m³/hr) as the minimum, light exercise (1.5 m³/hr) as the maximum, and the default activity-averaged breathing rate (0.92 m³/hr) as the mode. The distribution for activity-averaged breathing rate is shown in Figure 4.1-2.

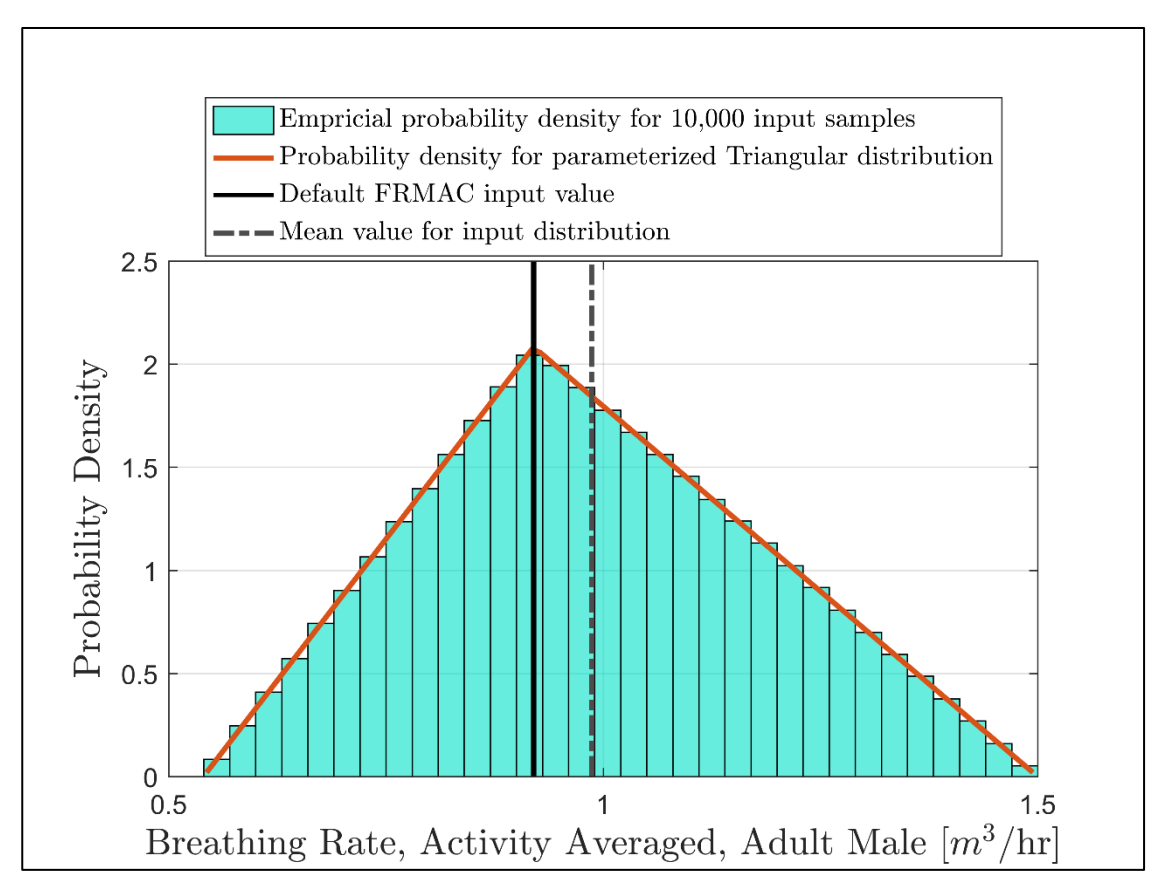


Figure 4.1-2. Empirical and parameterized probability densities for breathing rate, activity averaged, adult male.

#### 4.1.3.2. Light-Exercise Breathing Rate

The 2011 EPA Exposure Factors Handbook (EFH) [20] contains descriptive statistics on short-term gender-, age-, and activity-specific inhalation rates. This information was used to develop a distribution for the light-exercise breathing rate for this analysis. Table 6-17 of the EFH provides information for males performing "moderate intensity" activities, specifically. The "moderate intensity" activity level was used for this analysis because it is most comparable to the FRMAC default light-exercise breathing rate. The "21 to <30" age group was selected for this analysis because the  $BR_{LE}$  of 1.5 m<sup>3</sup>/hr used by default by FRMAC is cited as for a 30-year old male in Table B.15 of ICRP 66.

Table 6-17 of the EFH gives the mean and quantiles for the desired light-exercise breathing rate distribution, hereafter referred to as the empirical light-exercise breathing rate distribution. A truncated normal distribution was fit to this empirical distribution. This normal distribution uses the mean of 2.92E-2 m³/min (1.75 m³/hr) provided for the empirical distribution of the light-exercise breathing rate. The standard deviation (SD) for this distribution was calculated to minimize the root mean square error (RMSE) of the hypothesized normal distribution compared to the empirical distribution for the input, resulting in an SD value of 7.00E-3 m³/min (0.42 m³/hr). A Kolmogorov-Smirnov test was used to confirm that this distribution and its fitted

parameters are appropriate for the light-exercise breathing rate. The minimum of the truncated normal light-exercise breathing rate distribution is 9E-3 m³/min (0.54 m³/hr), the default FRMAC value for Adult Male sitting breathing rate, while the maximum is 5E-2 m³/min (3.0 m³/hr), the default FRMAC value for Adult Male heavy-exercise breathing rate. The distribution for the light-exercise breathing rate is shown in Figure 4.1-3.

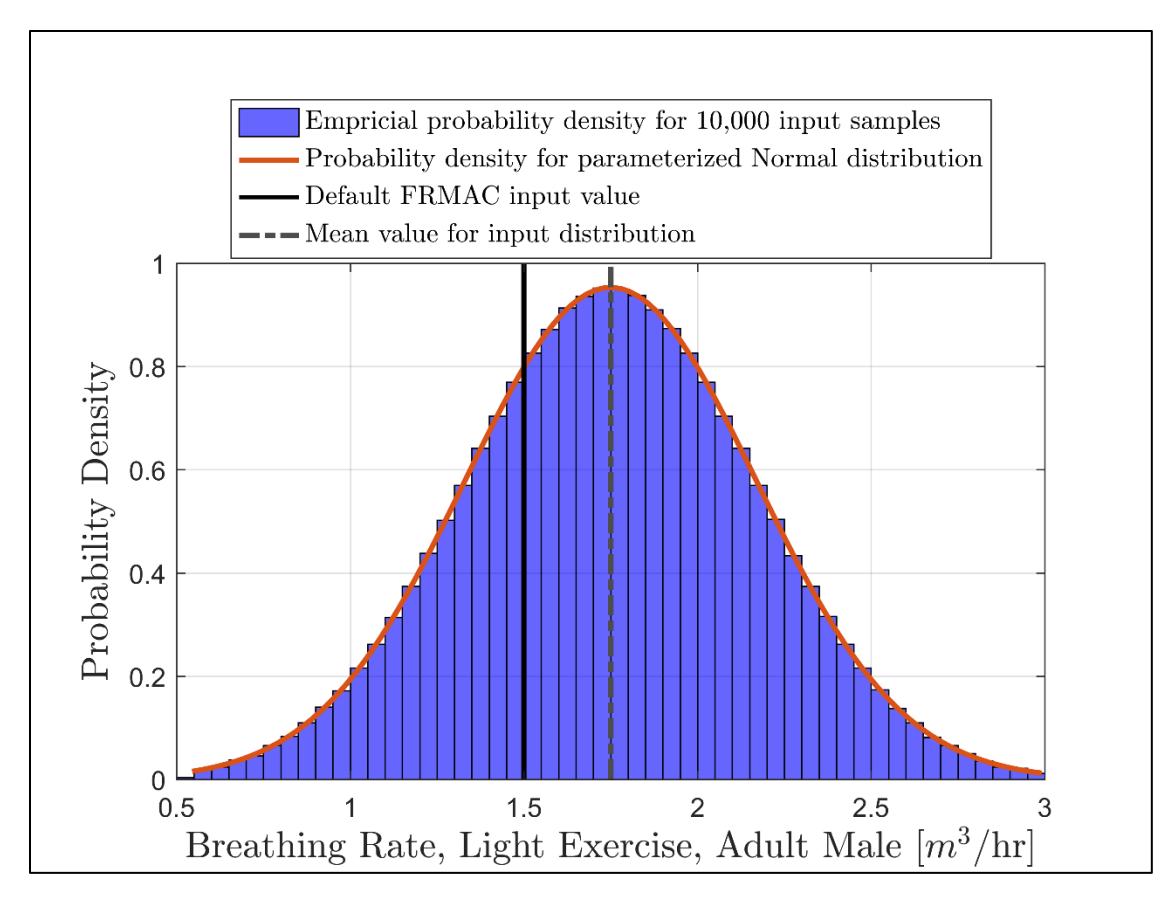


Figure 4.1-3. Empirical and parameterized probability densities for breathing rate, light exercise, adult male.

# 4.1.4. Deposition External Dose Coefficient

Keith Eckerman, Ph.D. of Oak Ridge National Laboratory recommends a multiplicative uncertainty for ground plane dose rate coefficients for all radionuclides and organs [21]. This multiplier is given a triangular distribution with a mode of 0.8, minimum of 0.5, and maximum of 1.5. This distribution is used by the NRC in their SOARCA uncertainty analyses [22]. The distribution for this parameter is shown in Figure 4.1-4.

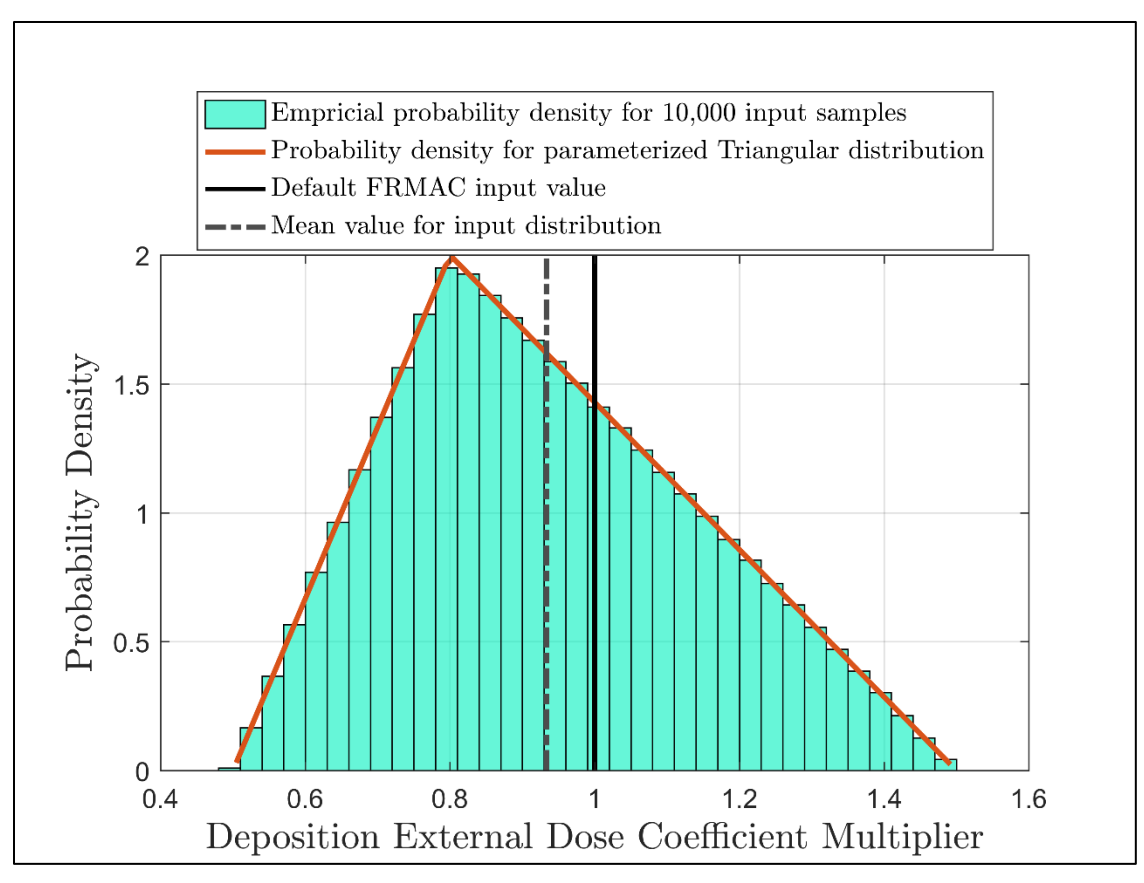


Figure 4.1-4. Empirical and parameterized probability densities for the deposition external dose coefficient multiplier.

# 4.1.5. Ground Roughness Factor

The deposition external dose coefficients used by FRMAC were calculated under the assumption that the radionuclides are deposited on an infinite flat plane. A ground roughness factor is used to account for the fact that this assumption is an approximation of reality. The default ground roughness factor used in FRMAC Assessment calculations is 0.82. This value is taken from Anspaugh et al. as specified in the equation for weathering [23]. A reference from the Anspaugh document by Likhtarev et al. states that "the initial migration or soil-roughness effect is taken into account by the factor 0.82 (which is the ratio of external gamma-exposure rate (EGER) in air due to Cs-137 source with a relaxation depth of 1 mm to that from an infinite plane source)" [24]. No uncertainty information is given in the Likhtarev document for this value.

Likhtarev cites Beck [25] for its cesium EGER ( $g_s$ ) values: "Because only dry deposition occurred in Ukraine during April-May 1986, for all radionuclides except cesium values of  $g_s$  were used that are appropriate for an initial migration into soil that can be described by an exponential decrease in concentration with depth with a relaxation depth of 1 mm and a soil density of 1.6 g/cm<sup>3</sup>." This depth corresponds to a relaxation length of 0.16 g/cm<sup>2</sup>. Using the tables in Beck, this corresponds to a  $g_s$  ratio of 0.16 g/cm<sup>2</sup> to "plane" of 0.87. Beck estimates that "the majority of the conversion factors given...are accurate to  $\pm 5$ -10% for locations meeting the

criteria of uniform deposition over an approximately 10-meter radius from the point of measurement for reasonably flat soil surfaces." In summary, uncertainty in the ground roughness factor is most likely driven by uncertainty in transport calculations and laboratory and field measurements. An uncertainty of 10% is assumed for purposes of this analysis. The distribution has a maximum of 1. A distribution type is not specified by Beck, so a normal distribution is assumed for this analysis. The distribution for this parameter is shown in Figure 4.1-5.

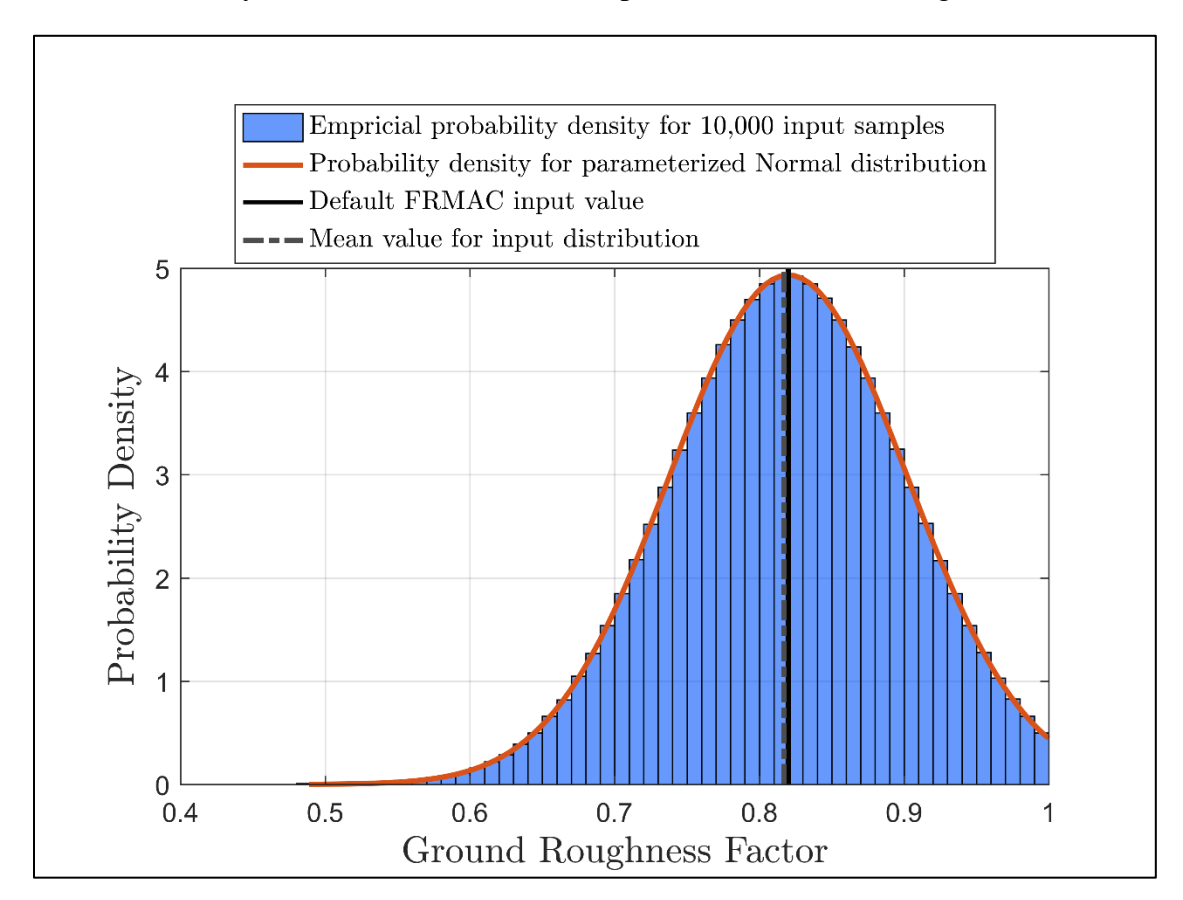


Figure 4.1-5. Empirical and parameterized probability densities for the ground roughness factor.

The MELCOR Accident Consequence Code System (MACCS) used for SOARCA includes a variable called "GSHFAC" which is a groundshine shielding factor [26]. GSHFAC is "a multiplier on the value of groundshine dose that would have been received if the person were standing outside and the ground were a perfectly flat surface. A value of 0 indicates complete shielding from groundshine; a value of 1 indicates no protection." The SOARCA Sequoyah uncertainty analysis [22] provides a distribution for GSHFAC which is combined with GSDE, "a dimensionless scaling factor used to account for the amount of ionizing radiation energy deposited within various human organs from external radiation emanating from the ground." The GSDE used for the SOARCA Sequoyah uncertainty analysis is the multiplicative uncertainty provided by Eckerman for ground plane dose rate coefficients (see Section 4.1.4).

The distribution for GSHFAC accounts for uncertainties due to "indoor residence time, household shielding value, and departures from the infinite flat plane." The default FRMAC

assumption for the receptor is that they are outside in the contaminated area continuously during the time phase under consideration without any protective measures (e.g., shielding or respiratory protection). Therefore, it is not appropriate to apply the GSHFAC distribution to the ground roughness factor.

#### 4.1.6. Inhalation Dose Coefficient

Eckerman recommends lognormal distributions for radionuclide- and organ-specific inhalation dose coefficients [21]. For Cs-137 Type F (ICRP Recommended lung clearance type), a geometric standard deviation (GSD) of 1.50 is given for leukemia, bone, breast, thyroid, liver, colon, and residual. A GSD of 1.55 is given for lung. This distribution (truncated lognormal using 90% CI as upper and lower values) was used for the SOARCA uncertainty analyses. An effective dose coefficient was not included in SOARCA because MACCS was used to calculate dose to the specific organs (cancer sites) previously listed. In a conversation with Eckerman on March 20, 2017, he recommended using a GSD of 1.50 for the Cs-137 effective dose coefficient.

Turbo FRMAC<sup>©</sup> assigns dose coefficients to radionuclides by calling them from a dose coefficient library rather than by direct user input. Instead of replacing the dose coefficient in the software with a sampled value for every realization, a dose coefficient multiplier was used to apply dose coefficient uncertainty. The inhalation dose coefficient uncertainty multiplier was assigned a lognormal distribution with a geometric mean (GM) of 1 and GSD of 1.50. The distribution for the inhalation dose coefficient uncertainty multiplier is shown in Figure 4.1-6.

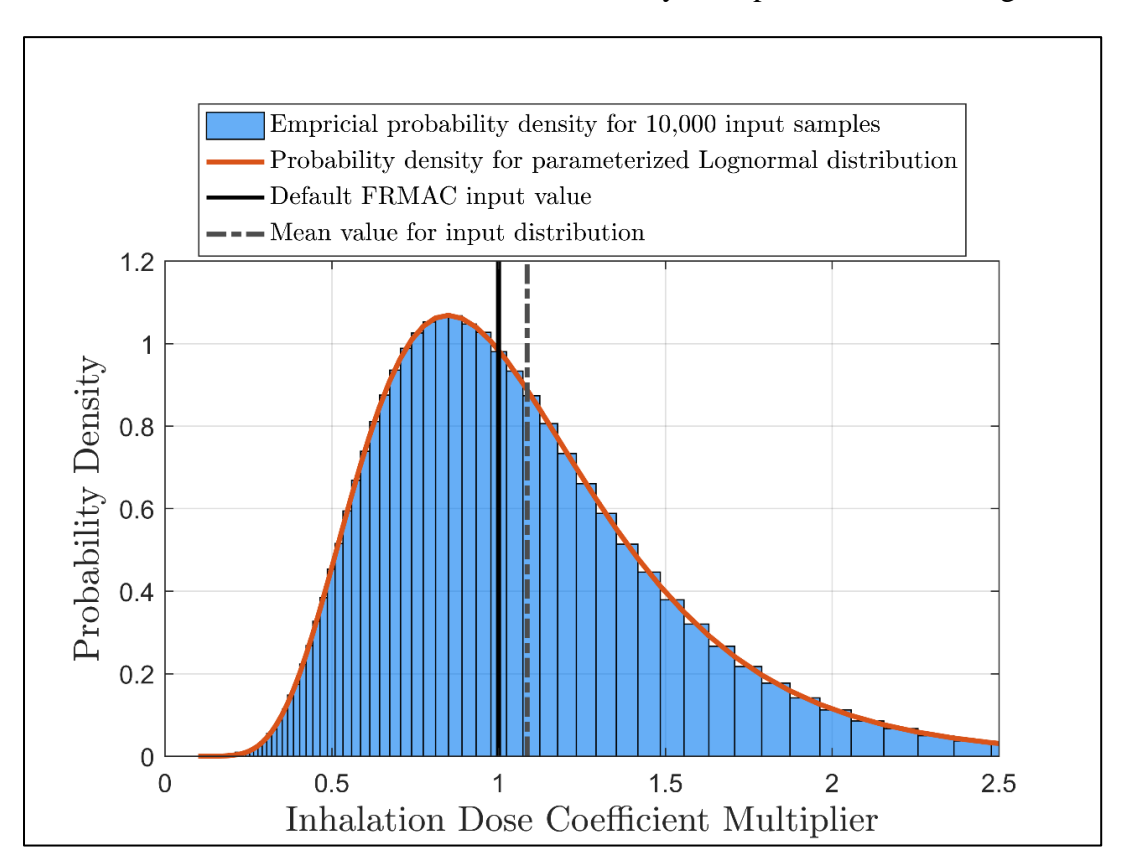


Figure 4.1-6. Empirical and parameterized probability densities for the inhalation dose coefficient multiplier.

# 4.1.7. Resuspension Factor

The resuspension factor used by FRMAC comes from Maxwell and Anspaugh [27]. Maxwell and Anspaugh provide an uncertainty estimate of  $4.2^{\pm 1}$ , to be interpreted as a GSD. The GSD is to be applied to the entire resuspension factor, K, as shown in Equation (1) below:

$$K_t = \left[10^{-5} \exp(-0.07t) + 7 \times 10^{-9} \exp(-0.002t) + 10^{-9}\right] \times 4.2^{\pm 1}$$
 (1)

#### 4.1.7.1. Resuspension Coefficient Uncertainty Multiplier

The resuspension factor is integrated over a given time phase along with radioactive decay and in-growth to calculate a resuspension parameter, which is ultimately used to calculate the Resuspension Inhalation DP. Uncertainty was applied to the calculated resuspension parameter by multiplying the resuspension coefficients used in Turbo FRMAC<sup>©</sup> to calculate the resuspension parameter by an uncertainty multiplier constant. This multiplier was sampled using Dakota and applied to three resuspension coefficients using the Python executable described in this section.

The resuspension parameter, *KP*, is calculated without uncertainty using Equation (2) (Eq. 1 and Eq. 2 of Section F2.1 of FRMAC Assessment Manual, Vol. 1 [3]):

$$KP_{i,TP} = \int_{t_1}^{t_2} \left[ (r_1 * e^{-8.1E - 07*t} + r_2 * e^{-2.31E - 08*t} + r_3) * Dp_{i,t} \right] dt$$
 (2)

where  $r_1 = 1 \times 10^{-5}$ ,  $r_2 = 7 \times 10^{-9}$ , and  $r_3 = 1 \times 10^{-9}$  are the resuspension coefficients used by default in this calculation.

Ideally, the application of uncertainty to the resuspension parameter would occur after this parameter is calculated. However, this is not practical to implement in the Turbo FRMAC<sup>©</sup> software. Instead, the uncertainty multiplier constant,  $u_1$ , was applied to each of the resuspension coefficients given in the equation above. Mathematically, this is the same as applying the uncertainty multiplier constant to resuspension parameter after it is calculated, as shown in Equation (3):

$$u_{1} * KP_{i,TP} = u_{1} * \int_{t_{1}}^{t_{2}} [(r_{1} * e^{-8.1E-07*t} + r_{2} * e^{-2.31E-08*t} + r_{3}) * Dp_{i,t}]dt$$

$$= \int_{t_{1}}^{t_{2}} u_{1} * [(r_{1} * e^{-8.1E-07*t} + r_{2} * e^{-2.31E-08*t} + r_{3}) * Dp_{i,t}]dt$$

$$= \int_{t_{1}}^{t_{2}} [(u_{1} * r_{1} * e^{-8.1E-07*t} + u_{1} * r_{2} * e^{-2.31E-08*t} + u_{1} * r_{3}) * Dp_{i,t}]dt$$

$$(3)$$

The uncertainty multiplier constant  $u_1$  is constant for each calculation of the resuspension parameter as shown in the equation above. However, this multiplier is sampled from a distribution for each Turbo FRMAC<sup>©</sup> realization, allowing uncertainty to be applied to the resuspension parameter.

### 4.1.7.2. Resuspension Coefficient Multiplier Distribution

The distribution for the resuspension coefficient uncertainty multiplier is shown in Figure 4.1-7.

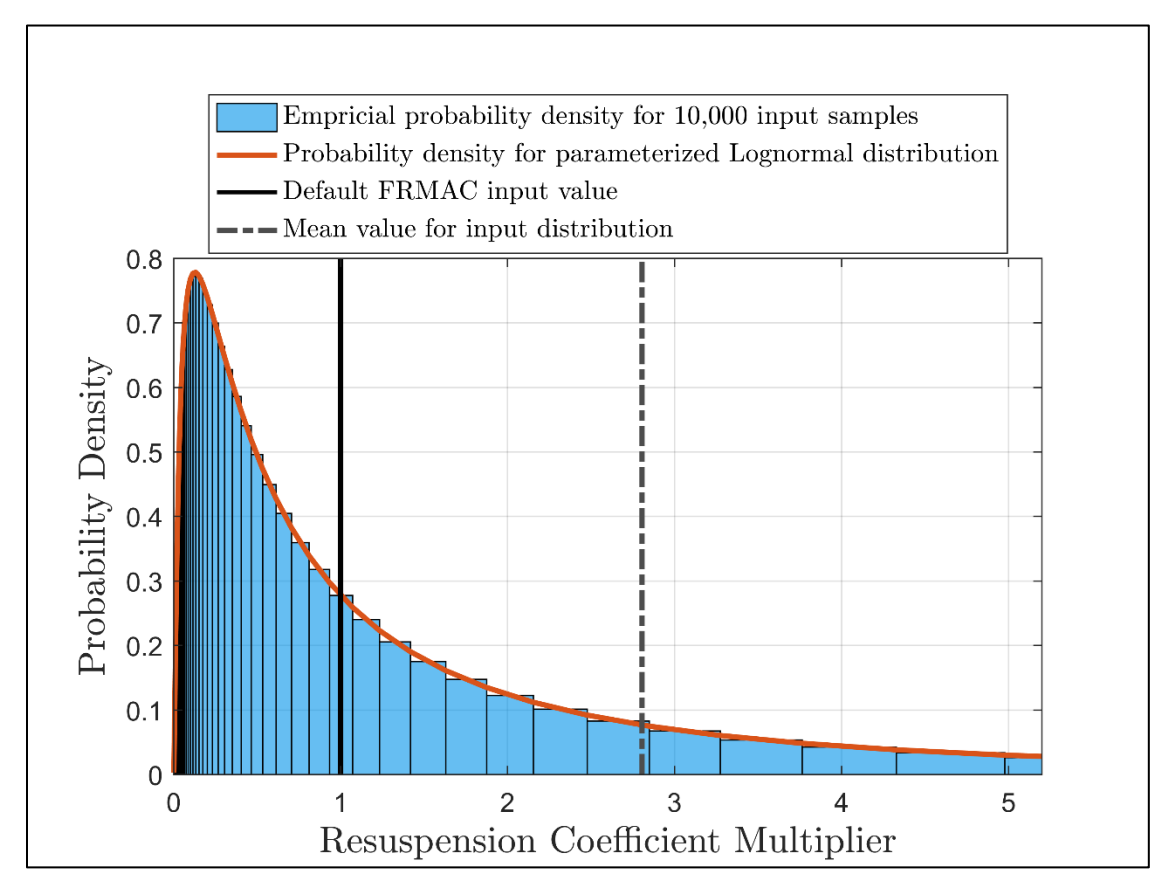


Figure 4.1-7. Empirical and parameterized probability densities for the resuspension coefficient multiplier.

#### 4.1.8. Protective Action Guide

There is no uncertainty associated with a PAG, so it was not sampled from a distribution.

#### 4.1.9. Plume External Dose Coefficient

Eckerman does not provide uncertainty information for plume external dose coefficients because the document was written in support of the SOARCA uncertainty analyses, in which "the dominant route of exposure...is exposure to contaminated ground surfaces" [21]. The Sequoyah SOARCA uncertainty analysis itself states that "cloudshine uncertainty is not treated because it is a relatively unimportant dose pathway compared with groundshine and inhalation" [22]. In a conversation on March 20, 2017, Eckerman recommended using the uncertainty for ground plane dose rate coefficients (described in Section 4.1.4) for the plume submersion dose coefficients.

The plume external dose coefficient uncertainty is applied in Turbo FRMAC<sup>©</sup> by using a multiplier. The distribution for the plume external dose coefficient uncertainty multiplier is shown in Figure 4.1-8.

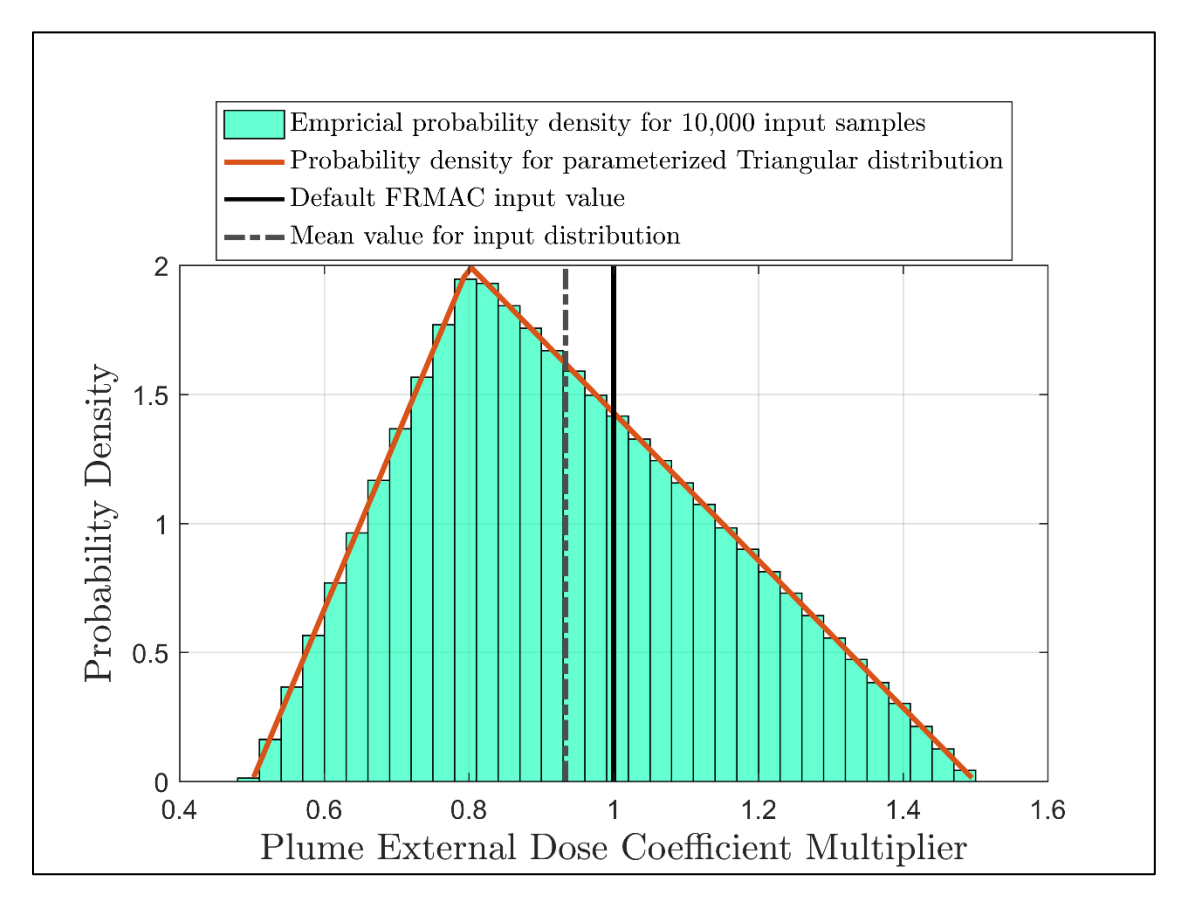


Figure 4.1-8. Empirical and parameterized probability densities for the plume external dose coefficient multiplier.

## 4.1.10. Exposure to Dose Conversion Factor

FRMAC Assessment uses a chronic exposure to dose conversion factor of 1 as a measure of conservativism. This value was assumed to be fixed for this uncertainty analysis.

## 4.1.11. Weathering Factor

The weathering factor used by FRMAC comes from Anspaugh et al. [23]. No uncertainty information is given for this equation by Anspaugh.

Golikov et al. [28] used a lognormal fit for weathering in their study of external exposure in areas contaminated by the Chernobyl accident. The average of the time-dependent GSDs associated with the fit was 1.2. This GSD and a lognormal distribution was used for weathering in this analysis given a lack of uncertainty information in the Anspaugh paper.

#### 4.1.11.1. Weathering Coefficient Uncertainty Multiplier

The weathering factor is integrated over a given time phase along with radioactive decay and ingrowth to calculate a weathering parameter, which is ultimately used to calculate the Groundshine DP. Uncertainty was also applied to the weathering parameter by multiplying the weathering coefficients used in Turbo FRMAC<sup>©</sup> to calculate the weathering parameter by an uncertainty multiplier constant, similar to what was done for the resuspension parameter. Again, this multiplier was sampled using Dakota and applied to the two weathering coefficients using the Python executable described in this section.

The weathering parameter, WP, is calculated without uncertainty using Equation (4) (Eq. 4 and Eq. 5 of Section F2.2 of FRMAC Assessment Manual, Vol. 1 [3]):

$$WP = \int_{t_1}^{t_2} \left[ (w_1 * e^{-1.46E - 08t} + w_2 * e^{-4.44E - 10t}) * Dp_{i,t} \right] dt$$
 (4)

where  $w_1 = 0.4$  and  $w_2 = 0.6$  are the weathering coefficients used by default in this calculation.

As described for the resuspension parameter, the application of uncertainty to the weathering parameter would ideally occur after this parameter is calculated but this is not practical to implement in Turbo FRMAC<sup>©</sup>. An uncertainty multiplier,  $u_2$ , is applied to each of the weathering coefficients given in the equation above to apply uncertainty to the weathering parameter under this implementation constraint. Mathematically, this is the same as applying the uncertainty multiplier constant to the weathering parameter after it is calculated, as shown in Equation (5):

$$u_{2} * WP = u_{2} * \int_{t_{1}}^{t_{2}} \left[ (w_{1} * e^{-1.46E - 08t} + w_{2} * e^{-4.44E - 10t}) * Dp_{i,t} \right] dt$$

$$= \int_{t_{1}}^{t_{2}} u_{2} * \left[ (w_{1} * e^{-1.46E - 08t} + w_{2} * e^{-4.44E - 10t}) * Dp_{i,t} \right] dt$$

$$= \int_{t_{1}}^{t_{2}} \left[ (u_{2} * w_{1} * e^{-1.46E - 08t} + u_{2} * w_{2} * e^{-4.44E - 10t}) * Dp_{i,t} \right] dt$$
(5)

Note that the weathering coefficients  $w_1$  and  $w_2$  still sum to one as required. The application of the uncertainty multiplier  $u_2$  applies uncertainty to the weathering parameter WP using the coefficients but does not change the meaning of the coefficients as shown in Equation (5).

The uncertainty multiplier constant  $u_2$  is constant for each calculation of the weathering parameter as shown in the equation above. However, this multiplier is sampled from a distribution for each Turbo FRMAC<sup>©</sup> realization, allowing uncertainty to be applied to the weathering parameter.

# 4.1.11.2. Weathering Coefficient Uncertainty Multiplier Distribution

The distribution for the weathering coefficient uncertainty multiplier is shown in Figure 4.1-9.

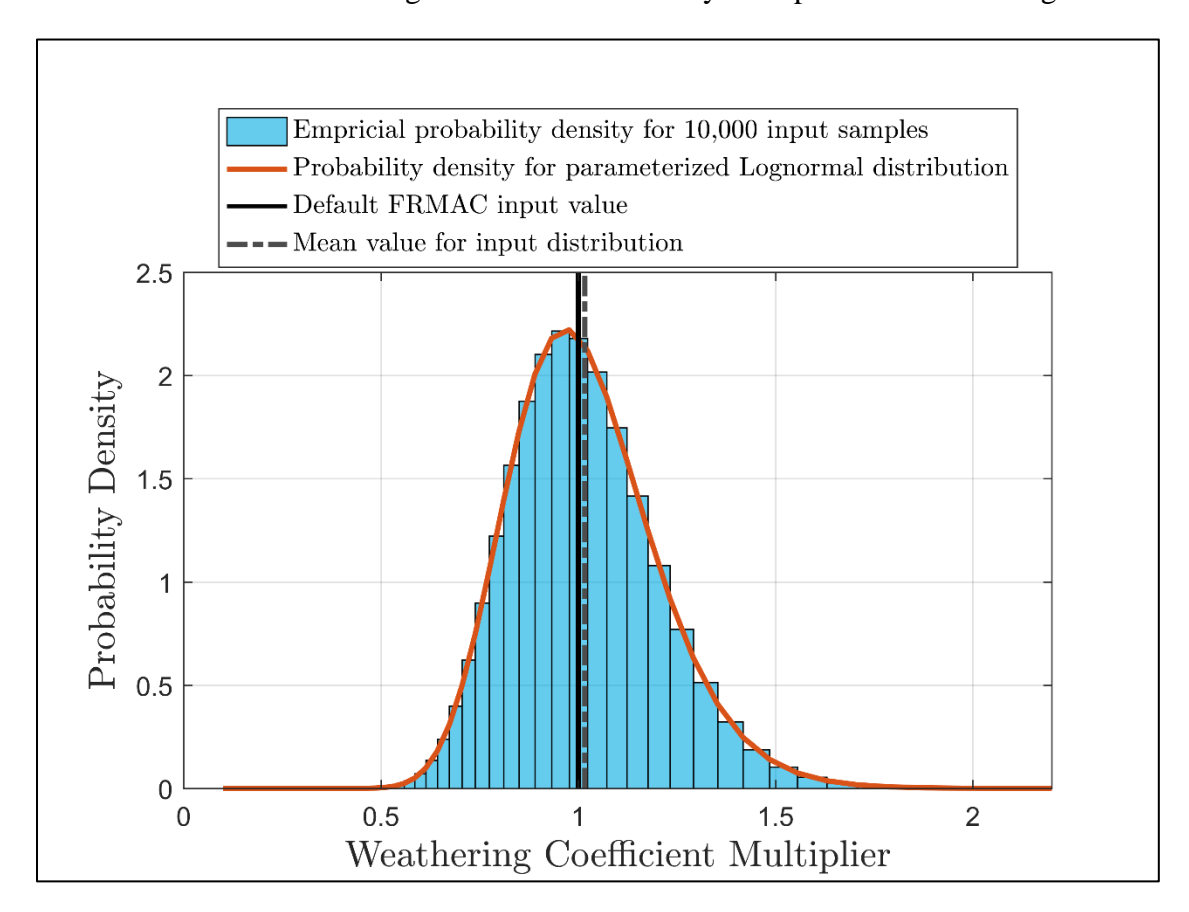


Figure 4.1-9. Empirical and parameterized probability densities for the weathering coefficient multiplier.

### 4.1.12. Yield

Alpha and beta yields were assumed to be well-characterized radioactive decay data with no associated uncertainty.

# 4.2. Data Collection Sources of Uncertainty

The health physics dose calculations are based on measured or projected concentrations of radionuclides in the environment. Measured values can be provided through multiple sources, including analytical laboratory results or field measurements obtained either through aerial measuring systems or ground-based monitoring teams. Projections are usually obtained from atmospheric modelling calculations performed using NARAC plume projections. Source terms can also be obtained from computer models such as RASCAL RASCAL uncertainty is not covered in this analysis, but could be incorporated if that information becomes available in the future.

Sources of uncertainty in measurement values are discussed in this section. Sources of uncertainty from NARAC modelling projections are discussed in Section 4.3.

# 4.2.1. Laboratory Analysis

The scenario analyzed for characterization of laboratory analysis uncertainty involves the release of Cs-137 to the environment. Ba-137m (daughter of Cs-137) emits a gamma at 662 keV, which is near the middle of the detectable range of energies for most gamma spectroscopy systems (40 keV - 3 MeV). Important facts about expanding the source term beyond this simple case while still using the uncertainty estimates given here are:

- 1. Because every radionuclide emits different radiation, the detectability, radiative yield, and relative abundance in the mixture must be considered for each scenario as these impact the method used for detection, the total propagated uncertainty (TPU), and the achievable detection limits.
- 2. The assumptions made for this scenario are only applicable to gamma spectroscopy. Many nuclides do not emit reliable photons with radiative yields above 1% and energies between 40keV and 3MeV. The calculation of TPU for these radionuclides is much different as other methods must be used to quantify them.

A simple case was chosen to estimate the analytical TPU. A deposited concentration of 330  $\mu$ Ci/m² was assumed as is described in Chapter 2. The sample collected in this case was a standard FRMAC ground deposition sample. This sample is essentially a 10cm x 10cm x 2cm plug out of the ground including the vegetation above the soil, the results of which are for a 100-cm² area. To proceed in the calculations from here an important assumption is made that *the material is uniformly deposited on the ground with a resolution of a minimum of 1 m*². This means that anywhere in a given square meter a sample of 100 square centimeters will yield the same result and that a 100-cm² sample is *representative* of the square meter.

The detector used to measure the sample is assumed to be the FRMAC Fly Away Laboratory (FAL) FALCON 5000 High-Purity Germanium Gamma Spectrometer. This detector system is utilized in the field to perform rapid gamma spectroscopy of samples collected by CM field teams. The system is calibrated with a mixed nuclide source for quantifying radionuclides emitting photons in the energy range of 40 keV to 3 MeV which is fairly standard in most radiochemistry laboratories. Furthermore, the relative efficiency of the FALCON 5000 is around 20% that of a 3x3 NaI detector, a standard size for many gamma spectrometers in laboratories.

This detector was chosen because it can be reasonably considered average when compared with other gamma spectrometers used in the industry.

The standard stand-off distance for ground deposition samples in the FRMAC FAL is 1 foot away to maximize the solid angle of detection and to minimize any dead time that may be witnessed for samples that are more radioactive. The count time was chosen to be 10 minutes which is fairly standard for fast turn-around samples and has proven to be a reasonable amount of time to yield statistically significant results for contaminated samples. The background for the instrument is assumed to be taken in Albuquerque, New Mexico (a fairly large background compared to other locations to remain conservative).

### 4.2.1.1. Laboratory Analysis Uncertainty Model

A standard Poisson-based uncertainty model is applied to gamma spectroscopy. This assumes that the uncertainty in any measurement of radioactivity is proportional to the square root of the number of counts observed. When any adjustment or correction is made to the number of counts observed, their errors are combined in quadrature following the law of propagation of uncertainty [29]. The expected measured counts per minute is calculated as shown in Equation (6):

$$C_i = \epsilon_i(E) * \tau_i * \nu * \kappa * \gamma_i(E)$$
 (6)

where:

 $C_i$ : Observed counts per minute of the detector system for nuclide, i (cpm)

 $\epsilon_i(E)$ : Detection efficiency at the energy in keV of the primary gamma ray of nuclide, i (cpm/dpm)

 $\tau_i$ : Deposited radioactivity for the nuclide,  $i \, (\mu \text{Ci/m}^2)$ 

 $\nu$ : Surface area for a standard ground deposition sample (0.01 m<sup>2</sup>)

 $\kappa$ : Conversion factor from  $\mu$ Ci to dpm (2.22E6 dpm/ $\mu$ Ci)

 $\gamma_i(E)$ : Radiative yield of the primary gamma ray of nuclide, i (gammas per disintegration)

The detection efficiency and yield of the primary line are functions of the gamma ray energy and radionuclide of interest, respectively. The efficiency is determined from a calibration curve that is either measured from a known standard traceable to the National Institute of Standards and Technology (NIST) or by the modeling of the geometry in a Monte-Carlo based simulation program. The efficiency calibration curve is a function of energy, counting geometry, and sample size, shape, and density. For this case of ground deposition sample counted 1 foot away from a FALCON 5000, a previous calibration was used to determine the efficiency. The curve used could theoretically be applied to other scenarios for other radionuclides as long as the same assumptions for sample size and counting geometry are made. The efficiency function for this geometry is shown in Equation (7):

$$\epsilon_i(E) = 10^{\left\{ [-1.659e - 4*E] - [3.780] + \left[ \frac{2.65e2}{E} \right] - \left[ \frac{2.66e4}{E^2} \right] + \left[ \frac{1.256e6}{E^3} \right] - \left[ \frac{2.191e7}{E^4} \right] \right\}}$$
(7)

Note that for any other counting geometry, the coefficients will be different but the shape of the curve and form of the equation will be similar. Using Equation (7) for the 662 keV gamma ray from Ba-137m, the efficiency equals 2.85E-04 cpm/dpm. Using Equation (6), the observed counts per minute is calculated to be 1775 cpm.

The number of observed counts is calculated using Equation (8):

$$G_i = C_i * T \tag{8}$$

where:

 $G_i$ : Gross observed number of counts in the measurement of nuclide, i (counts)

 $C_i$ : Observed counts per minute of the detector system for nuclide, i (cpm)

T: Count time of the measurement (min)

For this case, a ten-minute count time yields 17,750 gross counts.

Every gamma spectroscopy system will respond to background differently as it is a function of the detector size (efficiency), the location of the count, and the amount of shielding around the detector. For the purpose of this estimation, a standard background spectrum was taken from a FALCON 5000 instrument in Albuquerque, New Mexico. A region of interest (ROI) was drawn around where the Ba-137m emission at 662 keV would be observed and the net count rate in this ROI was calculated. This yielded 20 counts in a 10-minute measurement. When compared to the net signal of 17750 counts, this background can be assumed to be negligible in the calculation of the TPU. It is important to note that when there is a significant background (greater than a few percent of the gross measured value) the uncertainty in the background must be considered. For the more general case, the net counts are calculated using Equation (9):

$$N_i = (G_i - B_i) * T_b \tag{9}$$

where:

 $N_i$ : Net observed number of counts in the measurement of nuclide, i

 $G_i$ : Gross observed counts per minute of the detector system for nuclide, i (cpm)

 $B_i$ : Observed counts per minute of the background spectrum in the ROI for nuclide, i (cpm)

 $T_h$ : Count time of the background (min)

Equation (10) shows that the counting uncertainty is the square root of the number of net counts observed:

$$\sigma_i = \sqrt{N_i} \tag{10}$$

where:

 $\sigma_i$ : 1-sigma counting uncertainty of the measurement

 $N_i$ : Net observed number of counts in the measurement of nuclide, i

The relative counting uncertainty is then calculated as shown in Equation (11):

$$\sigma_i(\%) = \left(\frac{\sqrt{N_i}}{N_i}\right) * 100 \tag{11}$$

where:

 $\sigma_i$  (%): Relative 1-sigma counting uncertainty of the measurement

 $N_i$ : Net observed number of counts in the measurement of nuclide, i

For this case, the relative 1-sigma counting uncertainty is calculated to be 0.75%.

In the calculation of radioactivity the net count rate is corrected for efficiency, decay correction, radiative yield, and cascade summing (if applicable). Furthermore, there is uncertainty in the actual sampling that is usually very difficult to quantify and is often assumed to be zero. For the purpose of this example, the uncertainty in the calibration and decay/radiative yield corrections are assumed based on professional judgement. Similar assessments as were made for the counting uncertainty could be made for each of these components but it is deemed unnecessarily complicated for the purpose of these estimations. Table 4.2-1 shows the typical uncertainties that are expected from each of these components based on historical data from the radiochemistry laboratory at SNL.

Table 4.2-1. Laboratory Analysis sources of uncertainty.

Uncertainty Component	Approximate Relative Uncertainty		
Efficiency Calibration (includes calibration measurement uncertainty and certified activity uncertainty of the calibration source)	5%		
Decay Correction and Radiative Yield (based on reference material)	1%		
Sampling uncertainty	0% but is likely much larger and unquantifiable		

### 4.2.1.2. Calculating the Total Propagated Uncertainty for Laboratory Analysis

Applying the law of uncertainty propagation as defined by NIST [29], these uncertainties can be combined in quadrature to yield the TPU, as shown in Equation (12):

$$TPU\sigma_i(\%) = \sqrt{\sigma\%_i^2 + \sigma\%_\epsilon^2 + \sigma\%_\gamma^2}$$
 (12)

where:

 $TPU\sigma_i(\%)$ : Relative 1-sigma total propagated uncertainty (%)

 $\sigma_{i}^{2}$ : Relative 1-sigma counting uncertainty (%)

 $\sigma\%_{\epsilon}^2$ : Relative 1-sigma uncertainty in the efficiency calibration (%)

 $\sigma_{\nu}^{2}$ : Relative 1-sigma uncertainty in the yield and decay correction (%)

Using the previously-calculated relative 1-sigma counting uncertainty and the values in Table 4.2-1, the TPU is calculated to be 5.2%.

The radiochemical analysis of a ground deposition sample in this example should be modeled with a normal distribution. The mean in this case is the expected radioactivity in a  $100\text{-cm}^2$  ground deposition sample taken at the probed location. The SD of the distribution is the TPU for the measurement of this ground deposition sample. For the purposes of modeling the uncertainty for this specific case in a global uncertainty budget, a distribution is constructed with a mean of  $330 \, \mu \text{Ci/m}^2$  and an SD of  $17 \, \mu \text{Ci/m}^2$ . The final distribution for the activity value calculated with the uncertainty given for in laboratory measurements is shown in Figure 4.2-1.

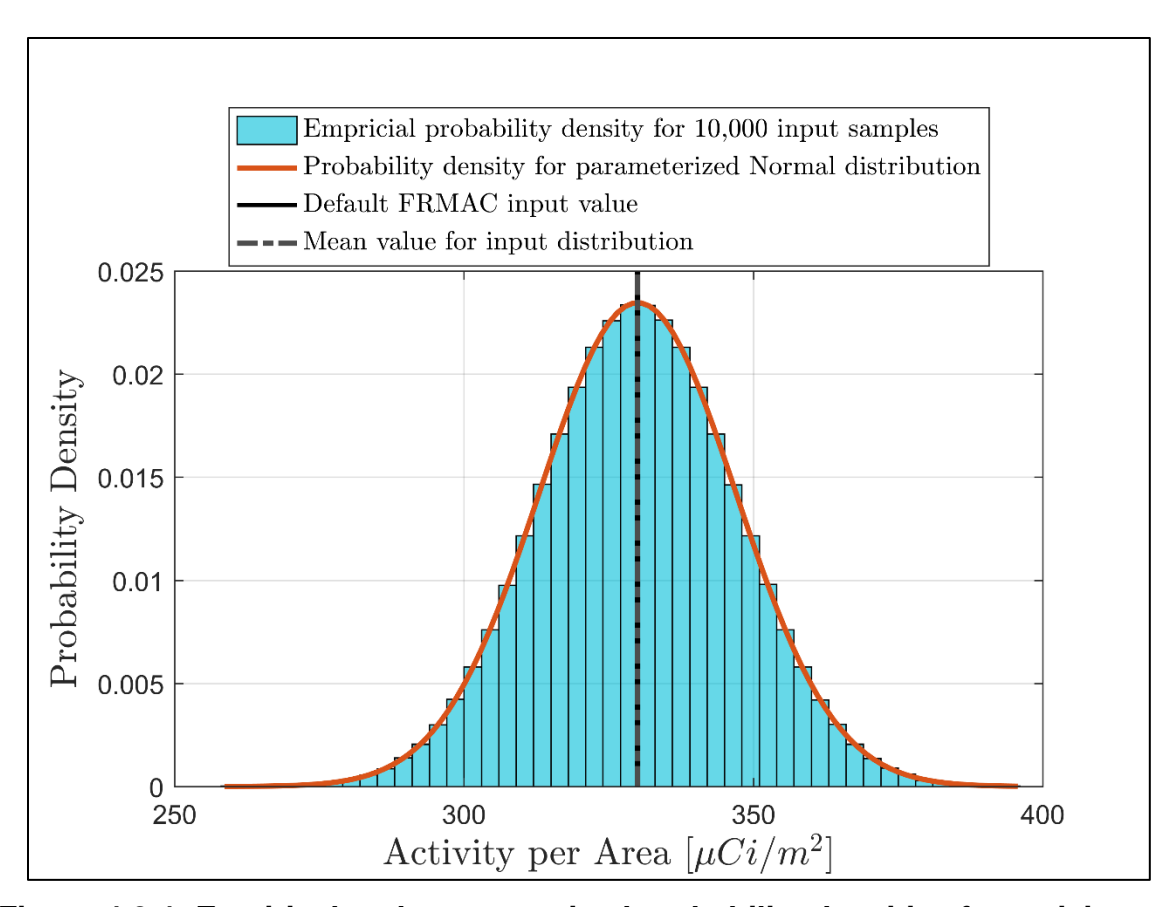


Figure 4.2-1. Empirical and parameterized probability densities for activity per area for laboratory measurements.

# 4.2.2. In Situ Deposition Measurements

In situ measurements of radioactive material on or in the soil are performed by directing the working end of a gamma ray spectroscopic detector toward the contaminated ground, as shown in Figure 4.2-2. Typically, the detector is on a tripod with the face of the detector at 1 meter above the ground. A gamma ray spectrum is collected and analyzed to determine the concentration of radioactive material.

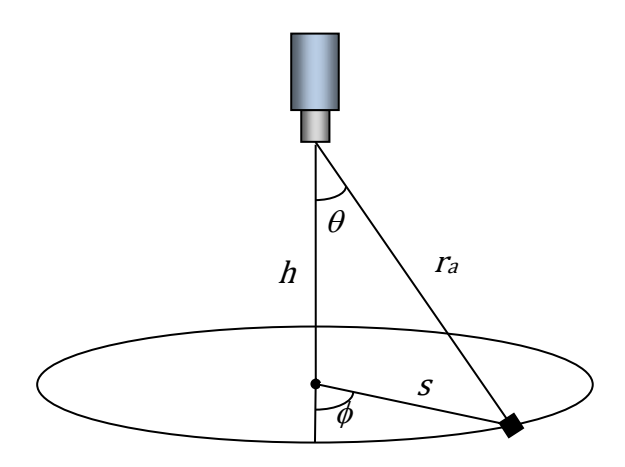


Figure 4.2-2. In situ measurement geometry.

### 4.2.2.1. In Situ Uncertainty Model

When the analysis is performed, the count rate for a peak in the gamma ray spectrum is modified by an expected yield per decay for the gamma ray, and an efficiency factor to obtain the activity concentration, as shown in Equation (13):

$$N(E) = tAy(E) \int_{0}^{\infty} 2\pi s ds \frac{\varepsilon(E, \theta)}{4\pi r_a^2} e^{-\mu_a(E)r_a} = tAy(E)\varepsilon_{dep}(E)$$
 (13)

where:

N(E): Counts in the peak at energy E of a gamma ray spectrum

t: Live time of the spectrum (s)

A: Deposition concentration of the radioactivity (Bq/m<sup>2</sup>)

y(E): Gamma rays per decay at energy E

 $\varepsilon(E,\theta)$ : Point-like source efficiency for gamma rays of energy E and angle  $\theta$ 

 $\mu_a(E)$ : Attenuation coefficient for gamma rays of energy E in air (m<sup>-1</sup>)

 $\varepsilon_{dep}(E)$ : Efficiency for ground deposited gamma rays of energy E (cps Bq<sup>-1</sup> m<sup>2</sup>)

The efficiency factors are computed with the assumption that the ground is an infinite plane, and that the distribution in the soil is described by one of three cases:

- 1. Material is uniformly distributed on the surface;
- 2. Material is uniformly mixed into the soil to an infinite depth;
- 3. Material is weathered into the soil so that the concentration as a function of depth can be described by an exponential distribution with a relaxation length.

The first two cases are special instances of the third case where the relaxation length is very short (surface contamination) or very long (uniform in the soil). Sources of uncertainty associated with the analysis results from in situ measurements include:

- 1. Statistical errors on the count rates for the gamma ray peaks and the spectrum background;
- 2. Systematic errors on the factors used to convert between count rates and gamma ray emission rates:
- 3. Geometric errors resulting from performing measurements in locations which are different from the infinite plane which is used in calculating the conversion factors.

The error that results from measurements being performed in non-ideal geometries cannot be addressed. These can be infinite in their complexity and include such issues as non-flat terrain, non-uniform deposition of material, potential hold-up of material in vegetation, and the presence of man-made structures that enhances or reduces the apparent signal.

The statistical uncertainty for the counts in a gamma ray peak is a combination of the uncertainty for the peak area and the underlying continuum. These are both Gaussian in nature. The error on the efficiency factor to convert between a count rate and an activity concentration has multiple contributions.

- 1. The efficiency for measurements of deposited activity is derived from efficiencies for point-like radioactive source at a variety of angles. There is uncertainty for the point-like source efficiency. The sources of the uncertainty are described below.
  - a. There is uncertainty in the activities of the radioactive sources. The radioactive sources are produced with a certificate. The certificate states the activities and emissions, along with uncertainties, that are valid at a point in time. The uncertainty in source activities is assumed to be uniform at 3%.
  - b. There is uncertainty in the counts in a gamma ray peak. As a source emits gamma rays, some of them will interact in the detector. Those interactions which deposit their full energy in the detector will contribute to a peak in the gamma ray spectrum. The number of events recorded in a peak are expected to follow a Gaussian distribution, thus the uncertainty will be equal to the square root of the number of events.

- c. There is uncertainty resulting from fitting the efficiency measurements at discrete energies to a function which can be used for determining the efficiency at other energies through interpolation. This will result in an uncertainty which is dependent upon the input measurements and the form of the function used. The uncertainty for different energies will also be correlated.
- 2. The point-like efficiencies as determined for several angles relative to the axis of the detector are combined through an angle-dependent weighting to obtain the efficiency for the deposited activity.

Because of the high degree of correlation among the different contributions to the uncertainty for the efficiency of an in situ measurement, it was determined that the best approach would be to apply variation to an existing set of point source efficiency measurements as follows:

- 1. Allow activities of the radioactive sources to vary uniformly  $\pm 3\%$  from their reported activities.
- 2. Adjust gamma ray peak counts according to the modified source activities.
- 3. Allow gamma ray peak counts to vary according to Gaussian statistics.
- 4. Calculate point source efficiencies based on the adjusted gamma ray peak counts and the reported source activities.
- 5. Fit the point source efficiencies to a function for interpolation.
- 6. Use the efficiency function to determine the efficiency for the specified energy.
- 7. Perform the weighted sum over angles to compute the efficiency for deposited material.

This process is carried out thousands of times to get a distribution for the deposition efficiency. Through this process, the mean efficiency for 662 keV gamma rays is 12.03 cps per gamma s<sup>-1</sup> cm<sup>-2</sup>. The distribution of efficiencies has an SD calculated as the square root of the variance, of 0.136 cps per gamma s<sup>-1</sup> cm<sup>-2</sup>. Figure 4.2-3 shows this distribution.

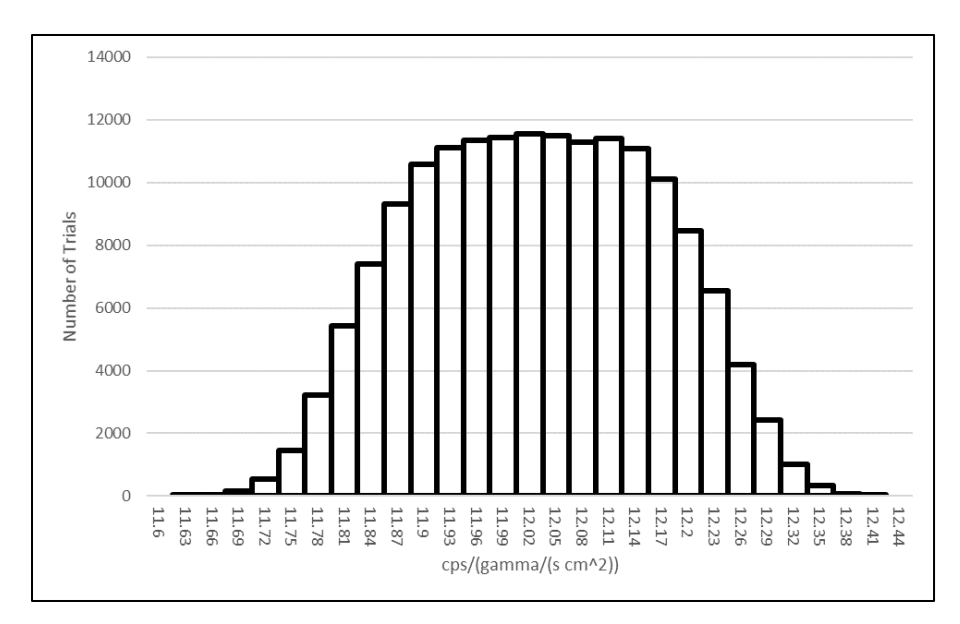


Figure 4.2-3. Distribution of the efficiency for a uniform surface deposition of 662 keV gamma rays for a DetectiveEX-100.

The contribution of the efficiency uncertainty to the uncertainty of an in situ measurement was examined for the specific case of the deposition of Cs-137 at 330  $\mu$ Ci/m² based on the assumptions described in Chapter 2. Cs-137 at 330  $\mu$ Ci/m² equates to 1.22E3 Bq/cm². Because a 662 keV gamma ray is emitted 85% of the time in Cs-137 decays, this corresponds to 1.04E3 gammas s⁻¹ cm⁻². The count rate in the detector is calculated by multiplying 1.04E3 gammas s⁻¹ cm⁻² by the efficiency of 12.03 cps per gamma s⁻¹ cm⁻², which yields 1.25E4 cps. For a spectrum with 300 seconds live time, the peak area is 3.75E6 counts.

The uncertainty of the counts in the peak is expected to follow normal counting statistics as shown in Equation (10). This yields an SD of 1.94E3 counts.

In this instance the uncertainty from the counts from the background in the spectrum is expected to be insignificant. If the background counts were greater than 10% of the peak counts, the background counts should be included in the calculation of the count peak uncertainty.

### 4.2.2.2. Calculating the Total Propagated Uncertainty for In Situ

With the counts in the peak, live time, and efficiency, the deposited activity can be re-calculated using Equation (14):

$$A = \frac{N}{t} \frac{1}{y(E)\varepsilon_{\text{den}}(E)} \tag{14}$$

The uncertainty on the deposited activity is calculated by combining the uncertainties for the counts and the efficiency as shown in Equation (15):

$$\sigma_{A} = \sqrt{\sigma_{N}^{2} \times \left(\frac{1}{ty(E)\varepsilon_{\text{dep}}(E)}\right)^{2} + \sigma_{\text{eff dep}}^{2} \times \left(\frac{N}{ty(E)\varepsilon_{\text{dep}}^{2}(E)}\right)^{2}}$$
(15)

where:

 $\sigma_A$ : Deposited activity uncertainty

 $\sigma_N$ : Count uncertainty

 $\sigma_{\rm eff \, dep}(E)$ : Efficiency uncertainty

For the case of a deposited activity of 330  $\mu$ Ci/m<sup>2</sup>, this propagation yields an SD of 3.74  $\mu$ Ci/m<sup>2</sup>. The final distribution for the activity value calculated with the uncertainty given for in situ deposition measurements is shown in Figure 4.2-4.

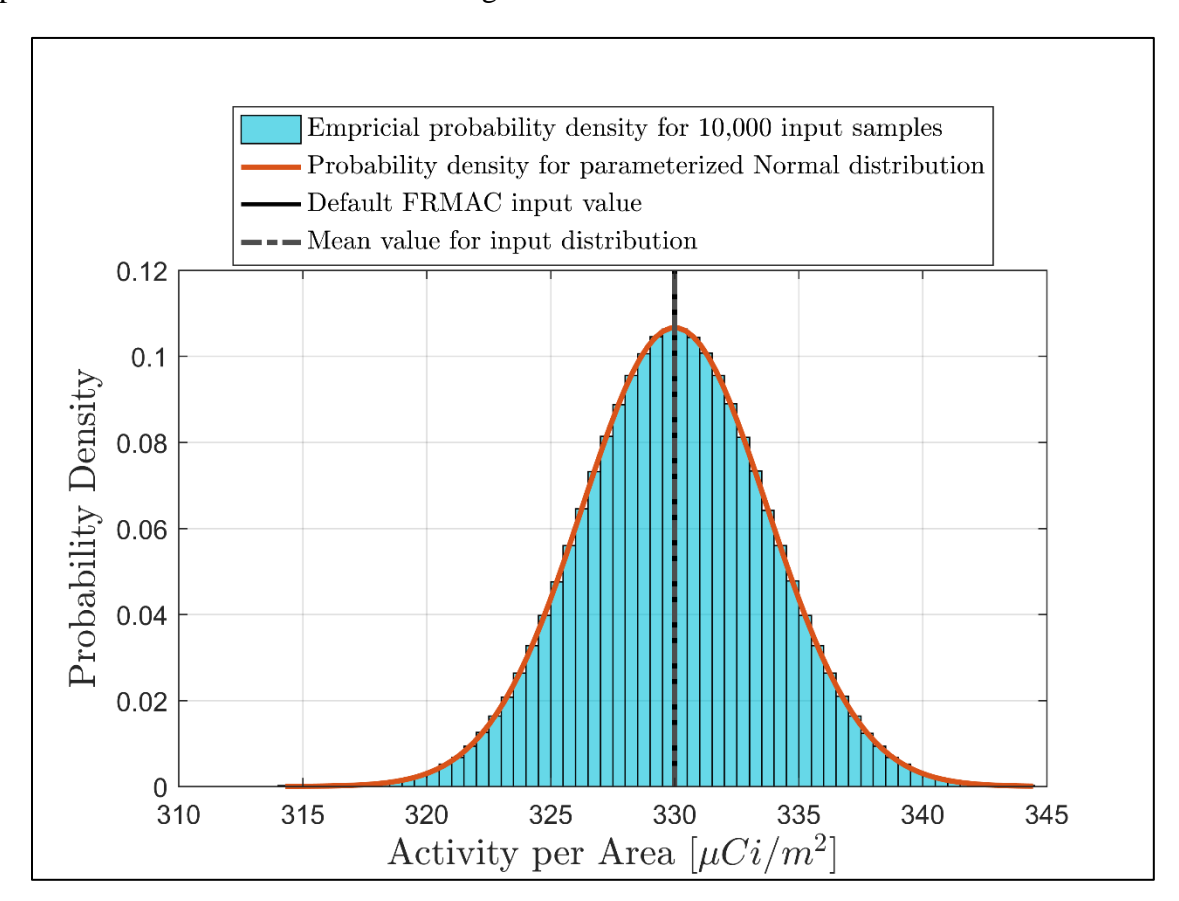


Figure 4.2-4. Empirical and parameterized probability densities for activity per area for in situ deposition measurements.

#### 4.2.3. AMS Measurements

For aerial measurements, the initial processing of the data converts the gross count rate in the detector to a corrected equivalent net count rate (N) at a nominal altitude. This process involves subtracting the background count rate, then adjusting from the altitude where the actual measurement was performed to the nominal altitude. The nominal altitude is the height at which the corrections to ground level activity are computed. The corrected net count rate is calculated as shown in Equation (16):

$$N = K(N_a - N_0)e^{B(z - z_0)}$$
(16)

where:

K: Conversion factor for count rate

 $N_a$ : Gross count rate in the detector during the measurement

 $N_0$ : Mean count rate estimate due to airborne background radiation

B: Effective attenuation coefficient (ft<sup>-1</sup>)

z: Altitude above ground level

 $z_0$ : Nominal altitude

The uncertainty for the coefficient to convert a net count rate in the aerial system to a ground-level quantity (exposure rate, or deposition concentration) depends upon the ground and aerial measurements along a calibration line. The aerial components of the uncertainty are related to the knowledge of the height above ground level (AGL) while performing the measurements at multiple altitudes (altitude spiral). When the radar altimeter (RA) is available, the uncertainty in the height is  $\pm 0.7$  m. When the GPS is used to measure the height, the uncertainty associated with the height above ellipsoid is approximately  $\pm 3$  m. Uncertainty related to an associated AGL correction depends on the resolution and accuracy of the digital elevation model chosen, but can be considered negligible for the assumed uniformly flat space of this analysis. These uncertainties in height correspond to 0.4% and 1.7% errors in the corrected count rates in the aerial detectors.

The uncertainty in the raw counts in the detector, either from the ground contamination or from the aircraft background, follow normal statistics. The background is assumed to be 3,500 cps for a 12-detector system as is used on the helicopter, or 870 cps in a 3-detector system as is used in the fixed-wing platforms. It should be noted that changes in naturally-occurring airborne radon have produced differences as much as 500 cps in the 12-detector system over the course of a two-hour flight. The error induced by this random uncertainty is small compared to the dominant source of counts in the scenario presented. The signal from the ground contamination will depend upon the level of contamination and the height of the measurement above the ground. Some estimated values for the 3-detector fixed wing and 12-detector rotary wing platforms at different altitudes above ground level are shown in Table 4.2-2. It should be noted that the RSI 701 system flown by AMS is rated to handle a throughput of 250,000 cps per crystal

without spectral degradation and therefore the scenario given is on the upper limit of applicability for the detector systems at 50 m.

Table 4.2-2. Estimated count rate in the aerial detectors flying over an area that is uniformly contaminated at 330 µCi/m².

Nominal Altitude	Helicopter, 12-detectors	Fixed-wing, 3-detectors
50 m AGL	$3.14x10^6 \text{ cps/}(330 \mu\text{Ci/m}^2)$	$7.85 \times 10^5 \text{ cps/}(330 \mu\text{Ci/m}^2)$
150 m AGL	1.89x10 <sup>6</sup> cps/(330 μCi/m <sup>2</sup> )	4.72x10 <sup>5</sup> cps/(330 μCi/m <sup>2</sup> )

There are multiple methods for determining the system background. The best method is to perform an altitude spiral over a large body of water at the same time that a spiral is performed over the calibration line. This results in an altitude dependent background which will include the contribution from airborne radioactive material (e.g., radon). A less detailed background can be obtained by performing a single pass over the large body of water. This does not give an altitude-dependent background, so any stratification of the radon will not be addressed. An alternative approach when no suitable water body is present is to use measurements performed at 900 m above ground level. At this height, the signal from the ground contamination is expected to have been reduced to zero because of attenuation in the air.

The uncertainty in the effective attenuation coefficient results from atmospheric conditions as well as the variability of the actual flight altitudes during passes over the calibration line. The height variability can result from the tools which are used to measure the altitude (RA or GPS), as well as the roughness of the terrain and the skill of the pilots. The atmospheric conditions include the temperature, pressure, and humidity. A number of data sets over a calibration line have been compiled for use in testing and training. The attenuation coefficient derived from this area is  $1.674 \times 10^{-3}$  ft<sup>-1</sup> with an SD of  $4.58 \times 10^{-5}$  ft<sup>-1</sup> (2.74%).

The uncertainty for the altitude above ground is related to the measurement method. As noted previously, the uncertainty associated with an RA is  $\pm 0.7$  m, and the uncertainty of GPS is  $\pm 3$  m. To calculate the total uncertainty for the aerial measurements, the contributions from the different components must be propagated. The variance is given by Equation (17):

$$\sigma_N^2 = \sigma_K^2 (N_g - N_0)^2 e^{2B(z - z_0)} + (\sigma_{N_g}^2 + \sigma_{N_0}^2) K^2 e^{2B(z - z_0)} + (\sigma_R^2 K^2 (N_g - N_0)^2 e^{2B(z - z_0)} (z - z_0)^2 + \sigma_Z^2 K^2 (N_g - N_0)^2 e^{2B(z - z_0)} B^2$$
(17)

Table 4.2-3 shows the results from the uncertainty propagation using Equation (17) for fixed-wing and helicopter at different nominal altitudes and using different altitude measurement methods. In evaluating this, a simplifying assumption is made that the aircraft is flown precisely at the nominal altitude (i.e.,  $z = z_0$ ). In reality this will not be the case, and the difference could be significant, especially in surveys conducted over rugged terrain.

Table 4.2-3. Uncertainty in estimated count rate in the aerial detectors flying over an area that is uniformly contaminated at 330 µCi/m<sup>2</sup>.

Platform	Nominal Altitude	Altitude Measure Method	cps/(330 μCi/m²)	Background cps	Altitude Uncertainty (m <sup>-1</sup> )	Uncertainty of corrected counts	Percent uncertainty
50	50 m AGL	GPS	$7.85 \times 10^5$	870	3.0	1.85x10 <sup>4</sup>	2.36
Fixed-wing	50 AC	RA	$7.85 \times 10^5$	870	0.7	$4.43x10^3$	0.56
Fixed-	GPS	4.72x10 <sup>5</sup>	870	3.0	1.11x10 <sup>4</sup>	2.36	
	Fix 150 m AGL	RA	4.72x10 <sup>5</sup>	870	0.7	1.85x10 <sup>4</sup>	0.57
	opter 50 m AGL	GPS	$3.14x10^6$	3500	3.0	$7.40 \times 10^4$	2.36
opter		RA	$3.14x10^6$	3500	0.7	$1.74 \times 10^4$	0.56
Helicopter 150 m 50 AGL AC	) m 3L	GPS	1.89x10 <sup>6</sup>	3500	3.0	4.46x10 <sup>4</sup>	2.36
	RA	1.89x10 <sup>6</sup>	3500	0.7	$1.05 \times 10^4$	0.56	

At a ground contamination level of 330  $\mu$ Ci/m², the uncertainty in the corrected count rate is dominated by uncertainty in the altitude during the altitude spiral and the survey measurements. The uncertainty from the counting statistics in the detector system is approximately equal to the uncertainty from the altitude measuring system at 30  $\mu$ Ci/m² when the RA is available, and 7  $\mu$ Ci/m² when the GPS is used.

An additional factor must be included in order to convert the aerial measurement to ground contamination values for use in the Turbo FRMAC<sup>©</sup> calculations. K is a scaling factor determined by a combination of aerial and ground measurements at a calibration area as shown in Equation (18):

$$K = \frac{A'}{N'} \tag{18}$$

where A' is the activity concentration on the calibration line from in situ measurements and N' is the corrected aerial count rate. For this analysis, a calibration line activity concentration of  $7 \,\mu\text{Ci/m}^2$  was assumed. Using the value for the fixed-wing, 3-detector platform at 150 m shown in Table 4.2-2, K is equal to 6.99E-04 ( $\mu\text{Ci/m}^2$ )/cps. This yields a corrected aerial count rate of 10,012 cps.

The uncertainty for K is obtained by considering the uncertainty in the in situ measurements and aerial measurements in the calibration area,  $\sigma_{A'}$  and  $\sigma_{N'}$ , respectively. The propagated uncertainty for K,  $\sigma_{K}$ , is defined in Equation (19):

$$\sigma_K = \frac{A'}{N'} * \sqrt{\left(\frac{\sigma_{A'}}{A'}\right)^2 + \left(\frac{\sigma_{N'}}{N'}\right)^2}$$
 (19)

The uncertainty in A',  $\sigma_{A'}$ , is determined using the method previously discussed for in situ uncertainty. The uncertainty in the aerial calibration measurements,  $\sigma_{N'}$ , is the square root of the count rate at the nominal altitude above the calibration line. For the assumed calibration line activity of 7  $\mu$ Ci/m<sup>2</sup>,  $\sigma_{K'}$  is equal to 1.08E-05 ( $\mu$ Ci/m<sup>2</sup>)/cps.

Ground contamination, A, is then calculated as shown in Equation (20):

$$A = K * N \tag{20}$$

where *N* is the count rate at the nominal altitude above the 330  $\mu$ Ci/m<sup>2</sup> contaminated area and *K* is the previously described scaling factor. For a ground contamination level of 330  $\mu$ Ci/m<sup>2</sup>, *N* is equal to 4.72E+05 cps for the fixed-wing, 3-detector platform at 150 m (Table 4.2-2). The uncertainty in *A*,  $\sigma_A$ , is defined in Equation (21):

$$\sigma_A = (K * N) * \sqrt{\left(\frac{\sigma_K}{K}\right)^2 + \left(\frac{\sigma_N}{N}\right)^2}$$
 (21)

where  $\sigma_K$  is the previously-calculated 1.08E-05 ( $\mu$ Ci/m²)/cps and  $\sigma_N$  is 1.11E+04 for the fixed-wing at 150 m using GPS (Table 4.2-3). The propagation in Equation (21) yields a final ground contamination uncertainty of 9.29  $\mu$ Ci/m² for AMS measurements. The final distribution for the activity value calculated with the uncertainty given for AMS measurements is shown in Figure 4.2-5.

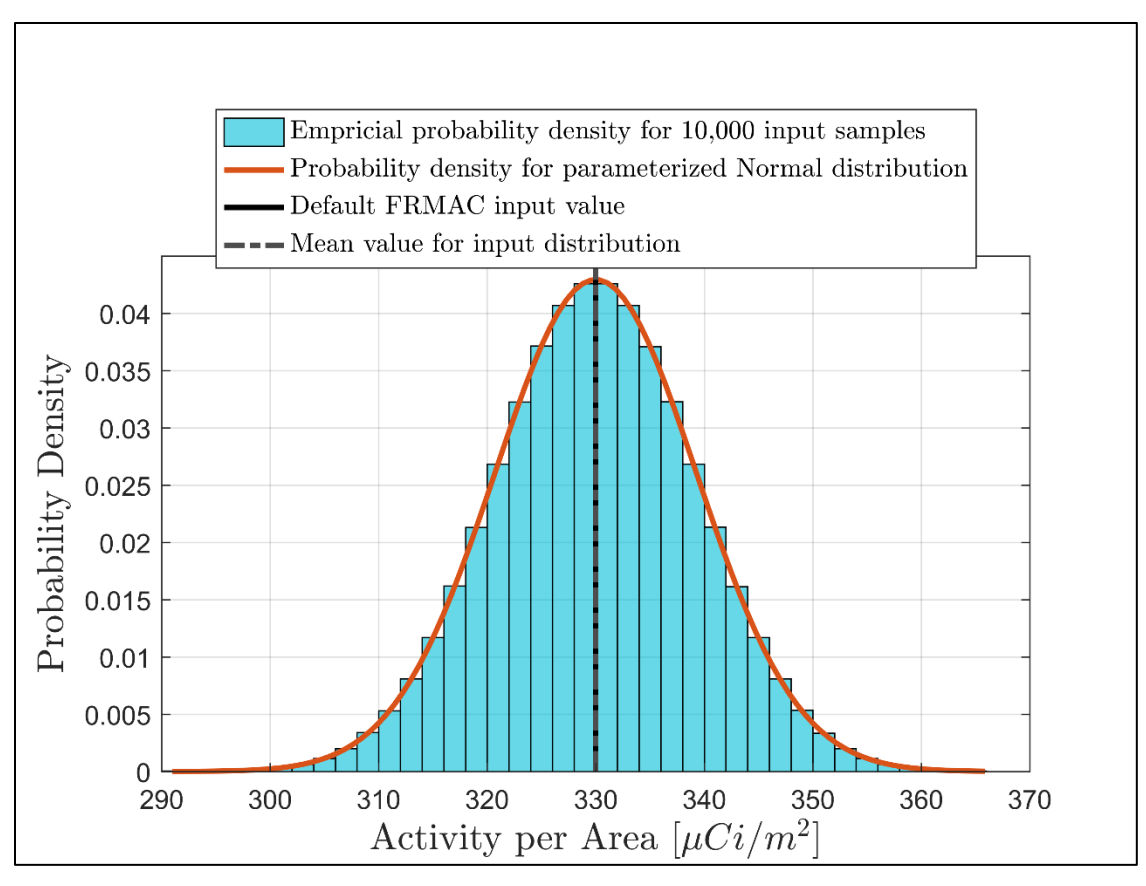


Figure 4.2-5. Empirical and parameterized probability densities for activity per area for AMS measurements.

# 4.3. NARAC Atmospheric Dispersion Sources of Uncertainty

This section documents the method used to quantify NARAC deposition plume uncertainty in relation to the project demonstration case study scenario. In Section 4.3.1, NARAC predicted air concentration uncertainty metrics developed using experimental data are discussed. NARAC air concentration uncertainty quantification for an idealized scenario is documented in Section 0. Final quantified NARAC plume uncertainty for implementation in the uncertainty analysis is summarized in Section 4.3.3.

#### 4.3.1. Benchmark Data

NARAC utilizes concentration measurements from atmospheric dispersion field experiments to compare with predicted values to determine model accuracy. Near-surface atmospheric tracer gas dispersion experiments range from constant winds over flat terrain with uniform vegetation cover (e.g., Prairie Grass Experiment; [30]) to highly variable wind fields in complex terrain along a coastline (e.g., Diablo Canyon Tracer Experiment; [31]). Based on the project study scenario previously discussed, the Prairie Grass Experiment is the most relevant since it involves well resolved winds, uniform land cover and flat terrain. However, one caveat is that the experiment

measured air concentration while the project scenario involves surface contamination uncertainty. Deposition velocity and its associated probability distribution (as previously described in Section 4.1.2) was used to convert air concentration to surface contamination in the uncertainty analysis simulations.

A metric useful for quantifying dispersion model accuracy is the ratio, r, of observed concentration values to predicted values at the same time and location. Statistics such as r are useful for comparing observed and predicted air and depositions concentration values that can range over several orders of magnitude. The equation for the concentration comparison metric r is given by Equation (22):

$$r = \frac{observed\ value}{model\ predicted} \tag{22}$$

Based on the above equation, predicted concentration values within a factor of 2 of observations means  $\frac{1}{2} < r < 2$ . For example, if an arbitrary concentration measurement is 1 ng/m<sup>2</sup>, then both predicted values of 0.5 and 2 ng/m<sup>2</sup> are within a factor of 2 of the observed value.

The distribution of *r* values for NARAC simulations of the Prairie Grass tracer experiment are shown in Table 4.3-1 [32]. Roughly 50% of NARAC simulated air concentration values are within a factor of 2 of the observed value. Just over 80% of NARAC predicted values are within a factor of 10 of measured concentrations. Since the Prairie Grass experiment closely matches the project study scenario, the comparison metric values provided in Table 4.3-1 are the best analog for quantifying NARAC uncertainty for <u>air concentrations</u>. As a side note, observed to predicted concentration comparison metric values for the Diablo Canyon tracer experiment are also provided in Table 4.3-1 to illustrate the significant decrease in model accuracy when dispersion simulations occur in complex terrain with non-uniform wind fields.

Table 4.3-1. Distribution of NARAC observed to predicted concentration ratios for the Prairie Grass and Diablo Canyon tracer gas experiments.

Experiment	% r in factor 2	% r in factor 5	% <i>r</i> in factor 10
Prairie Grass	49	73	83
Diablo Canyon	18	41	56

# 4.3.2. Quantifying NARAC Concentration Uncertainty

A NARAC RDD dispersion simulation was used to generate scenario-dependent concentration uncertainty metrics (i.e., error mean and variance) based on the assumptions made for this project. The specifics of the RDD dispersion run are as follows:

Source term: 1500 Ci of <sup>137</sup>Cs

• HE amount: 10 lbs of high explosive

• PSD: All particles with a size of 1 µm

• Meteorology: 4 m/s wind speed, no wind shear, neutral stability, no precipitation

As a point of reference, the RDD scenario results in a deposition concentration of 90.2  $\mu$ Ci/m<sup>2</sup> at a distance of 1 km from the source location.

With predicted air concentration values provided by the RDD dispersion run, the next step in quantifying scenario dependent error metrics is to generate synthetic observations that will produce a NARAC r distribution similar to the Prairie Grass experiment (Figure 4.3-1).

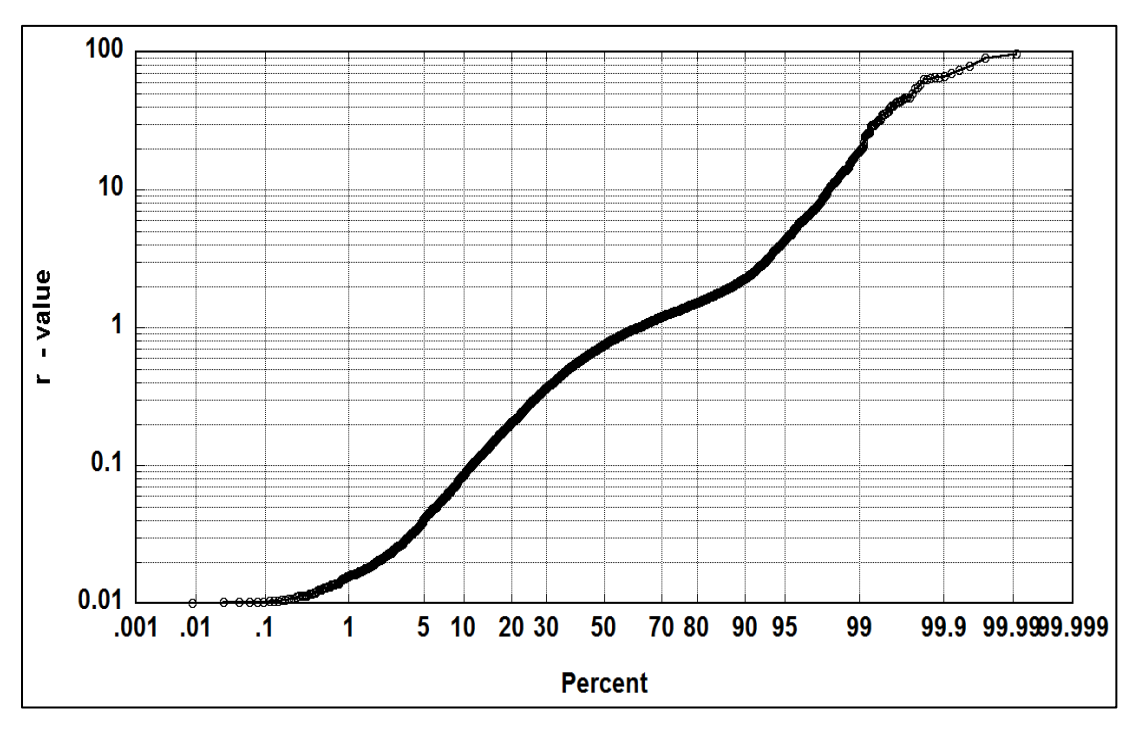


Figure 4.3-1. NARAC r value probability function for the Prairie Grass Experiment.

Prairie Grass r value outliers that are more than two orders of magnitude greater or less than the median of the distribution were not included in the analysis. As a result, a total of 5711 individual r values are available in the Prairie Grass NARAC benchmark distribution. Next, the predicted 1-hour average air concentration plume following the RDD release was analyzed. Predicted concentrations along the plume edge (< 0.01  $\mu$ Ci/m³) were removed from the analysis to avoid skewing statistics with extremely low concentration values. A synthetic concertation

observation was then generated for each unique predicted concentration value (n=3505) by multiplying the predicted value by a r value randomly selected from the Prairie Grass distribution.

The final result of the analysis was a table of predicted and corresponding synthetic concentration observations specific to the project RDD scenario source term and PSD that has a r value distribution similar to NARAC model benchmarking tests using Prairie Grass Experiment measurements. A comparison of the predicted and synthetic concentration data results in a GM (log form) of 0.616 and a geometric variance (log form) of 8.34. A log form of the error metrics is used since the concentration predictions span several orders of magnitude.

It is worth noting that the NARAC model uncertainty estimated for the simplified project RDD release scenario is on the low range of NARAC predicted concentration error. For example, the following key assumptions were necessary to quantify NARAC error for the project scenario:

- Meteorology is known
- RDD source term, geometry, and particle size distribution are perfectly known
- The Prairie Grass r value distribution for a continuous release is valid for a puff release (RDD scenario)

NARAC predicted concentration errors will be much larger for real-world atmospheric releases where the source term and release mechanism are often poorly characterized. In addition, complex wind fields along coastlines and variable terrain and will significantly contribute to NARAC prediction error.

# 4.3.3. Implementation of NARAC Uncertainty for CM Probabilistic Assessment

The ratio of the observed value to the model prediction, given in Equation (22), was used to characterize the uncertainty in a prediction at a fixed point in the plume. A nominal air concentration value was selected for the scenario of interest. This nominal value was multiplied by a sampled value for an air concentration multiplier whose distribution is given by the comparison metric values calculated for the Prairie Grass tracer experiment, as described in Section 4.3.1. A lognormal distribution was fitted to this data. This distribution was found to have a GSD of approximately 0.59 and a GM of 3.99.

The distribution for the air concentration multiplier is shown in Figure 4.3-2.

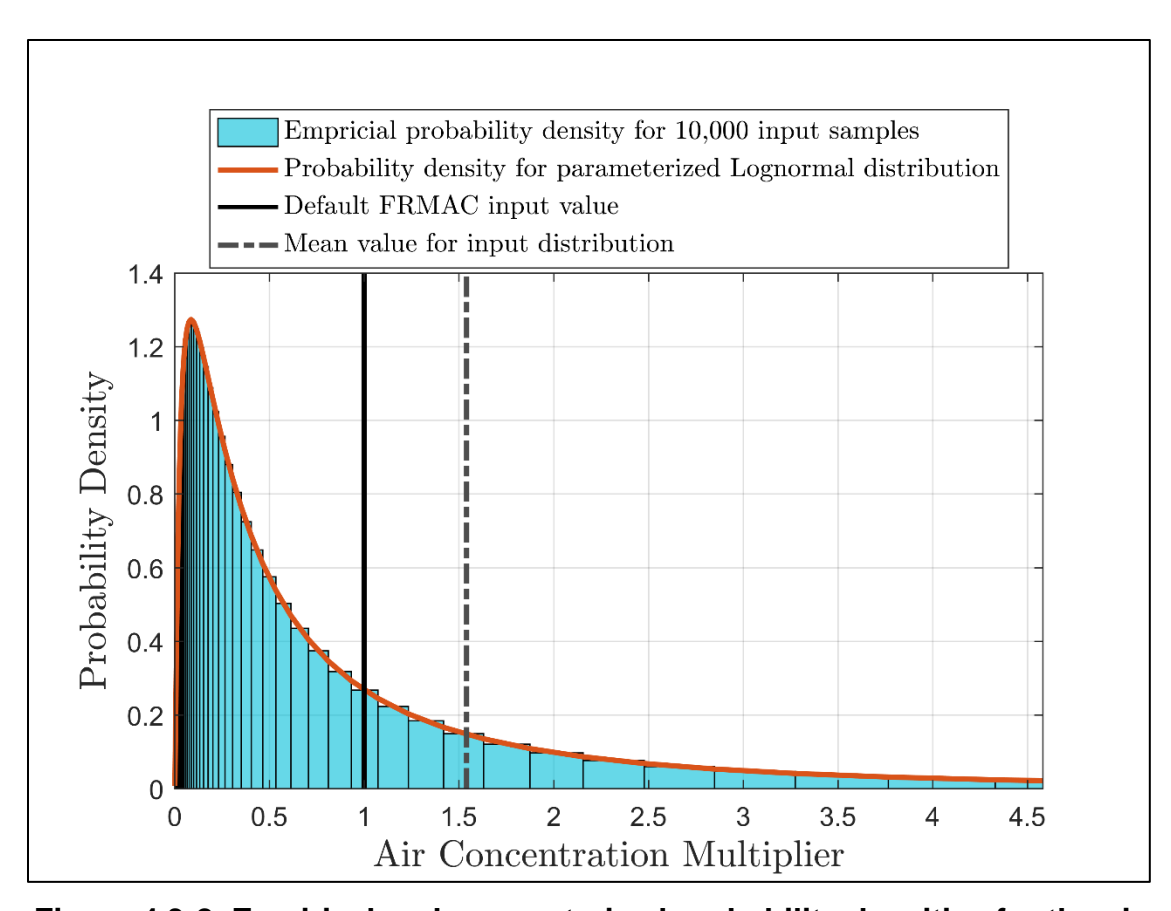


Figure 4.3-2. Empirical and parameterized probability densities for the air concentration multiplier.

The nominal integrated air activity for this analysis is the integrated air activity resulting from a deposition of 330  $\mu$ Ci/m² of Cs-137 using the FRMAC default for deposition velocity (see Eq. 4.5-1 in [3]). This equates to 1.10E5  $\mu$ Ci-s/m³. The air concentration multiplier was applied to this nominal value for each simulation to generate air concentration uncertainty.

# 4.4. Summary of Assigned Input Distributions

Table 4.4-1 summarizes the distributions assigned to the inputs to the Public Protection DRL calculation.

Table 4.4-1. Summary of input distributions for Public Protection DRL Calculation.

Input	Default Value	Distribution Type	Mean	SD	Mode	Lower Bound	Upper Bound	Units
Air Concentration Uncertainty Multiplier – NARAC*	1	Lognormal <sup>+</sup>	0.59	3.99				
Activity per Area – In Situ	330	Normal	330	3.74				μCi/m²
Activity per Area – AMS	330	Normal	330	9.29				μCi/m²
Activity per Area – Laboratory Analysis	330	Normal	330	17				μCi/m²
Deposition Velocity	3.00E-3	Triangular			3.00E-3	3.00E-4	3.00E-2	m/s
Breathing Rate – Light Exercise, Adult Male	1.50	Normal	1.75	0.42		0.54	3.00	m <sup>3</sup> /hr
Breathing Rate – Activity-Averaged, Adult Male	0.92	Triangular			0.92	0.54	1.50	m <sup>3</sup> /hr
Ground Roughness Factor	0.82	Normal	0.82	0.082		0	1	
Resuspension Coefficient Multiplier <sup>‡</sup>	1	Lognormal <sup>+</sup>	1	4.2				
Weathering Coefficient Multiplier <sup>‡</sup>	1	Lognormal <sup>+</sup>	1	1.2				
Deposition External Dose Coefficient Multiplier	1	Triangular			0.8	0.5	1.5	
Inhalation Dose Coefficient Multiplier <sup>§</sup>	1	Lognormal <sup>+</sup>	1	1.5				
Plume External Dose Coefficient Multiplier	1	Triangular			0.8	0.5	1.5	

<sup>\*</sup> This uncertainty multiplier is multiplied by a user-defined air concentration value to sample air concentration with uncertainty. This distribution is calculated from the comparison of NARAC predictions to experimental data.

<sup>+</sup> The means and standard deviations (SD) listed for lognormal distributions on this table are the geometric mean and geometric standard deviation, respectively. The lognormal distribution is defined by parameters  $\mu$ , the mean of the natural logarithm of the data, and  $\sigma$ , the standard deviation of the natural logarithm of the data. Then, the geometric mean (*GM*) is given by  $GM = e^{\mu}$  and the geometric standard deviation (*GSD*) is given by  $GSD = e^{\sigma}$ .

<sup>‡</sup> These multipliers are to be applied only to the coefficients outside the exponentials in the Resuspension and Weathering Factors

<sup>§</sup> This multiplier is specifically for Cs-137, Type F, Effective (Whole Body). Ba-137m is present at equilibrium with Cs-137 at the start of the time phase. The uncertainty in the Ba-137m inhalation dose coefficient is neglected because its ingrowth from Cs-137 over the dose commitment period dominates the delivered dose. The Cs-137 inhalation dose coefficient accounts for dose and uncertainty from the ingrowth of Ba-137m. (per communication with Keith Eckerman on May 10, 2017)

#### 5. PROBABILISTIC ANALYSIS RESULTS

In order to characterize the uncertainty in data products due to varying sources of activity information, a probabilistic analysis was completed for each activity source. The runs for Laboratory Analysis, In Situ Deposition, and AMS used a mixture based on activity per area with the same parameter distributions given in Section 4.4 except each of these runs uses a different SD. The runs for NARAC used a distribution for integrated air activity instead of activity per area.

The results for the Laboratory Analysis, In Situ, and AMS simulations are nearly the same, although slight differences can be seen in the DP outputs for these varying sources of deposition data. This is expected because the only difference between these simulations is the SD on the distribution for activity per area. For the sake of brevity, Laboratory Analysis was chosen to represent the results for this group because the results are similar enough that the same conclusions can be drawn for each deposition data source. The Laboratory Analysis results are included in this chapter because the activity per area distribution for Laboratory Analysis has the largest SD of the three. The results for the In Situ and AMS simulations are located in Appendix A. The NARAC results are presented following the Laboratory Analysis results.

Although the output from the Turbo FRMAC<sup>©</sup> batch runs was set up to include Exposure Rate, Alpha Deposition, Beta Deposition, Alpha Integrated Air, and Beta Integrated Air DRLs, these results are not included in the tables presented in this section. Because an exposure to dose conversion factor of 1 was assumed for this analysis, the Exposure Rate DRLs equal the Dose Rate DRLs. Similarly, because the beta yield is assumed to have no uncertainty and is equal to 1 for Cs-137, the Beta Deposition and Beta Integrated Air DRLs equal the Cs-137 Deposition and Cs-137 Integrated Air DRLs, respectively. Lastly, Cs-137 does not emit alpha radiation and thus the Alpha Deposition and Alpha Integrated Air DRLs are zero.

The results presented in this section were calculated using the methods described in Section 3.3. Section 3.3 provides an example showing the meaning of each of the metrics given in tables and provides the statistical background required for interpreting the results.

The goal of this project is to develop the methods that could be used to execute a probabilistic analysis for the values used to generate CM data products; this project does not seek to provide specific and final information regarding the uncertainty in data products as a whole. Therefore, the results presented in this report should be considered examples derived from a proof of concept of simulation methods and should not be explicitly applied or used to draw conclusions about the full range of potential uncertainties in data products. As the scope of the project is focused on the development of methods for characterizing uncertainty in data products, the discussion provided in this section could be expanded further as results are generated for other analyses in future work.

## 5.1. Laboratory Analysis

The Laboratory Analysis-based distribution for activity per area was used along with the other input distributions discussed in Section 4.1 to run 10,000 simulations of Turbo FRMAC<sup>©</sup>. The results of the statistical analysis of these simulations are given in the following subsections, including percentiles on the DRL and DP results for the Laboratory Analysis simulations, a

ranking of the important inputs for each of the DRL and DP results, and a convergence analysis for the simulations.

# 5.1.1. Uncertainty Analysis Results

The results for the uncertainty analysis of CM data products using the activity distribution derived from uncertainty in laboratory measurements are given in this section.

Table 5.1-1 and Table 5.1-2 below show the mean, 5<sup>th</sup>, 50<sup>th</sup>, and 95<sup>th</sup> for the DRL and DP results, respectively. These values are percentiles of the distribution for each output defined by the 10,000 realizations in the simulation for this activity source. The cumulative distribution functions (CDFs) for each of these outputs are also shown for the DRL outputs in Figure 5.1-1 through Figure 5.1-3 and for the DP outputs in Figure 5.1-4 through Figure 5.1-8. Note that because the distributions for each of the four pathway DPs are different, they cannot be directly summed to get the distribution for the Total DP.

Table 5.1-1. DRL uncertainty results for Laboratory Analysis simulations.

Output Name	Default	Mean	5th	50th	95th
Dose Rate DRL [mrem/hr]	1.98	3.869	0.989	3.779	7.066
Cs-137 Deposition DRL [µCi/m²]	3.31E2	712.550	194.564	683.833	1342.506
Cs-137 Integrated Air DRL [μCi-s/m³]	1.10E5	75856.595	35836.703	68270.251	140970.833

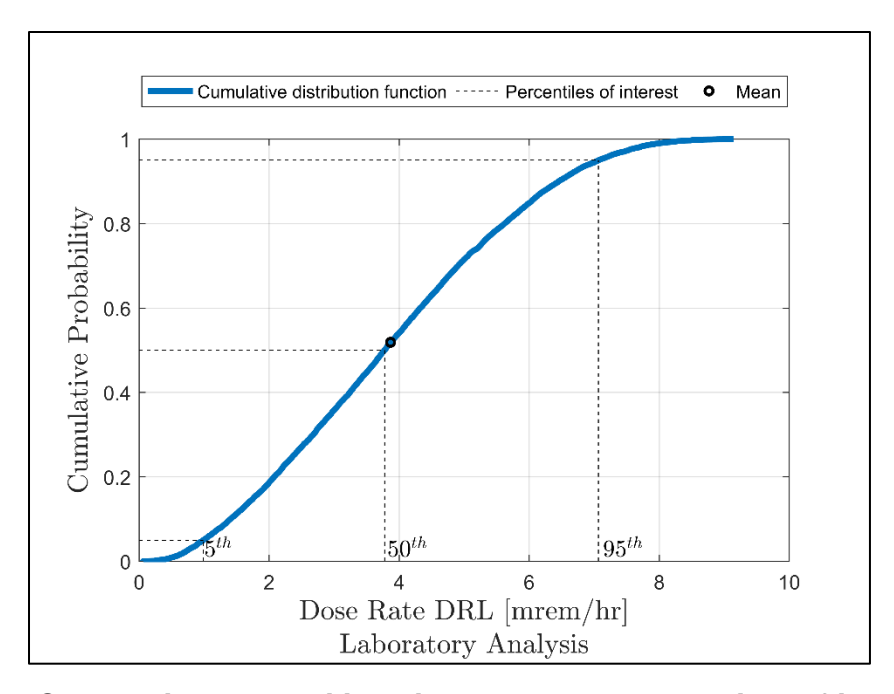


Figure 5.1-1. Cumulative probability with mean and percentiles of interest for the Dose Rate DRL for Laboratory Analysis.

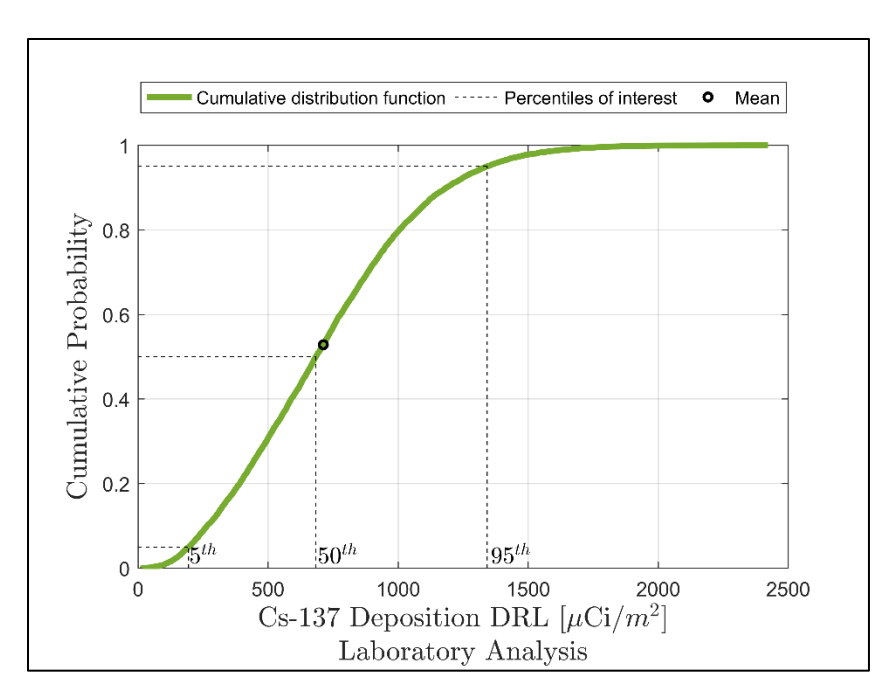


Figure 5.1-2. Cumulative probability with mean and percentiles of interest for the Cs-137 Deposition DRL for Laboratory Analysis.

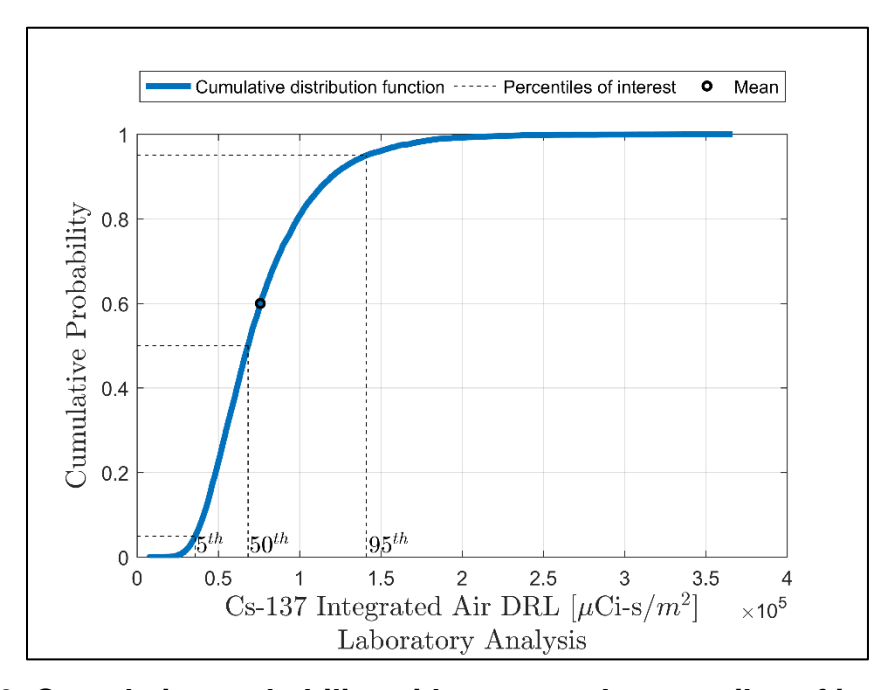


Figure 5.1-3. Cumulative probability with mean and percentiles of interest for the Cs-137 Integrated Air DRL for Laboratory Analysis.

Table 5.1-2. DP uncertainty results for Laboratory Analysis simulations.

Output Name	Default	Mean	5th	50th	95th
Cs-137 Plume Inhalation DP [mrem]	7.93E2	468.811	82.884	281.046	1415.731
Cs-137 Plume Submersion DP [mrem]	10.4	4.501	1.087	2.875	12.926
Cs-137 Resuspension Inhalation DP [mrem]	4.42	14.128	0.393	4.572	55.303
Cs-137 Groundshine DP [mrem]	1.89E2	179.447	102.408	171.332	285.943
Cs-137 Total DP [mrem]	9.97E2	666.886	242.166	485.638	1636.671

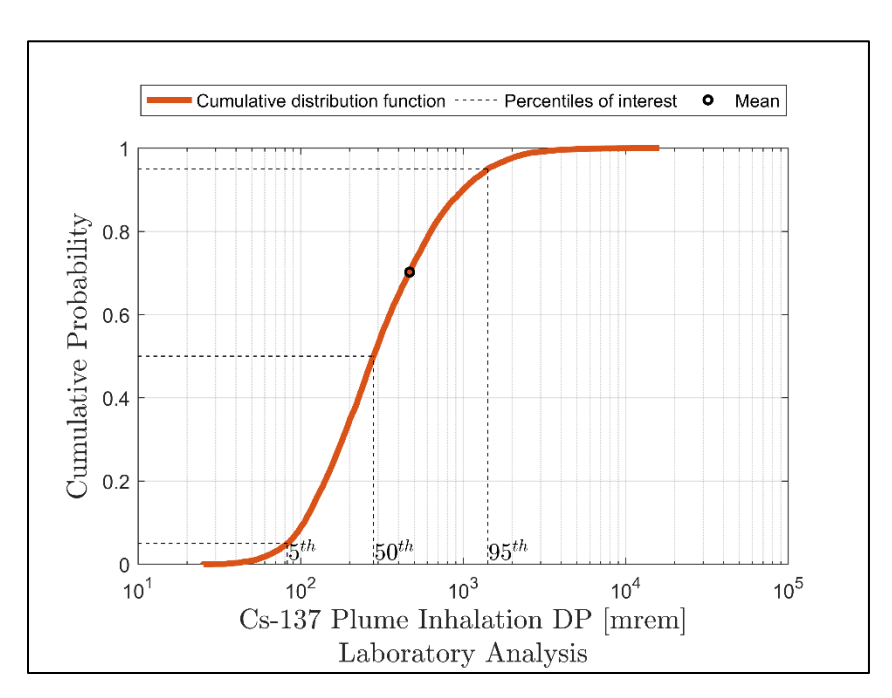


Figure 5.1-4. Cumulative probability with mean and percentiles of interest for the Cs-137 Plume Inhalation DP for Laboratory Analysis.

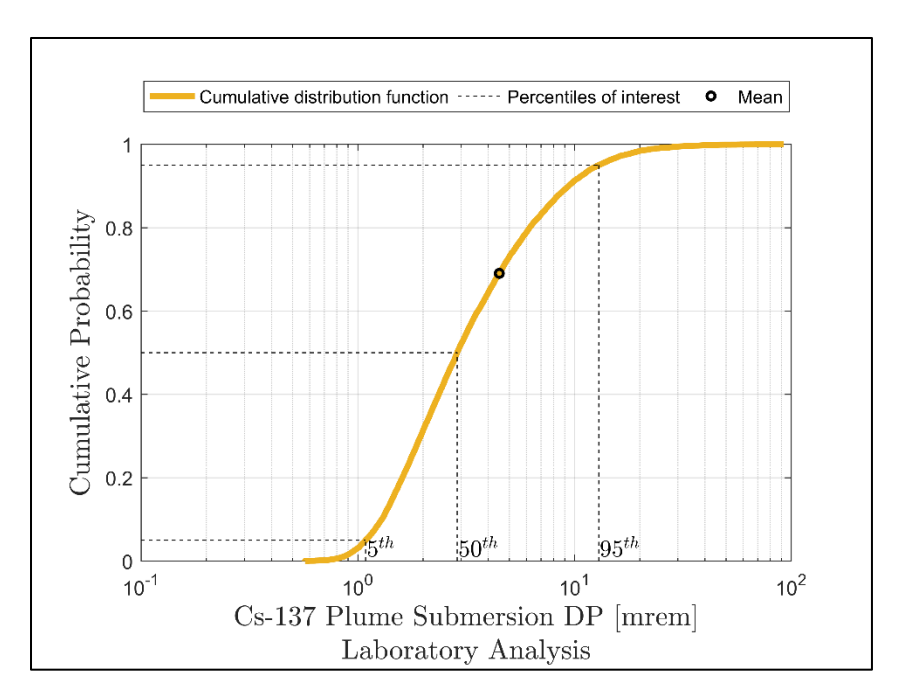


Figure 5.1-5. Cumulative probability with mean and percentiles of interest for the Cs-137 Plume Submersion DP for Laboratory Analysis.

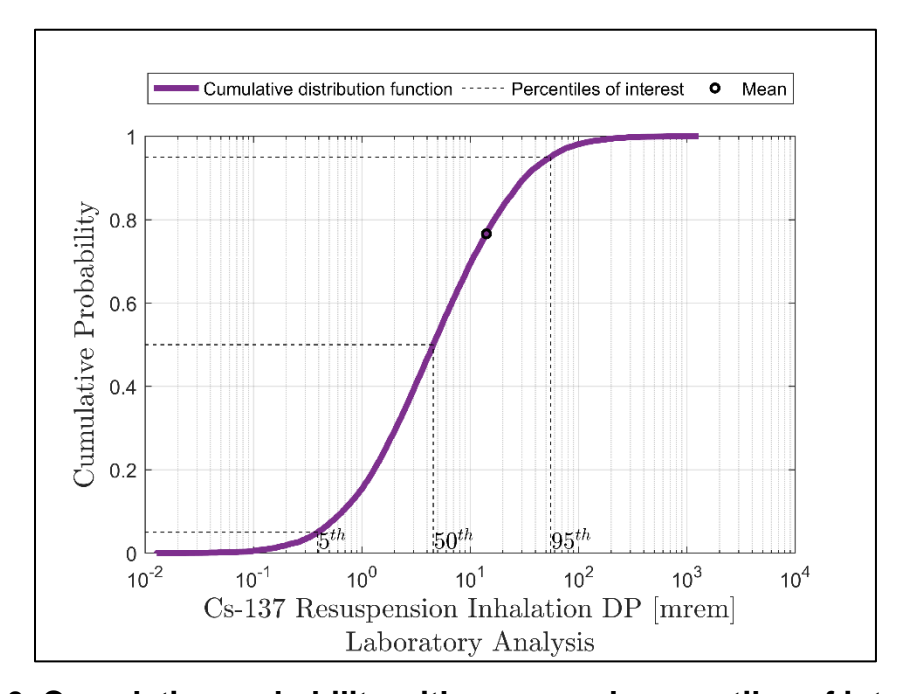


Figure 5.1-6. Cumulative probability with mean and percentiles of interest for the Cs-137 Resuspension Inhalation DP Laboratory Analysis.

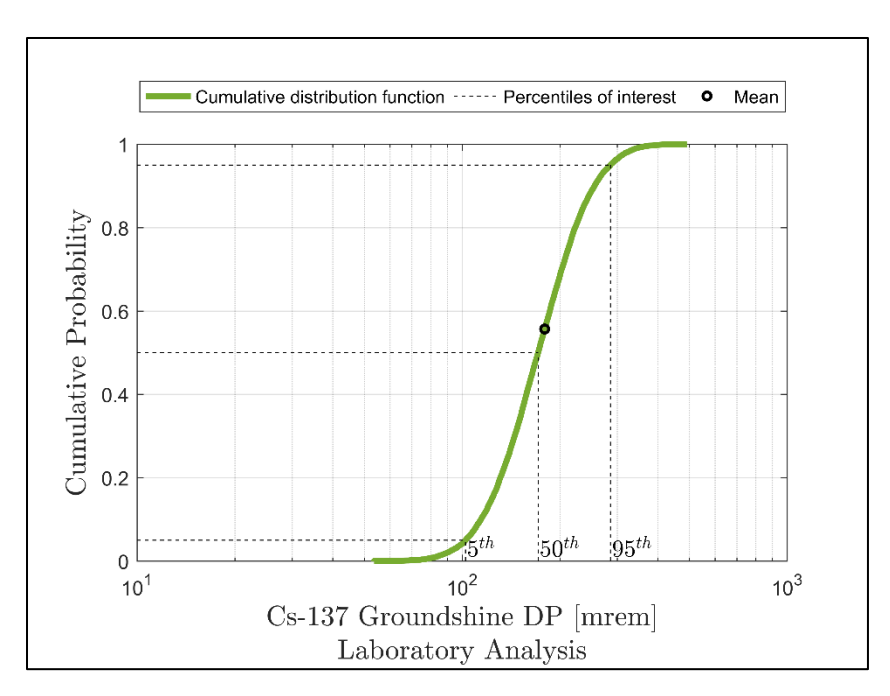


Figure 5.1-7. Cumulative probability with mean and percentiles of interest for the Cs-137 Groundshine DP Laboratory Analysis.

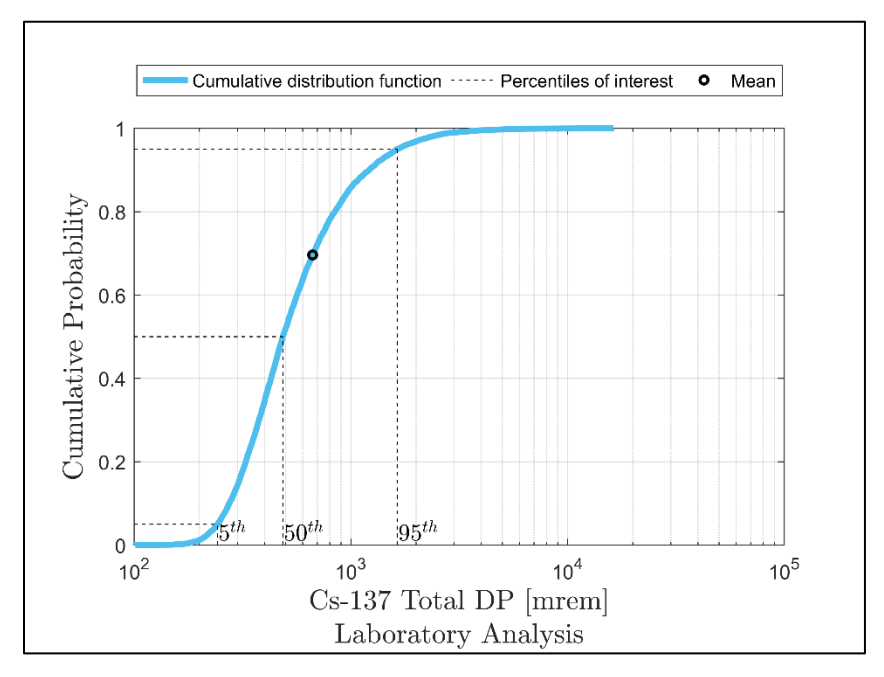


Figure 5.1-8. Cumulative probability with mean and percentiles of interest for the Cs-137 Total DP Laboratory Analysis.

The values given in the tables above describe the distributions of each of the outputs as approximated by the results of 10,000 Turbo FRMAC<sup>©</sup> simulations. The interpretation of these summary statistics provides information about the uncertainty in each of these outputs given the uncertainty in the inputs used in the study scenario. For example, the 95<sup>th</sup> percentile of the Dose Rate DRL is 7.066 mrem/hr. This means that 95% of the simulation results have a Dose Rate DRL that is less than 7.066 mrem/hr, but that 5% of the simulation results have a Dose Rate DRL that is greater than this value. The 5<sup>th</sup> percentile of the Dose Rate DRL is 0.989 mrem/hr. This means that 5% of the simulation results have a Dose Rate DRL that is less than 0.989 mrem/hr. This represents the "worst" portion of the Dose Rate DRL distribution from a CM perspective; this percentile used for the final Dose Rate DRL will result in a larger evacuation area.

The calculated values using the default inputs for each of the outputs shown in Table 5.1-1 and Table 5.1-2 lie between the 5<sup>th</sup> and 95<sup>th</sup> percentiles. This shows that the default values that are currently calculated and used to inform protective action decisions do not necessarily represent statistical outliers for this study scenario.

The mean Dose Rate and Deposition DRLs are double the default DRLs. This means that the default results for these DRLs are conservative. Deposition velocity is the greatest contributor to uncertainty. Figure 4.1-1 shows that the distribution for deposition velocity is skewed so that the mean deposition velocity is greater than the default, i.e., more material is deposited on the ground on average than in the default case. Because the mixture is based on activity per area for the Laboratory Analysis simulations, a higher deposition velocity reduces the amount of radioactive material in the air, therefore reducing the dose from the plume relative to contamination on the ground. This allows more activity to be on the ground to reach the PAG. Conversely, the mean Integrated Air DRL is half of the default DRL. This is because deposition velocity is inversely related to the Integrated Air DRL, unlike the other DRLs, as shown by the negative SRRC in the sensitivity analysis results given in Section 5.1.2. This means that less material is in the air than in the default case, allowing less to meet the PAG. The mean is much greater than the median for all DP results, demonstrating that the distributions of these results are more skewed than those for the DRL results in which the mean and median are much closer. This difference is reflected in the respective CDFs.

## 5.1.2. Sensitivity Analysis Results

The sensitivity analysis results for the DRLs and DPs are provided in Sections 5.1.2.1 and 5.1.2.2, respectively. A description of the statistical interpretation of these tables and figures is given in Section 3.3.2. In each table, the inputs are listed in order of importance with the most important input variable on the first row of each table. In this context, importance means that the variable has the strongest relationship with the output of interest and explains the greatest amount of output variance.

The equations for the four pathway DP results do not include some of the uncertain input variables that were used for each simulation. However, these inputs were included in the regression model to ensure a complete coverage of the uncertain input space. The regression results show that these inputs are not important to the uncertainty in the outputs, as would be expected. Inputs that are not included in result equations are shown in italics in the sensitivity analysis result tables for these DP outputs.

Note that the use of linear rank regression to quantify the relationship between input and output uncertainty assumes a model to describe this relationship and numerically approximates the behavior of this relationship. Spurious numerical results are possible, meaning that inputs that are not expected to have an impact on the final output uncertainty could have small individual R<sup>2</sup> and SRRC values. The overall R<sup>2</sup> values for each output show that the linear rank regression model appropriately captures the majority of output variance and that the ranking of the most important parameters is valid.

## 5.1.2.1. DRL Sensitivity Analysis Results

Table 5.1-3 through Table 5.1-5 include the sensitivity analysis results for the DRLs for the Laboratory Analysis simulations. Figure 5.1-9 through Figure 5.1-11 include scatter plots which show the relationship between the most important inputs and the output for each DRL.

The inputs for all three DRLs are ranked nearly the same, with deposition velocity contributing the most to the uncertainty in each DRL. Of the three DRLs, deposition velocity contributes the least to the Integrated Air DRL uncertainty. Inhalation dose coefficient multiplier uncertainty is the next most important input to DRL uncertainty, followed by light-exercise breathing rate uncertainty due to their contribution to the Total DP through the Plume Inhalation DP. Activity per area uncertainty does not contribute to DRL uncertainty because the mixture for this analysis is a single radionuclide, Cs-137. This means that Cs-137 (and daughter Ba-137m) is the sole contributor to the Total DP. As a result, activity per area is in both the numerator and denominator of the DRLs and is thus cancelled out. Activity-averaged breathing rate and the plume external dose coefficient multiplier appear to have little to no contribution to DRL uncertainty as well. This is partly because the distributions for these inputs are narrow relative to the other important inputs. Additionally, the activity-averaged breathing rate and plume external dose coefficient contribute to the Plume Submersion DP and Resuspension Inhalation DPs, respectively, and these DPs are dominated by the Plume Inhalation DP in the Total DP. Section 5.1.2.2 presents the DP sensitivity analysis results in greater detail.

Inputs that contribute to DRL uncertainty by contributing to Total DP uncertainty (in the denominator of the DRL equations) have a negative SRRC, meaning as those inputs increase, the DRL decreases. DRL inputs that have a positive SRRC are included in the numerator of the DRL equations, e.g., the weathering factor in the Dose Rate DRL and Cs-137 Deposition DRL. The SRRC for deposition velocity is positive for the Dose Rate and Cs-137 Deposition DRLs, as shown in the upper left scatter plots in Figure 5.1-9 and Figure 5.1-10, respectively. Conversely, the SRRC for deposition velocity is negative for the DRL to which it contributes least to uncertainty, the Cs-137 Integrated Air DRL. This relationship is shown in the upper left scatter plot in Figure 5.1-11.

Table 5.1-3. Sensitivity analysis results for the Dose Rate DRL for Laboratory Analysis.

Dose Rate DRL, R <sup>2</sup> = 0.936				
Variable Name	R <sup>2</sup> Individual	SRRC		
Deposition Velocity	0.574	0.758		
Inhalation Dose Coefficient Multiplier	0.186	-0.429		
Breathing Rate, Light Exercise, Adult Male	0.063	-0.249		
Deposition External Dose Coefficient Multiplier	0.061	0.249		
Weathering Coefficient Multiplier	0.037	0.192		
Ground Roughness Factor	0.011	0.105		
Resuspension Coefficient Multiplier	0.004	-0.062		
Activity per Area	0.000	0.000		
Plume External Dose Coefficient Multiplier	0.000	0.000		
Breathing Rate, Activity Averaged, Adult Male	0.000	-0.010		

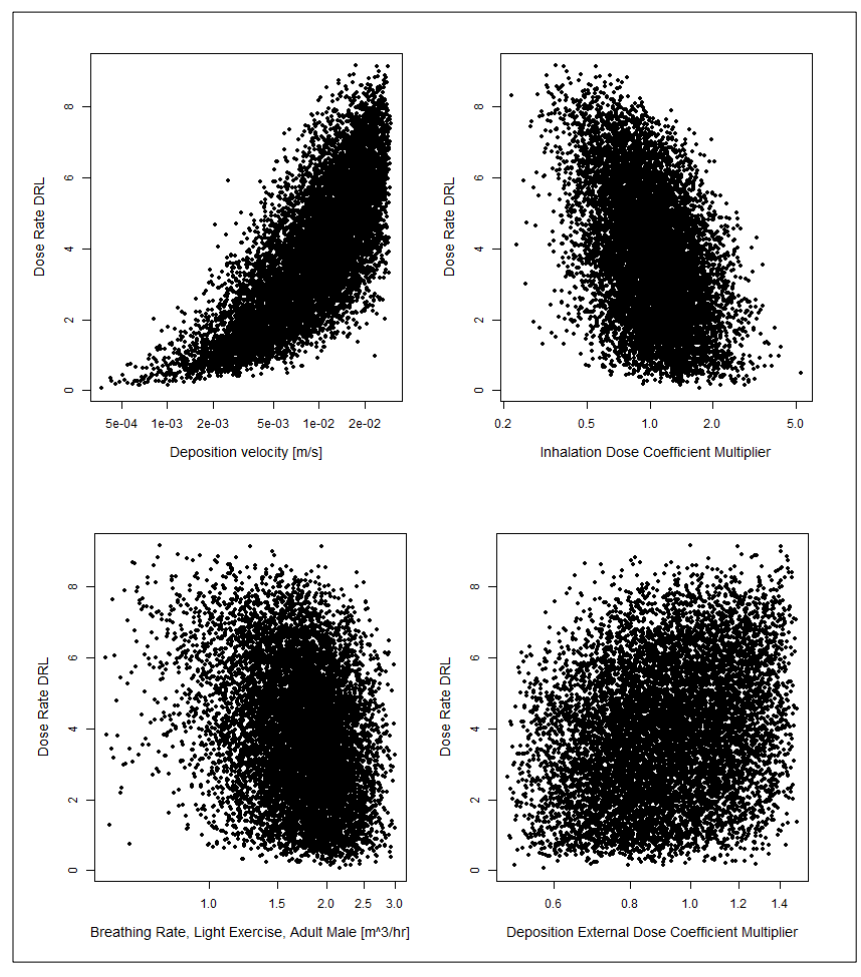


Figure 5.1-9. Scatter plots for the Dose Rate DRL for Laboratory Analysis and the first four inputs shown in Table 5.1-3.

Table 5.1-4. Sensitivity analysis results for the Cs-137 Deposition DRL for Laboratory Analysis.

Cs-137 Deposition DRL, R <sup>2</sup> = 0.924				
Variable Name	R <sup>2</sup> Individual	SRRC		
Deposition Velocity	0.603	0.777		
Inhalation Dose Coefficient Multiplier	0.187	-0.430		
Breathing Rate, Light Exercise, Adult Male	0.062	-0.250		
Weathering Coefficient Multiplier	0.036	0.189		
Deposition External Dose Coefficient Multiplier	0.027	-0.166		
Ground Roughness Factor	0.005	-0.069		
Resuspension Coefficient Multiplier	0.004	-0.059		
Activity per Area	0.000	0.000		
Plume External Dose Coefficient Multiplier	0.000	0.000		
Breathing Rate, Activity Averaged, Adult Male	0.000	-0.008		

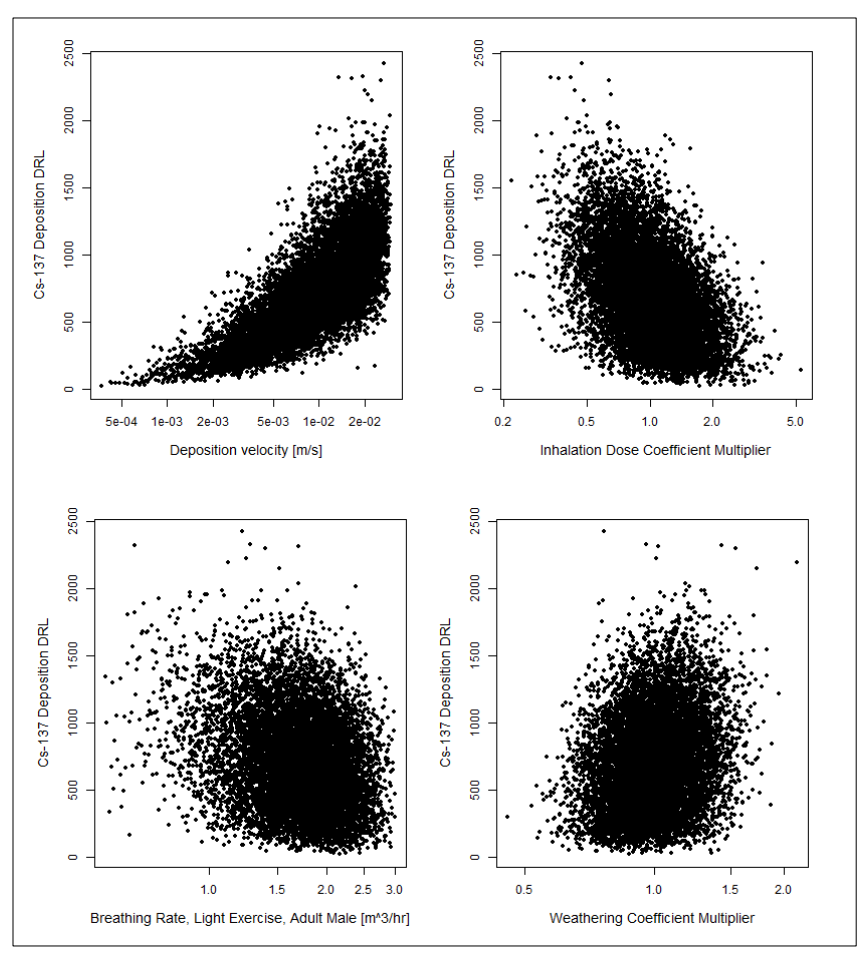


Figure 5.1-10. Scatter plots for the Cs-137 Deposition DRL for Laboratory Analysis and the first four inputs shown in Table 5.1-4.

Table 5.1-5. Sensitivity analysis results for the Cs-137 Integrated Air DRL for Laboratory Analysis.

Cs-137 Integrated Air DRL, R <sup>2</sup> = 0.905				
Variable Name	R <sup>2</sup> Individual	SRRC		
Deposition Velocity	0.379	-0.616		
Inhalation Dose Coefficient Multiplier	0.339	-0.580		
Breathing Rate, Light Exercise, Adult Male	0.113	-0.337		
Deposition External Dose Coefficient Multiplier	0.039	-0.198		
Weathering Coefficient Multiplier	0.026	-0.160		
Ground Roughness Factor	0.006	-0.078		
Resuspension Coefficient Multiplier	0.004	-0.064		
Activity per Area	0.000	0.000		
Plume External Dose Coefficient Multiplier	0.000	0.000		
Breathing Rate, Activity Averaged, Adult Male	0.000	-0.005		

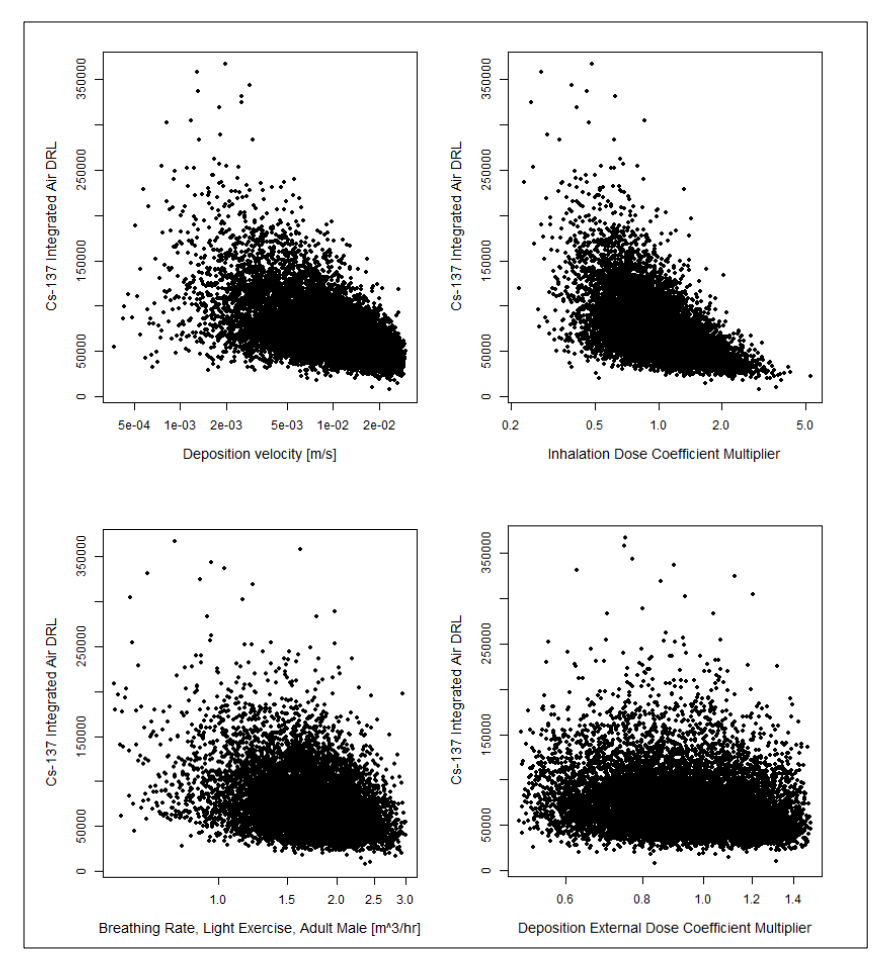


Figure 5.1-11. Scatter plots for the Cs-137 Integrated Air DRL for Laboratory Analysis and the first four inputs shown in Table 5.1-5.

## 5.1.2.2. DP Sensitivity Analysis Results

Table 5.1-6 through Table 5.1-10 provide the sensitivity analysis results for the DPs for the Laboratory Analysis simulations. Figure 5.1-12 through Figure 5.1-16 show scatter plots which demonstrate the relationship between the most important inputs and the output for each DP.

Deposition velocity contributes most to the uncertainty for the plume pathways for the Laboratory Analysis simulations, as shown by its rank in Table 5.1-6 and Table 5.1-7. Deposition velocity has the widest distribution of all of the plume pathway inputs. This input is not important for the ground pathways because ground pathways are based on activity per area. Conversely, the plume pathways are based on integrated air activity, and deposition velocity is used to convert activity per area to integrated air activity. The SRRC is negative for deposition velocity for the plume pathways because if activity per area is fixed and deposition velocity increases, integrated air activity decreases, thus decreasing the plume DPs (i.e., deposition velocity and plume dose are inversely related). This strong relationship is shown in the upper left scatter plots in Figure 5.1-12 and Figure 5.1-13. All of the other inputs have positive SRRCs and are therefore directly related to the DPs.

For the Laboratory Analysis simulations, the mean DP is greater than the default DP for the Resuspension Inhalation DP only, as shown in Table 5.1-2. The resuspension coefficient multiplier uncertainty dominates the Resuspension Inhalation DP due to its broad distribution relative to the other inputs used to calculate this parameter. This strong relationship is reflected in the SRRC in Table 5.1-8 and the upper left scatter plot in Figure 5.1-14. The mean of the distribution for the resuspension coefficient multiplier is nearly three times the default, as shown in Figure 4.1-7. Additionally, the spread between the 5<sup>th</sup> and 95<sup>th</sup> percentiles is also largest for the Resuspension Inhalation DP. As previously noted, the uncertainty in the plume DPs is mostly driven by the deposition velocity, for which the mean is also greater than the default. However, since deposition velocity has an inverse relationship with the plume DPs, the mean is not greater than the default for these outputs.

Table 5.1-9 shows that the deposition external dose coefficient multiplier uncertainty is the largest contributor to uncertainty in the Groundshine DP, followed by the weathering coefficient multiplier uncertainty and ground roughness uncertainty. These drivers for ground pathway uncertainty do not appear to be as important for the Total DP, which is the ultimate parameter used in the denominator of the DRL calculations. The Total DP uncertainty is driven by deposition velocity uncertainty, followed by Inhalation Dose Coefficient Multiplier uncertainty, as shown in Table 5.1-10. These are the most important inputs to the Plume Inhalation DP. Because 80% of the total dose comes from plume inhalation for the default case, these inputs are therefore important in the Total DP.

Table 5.1-6. Sensitivity analysis results for the Cs-137 Plume Inhalation DP for Laboratory Analysis.

Cs-137 Plume Inhalation DP, R <sup>2</sup> = 0.953				
Variable Name	R <sup>2</sup> Individual	SRRC		
Deposition Velocity	0.673	-0.820		
Inhalation Dose Coefficient Multiplier	0.203	0.449		
Breathing Rate, Light Exercise, Adult Male	0.073	0.271		
Activity per Area	0.003	0.058		
Ground Roughness Factor	0.000	0.000		
Resuspension Coefficient Multiplier	0.000	0.000		
Weathering Coefficient Multiplier	0.000	0.000		
Breathing Rate, Activity Averaged, Adult Male	0.000	0.000		
Deposition External Dose Coefficient Multiplier	0.000	0.000		
Plume External Dose Coefficient Multiplier	0.000	0.000		

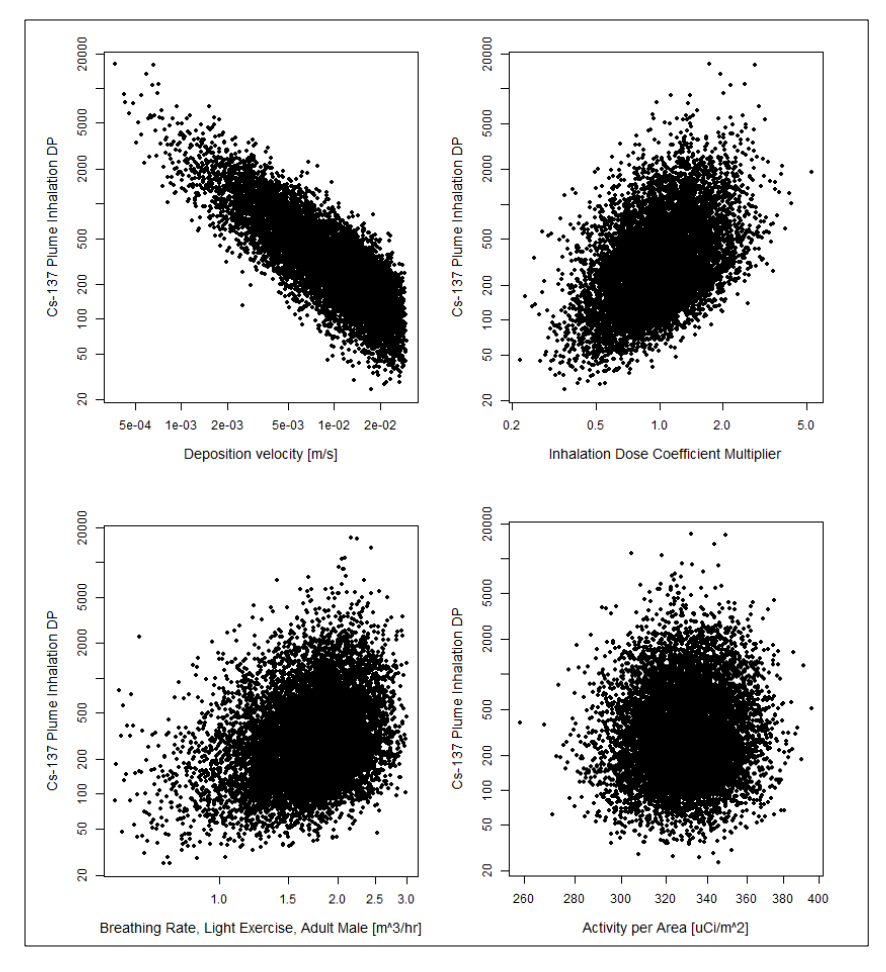


Figure 5.1-12. Scatter plots for the Cs-137 Plume Inhalation DP for Laboratory Analysis and the first four inputs shown in Table 5.1-6.

Table 5.1-7. Sensitivity analysis results for the Cs-137 Plume Submersion DP for Laboratory Analysis.

Cs-137 Plume Submersion DP, R <sup>2</sup> = 0.987				
Variable Name	R <sup>2</sup> Individual	SRRC		
Deposition Velocity	0.895	-0.945		
Plume External Dose Coefficient Multiplier	0.088	0.296		
Activity per Area	0.004	0.065		
Breathing Rate, Light Exercise, Adult Male	0.000	0.000		
Ground Roughness Factor	0.000	0.000		
Inhalation Dose Coefficient Multiplier	0.000	0.000		
Resuspension Coefficient Multiplier	0.000	0.000		
Weathering Coefficient Multiplier	0.000	0.000		
Breathing Rate, Activity Averaged, Adult Male	0.000	0.000		
Deposition External Dose Coefficient Multiplier	0.000	0.000		

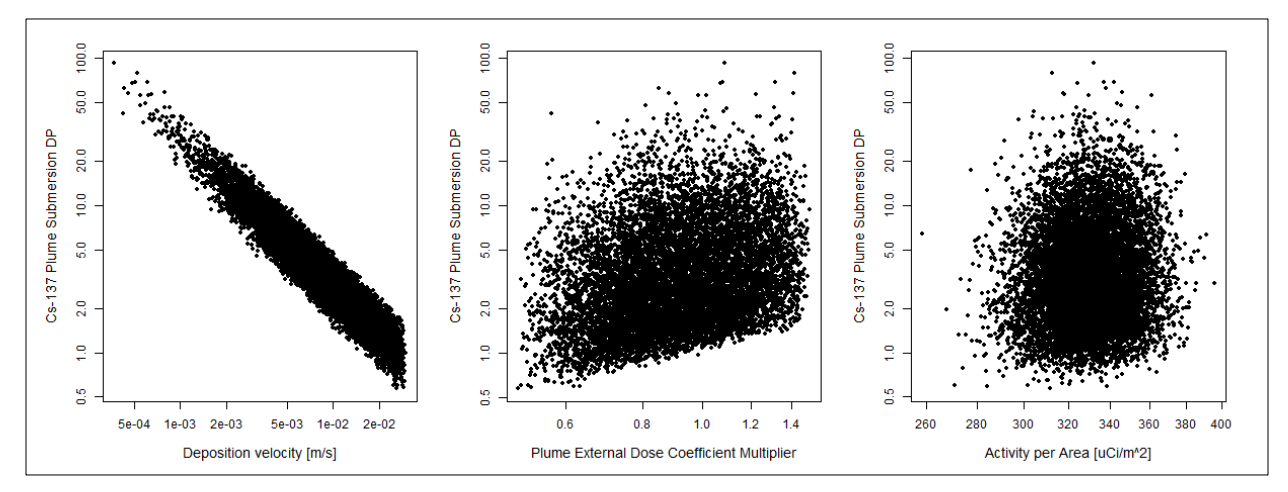


Figure 5.1-13. Scatter plots for the Cs-137 Plume Submersion DP for Laboratory Analysis and the first three inputs shown in Table 5.1-7.

Table 5.1-8. Sensitivity analysis results for the Cs-137 Resuspension Inhalation DP for Laboratory Analysis.

Cs-137 Resuspension Inhalation DP, R <sup>2</sup> = 0.985				
Variable Name	R <sup>2</sup> Individual	SRRC		
Resuspension Coefficient Multiplier	0.900	0.948		
Inhalation Dose Coefficient Multiplier	0.066	0.257		
Breathing Rate, Activity Averaged, Adult Male	0.017	0.131		
Activity per Area	0.001	0.032		
Breathing Rate, Light Exercise, Adult Male	0.000	0.000		
Ground Roughness Factor	0.000	0.000		
Weathering Coefficient Multiplier	0.000	0.000		
Deposition velocity	0.000	0.000		
Deposition External Dose Coefficient Multiplier	0.000	0.000		
Plume External Dose Coefficient Multiplier	0.000	0.000		

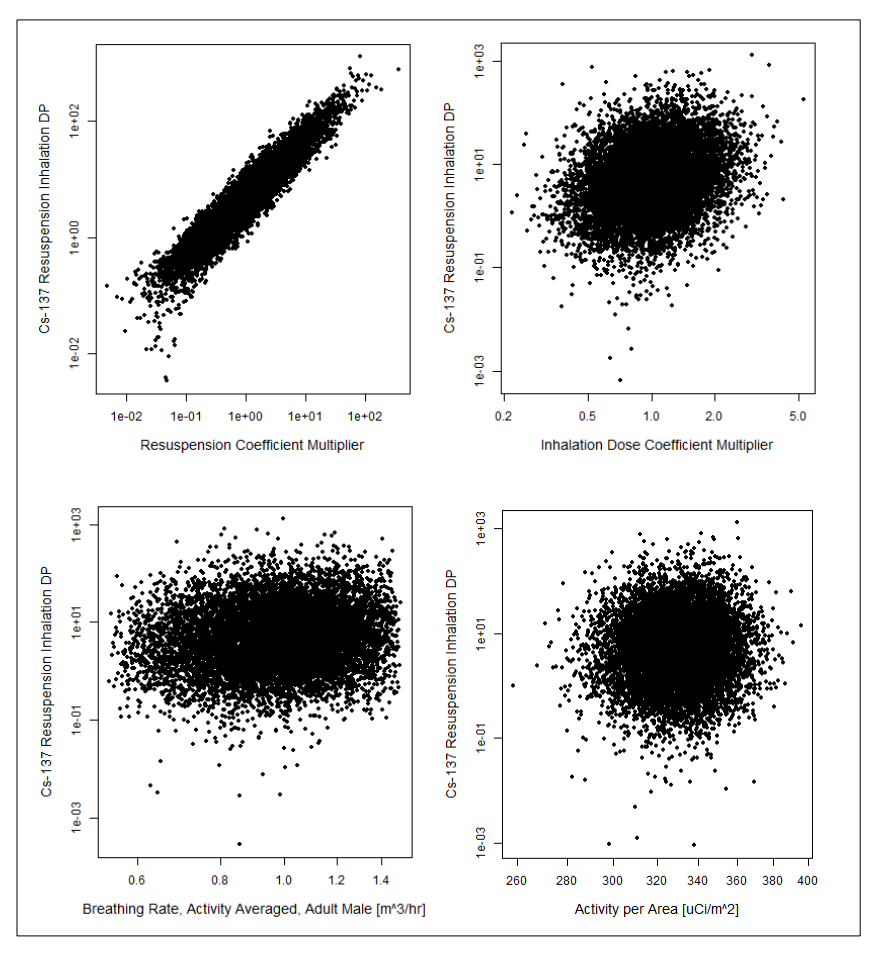


Figure 5.1-14. Scatter plots for the Cs-137 Resuspension Inhalation DP for Laboratory Analysis and the first four inputs shown in Table 5.1-8.

Table 5.1-9. Sensitivity analysis results for the Cs-137 Groundshine DP for Laboratory Analysis.

Cs-137 Groundshine DP, R <sup>2</sup> = 0.951				
Variable Name	R <sup>2</sup> Individual	SRRC		
Deposition External Dose Coefficient Multiplier	0.522	0.726		
Weathering Coefficient Multiplier	0.319	0.562		
Ground Roughness Factor	0.087	0.295		
Activity per Area	0.024	0.155		
Breathing Rate, Light Exercise, Adult Male	0.000	0.000		
Inhalation Dose Coefficient Multiplier	0.000	0.000		
Resuspension Coefficient Multiplier	0.000	0.000		
Deposition Velocity	0.000	0.000		
Breathing Rate, Activity Averaged, Adult Male	0.000	0.000		
Plume External Dose Coefficient Multiplier	0.000	-0.007		

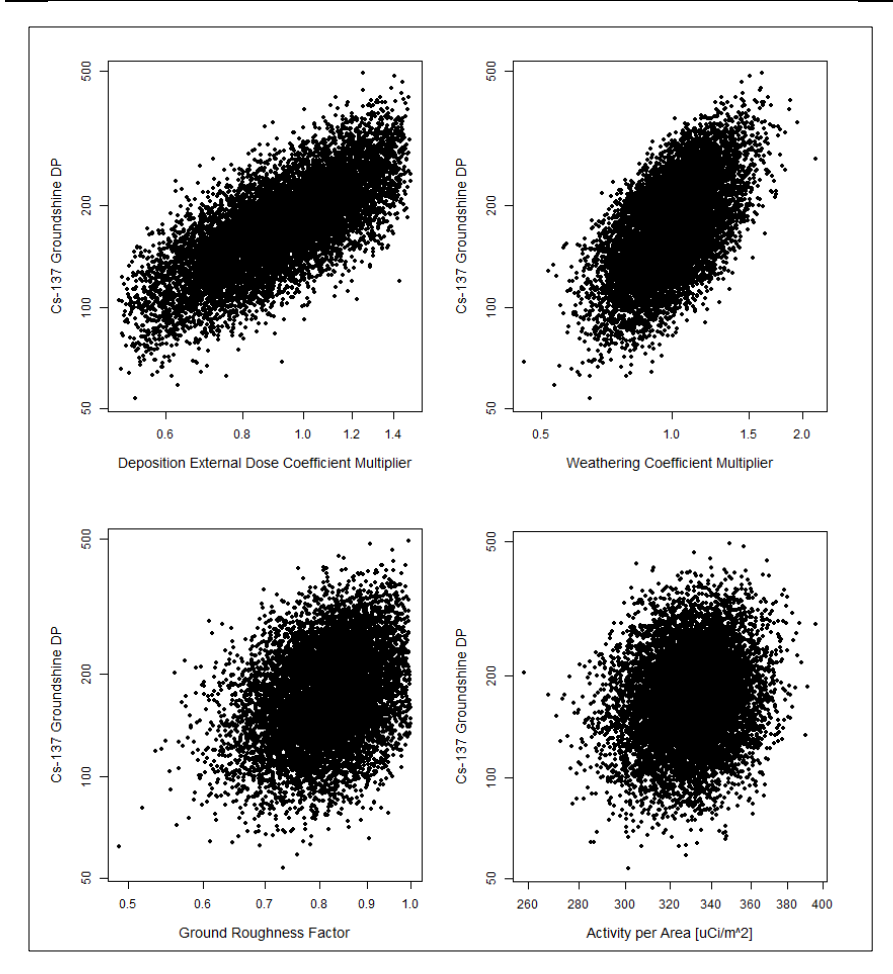


Figure 5.1-15. Scatter plots for the Cs-137 Groundshine DP for Laboratory Analysis and the first four inputs shown in Table 5.1-9.

Table 5.1-10. Sensitivity analysis results for the Cs-137 Total DP for Laboratory Analysis.

Cs-137 Total DP, R <sup>2</sup> = 0.919				
Variable Name	R <sup>2</sup> Individual	SRRC		
Deposition Velocity	0.612	-0.782		
Inhalation Dose Coefficient Multiplier	0.184	0.428		
Breathing Rate, Light Exercise, Adult Male	0.061	0.249		
Deposition External Dose Coefficient Multiplier	0.027	0.164		
Weathering Coefficient Multiplier	0.018	0.135		
Activity per Area	0.009	0.095		
Ground Roughness Factor	0.004	0.067		
Resuspension Coefficient Multiplier	0.004	0.059		
Breathing Rate, Activity Averaged, Adult Male	0.000	0.006		
Plume External Dose Coefficient Multiplier	0.000	0.000		

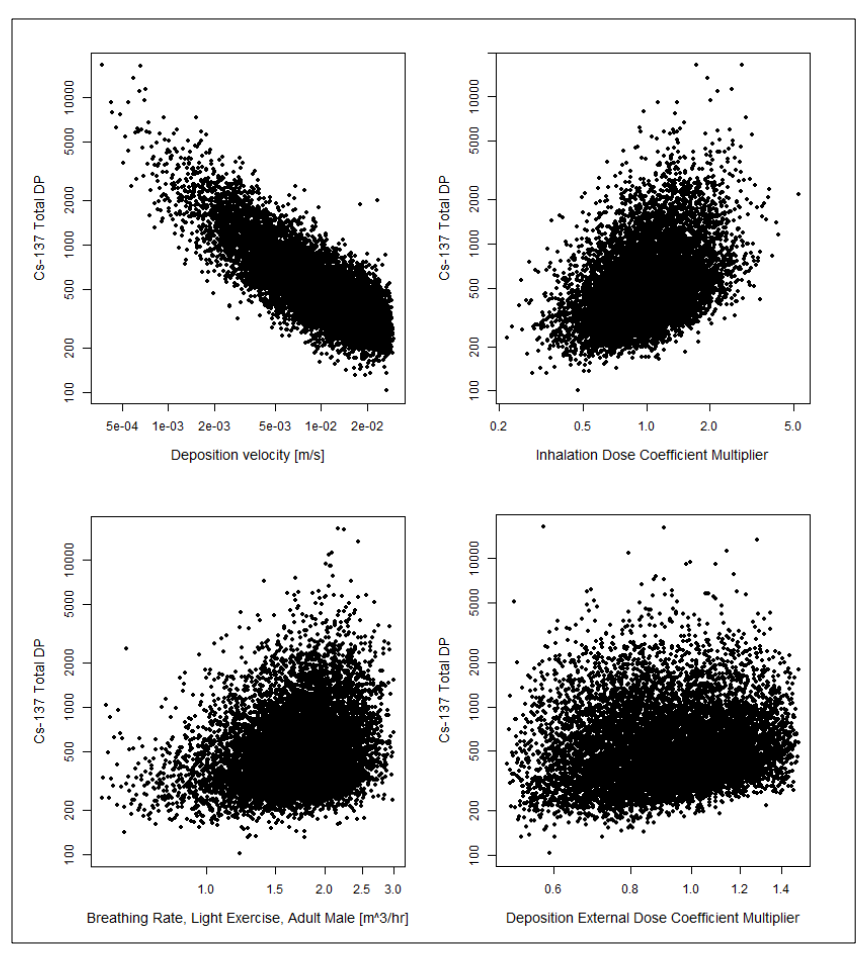


Figure 5.1-16. Scatter plots for the Cs-137 Total DP for Laboratory Analysis and the first four inputs shown in Table 5.1-10.

# 5.1.3. Sampling Confidence intervals

The table below shows the sampling CIs calculated about the mean for each output of interest. The sample mean is also shown for reference for each output. The steps used to calculate the CIs are described in Section 3.3.3. These 95% CIs are interpreted as follows: 'there is a 95% confidence that the true value of the mean falls within this interval.' The results given in Table 5.1-11 show that the estimate of the mean is well characterized by the 10,000 LHS samples used to quantify the uncertainty in each of the outputs of interest.

Table 5.1-11. Sampling confidence intervals for Laboratory Analysis simulations.

Output Name	Lower Bound of 95% CI	Mean	Upper Bound of 95% CI
Dose Rate DRL [mrem/hr]	3.83	3.87	3.91
Cs-137 Deposition DRL [μCi/m²]	706	713	719
Cs-137 Integrated Air DRL [µCi-s/m³]	75200	75900	76500
Cs-137 Plume Inhalation DP [mrem]	456	469	481
Cs-137 Plume Submersion DP [mrem]	4.40	4.50	4.60
Cs-137 Resuspension Inhalation DP [mrem]	13.4	14.1	14.9
Cs-137 Groundshine DP [mrem]	178	179	181
Cs-137 Total DP [mrem]	654	667	681

#### 5.2. NARAC

The NARAC-based distribution for integrated air activity was used along with the other input distributions discussed in Section 4.1 to run 10,000 simulations of Turbo FRMAC<sup>©</sup>. The results of the statistical analysis of these simulations are given in the following subsections, including percentiles on the DRL and DP results for the NARAC simulations, a ranking of the important inputs for each of the DRL and DP results, and a convergence analysis for the simulations.

# 5.2.1. Uncertainty Analysis Results

The results for the uncertainty analysis of CM data products using the activity distribution derived from uncertainty in NARAC air concentration are given in this section.

Table 5.2-1 and Table 5.2-2 below show the mean, 5<sup>th</sup>, 50<sup>th</sup>, and 95<sup>th</sup> for each of the outputs considered in this analysis. These values are percentiles of the distribution for each output defined by the 10,000 realizations in the simulation for this activity source. The CDFs for each of these outputs are also shown for the DRL outputs in Figure 5.2-1 through Figure 5.2-3 and for the DP outputs in Figure 5.2-4 through Figure 5.2-8. Note that because the distributions for each of the four pathway DPs are different, they cannot be directly summed to get the distribution for the Total DP.

Table 5.2-1. DRL uncertainty results for NARAC simulations.

Output Name	Default	Mean	5th	50th	95th
Dose Rate DRL [mrem/hr]	1.98	3.868	0.979	3.784	7.077
Cs-137 Deposition DRL [μCi/m²]	3.31E2	712.554	191.446	684.924	1337.570
Cs-137 Integrated Air DRL [μCi-s/m³]	1.10E5	75875.319	35851.234	68229.968	141719.457

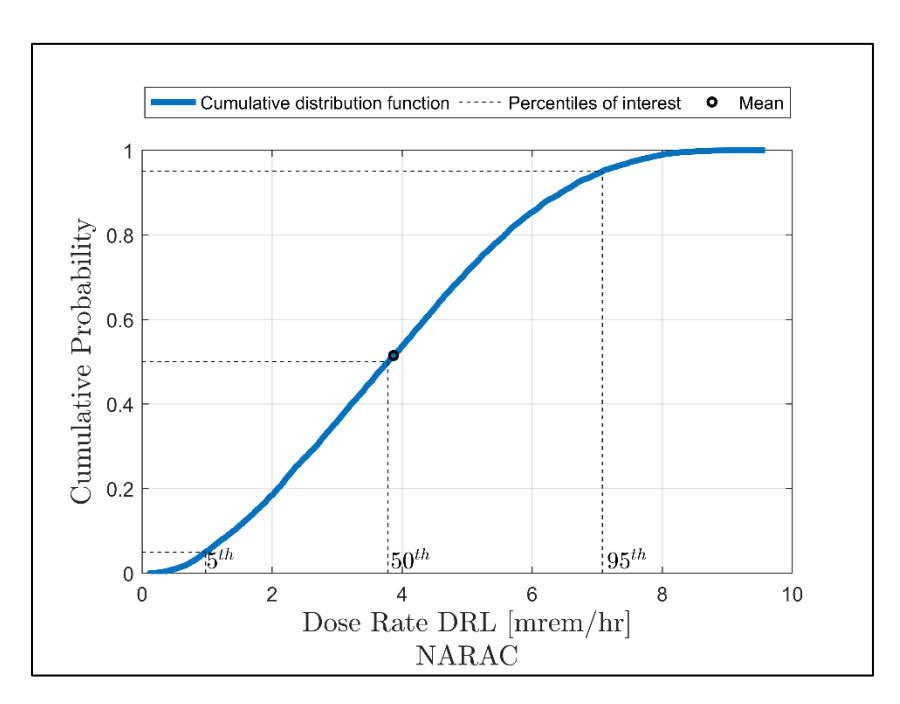


Figure 5.2-1. Cumulative probability with mean and percentiles of interest for the Dose Rate DRL results for NARAC.

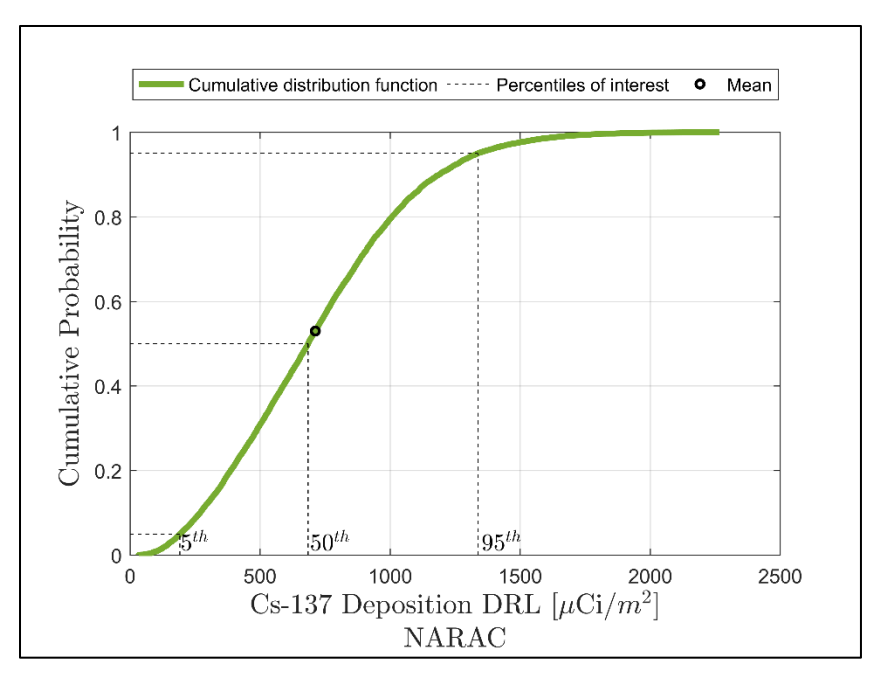


Figure 5.2-2. Cumulative probability with mean and percentiles of interest for the Cs-137 Deposition DRL for NARAC.

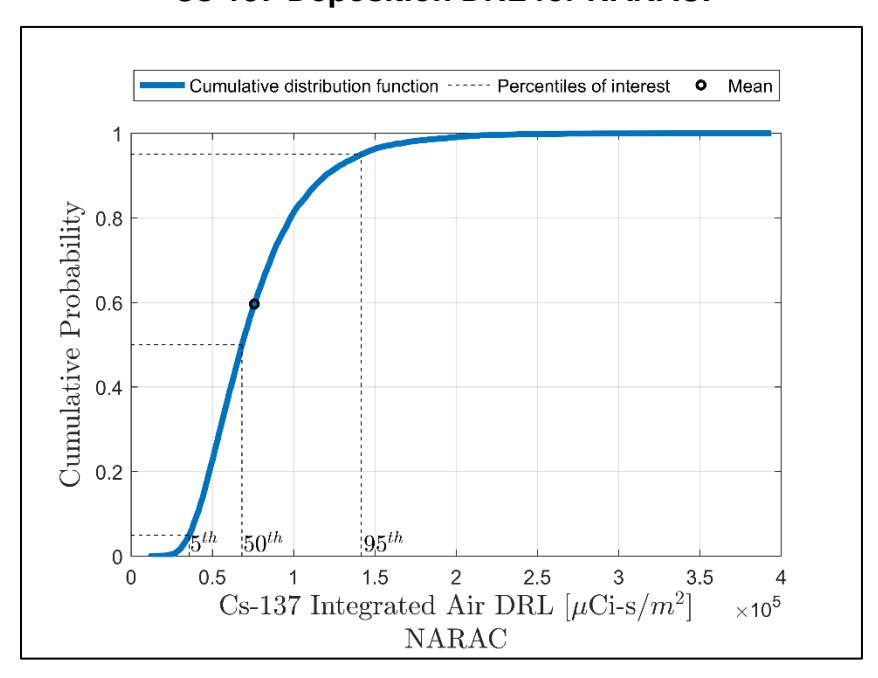


Figure 5.2-3. Cumulative probability with mean and percentiles of interest for the Cs-137 Integrated Air DRL for NARAC.

Table 5.2-2. DP uncertainty results for NARAC simulations.

Output Name	Default	Mean	5th	50th	95th
Cs-137 Plume Inhalation DP [mrem]	7.93E2	1545.600	46.646	543.879	5867.312
Cs-137 Plume Submersion DP [mrem]	10.4	14.704	0.548	5.556	56.854
Cs-137 Resuspension Inhalation DP [mrem]	4.42	78.834	0.222	8.040	300.661
Cs-137 Groundshine DP [mrem]	1.89E2	1023.456	20.256	303.108	4034.818
Cs-137 Total DP [mrem]	9.97E2	2662.594	85.605	965.488	10178.488

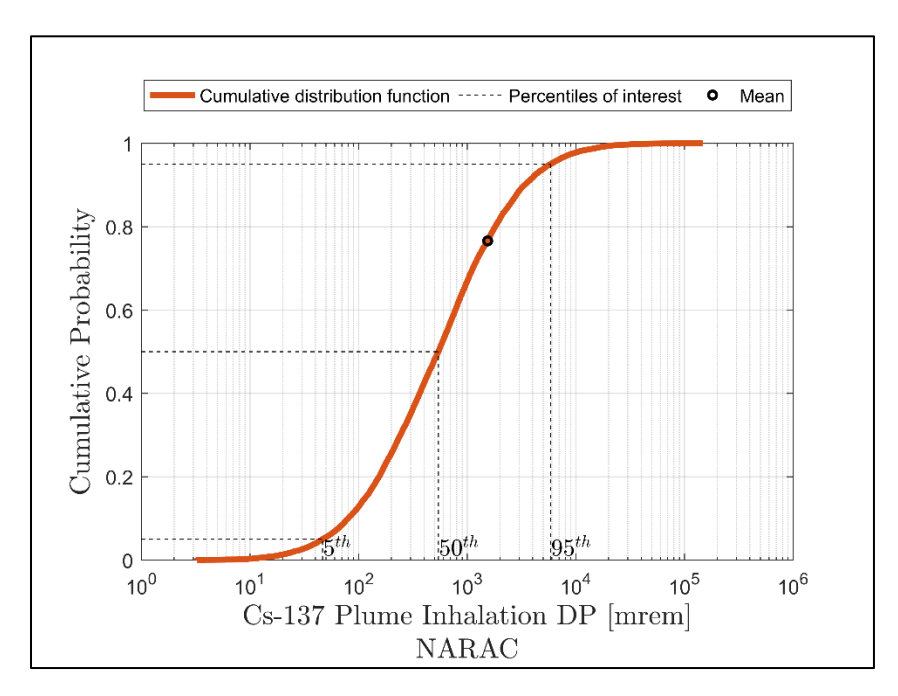


Figure 5.2-4. Cumulative probability with mean and percentiles of interest for the Cs-137 Plume Inhalation DP for NARAC.

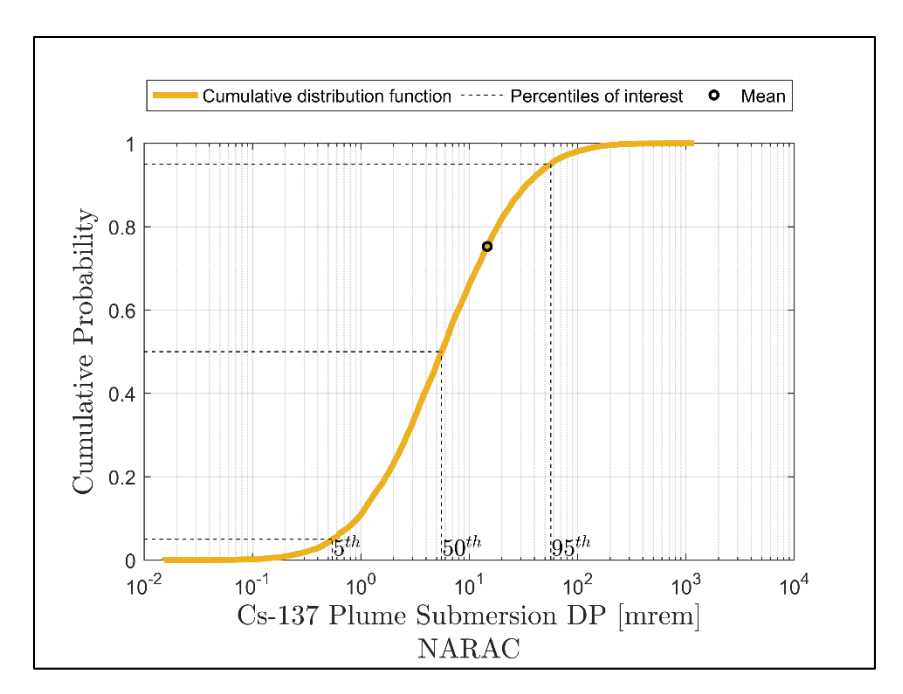


Figure 5.2-5. Cumulative probability with mean and percentiles of interest for the Cs-137 Plume Submersion DP for NARAC.

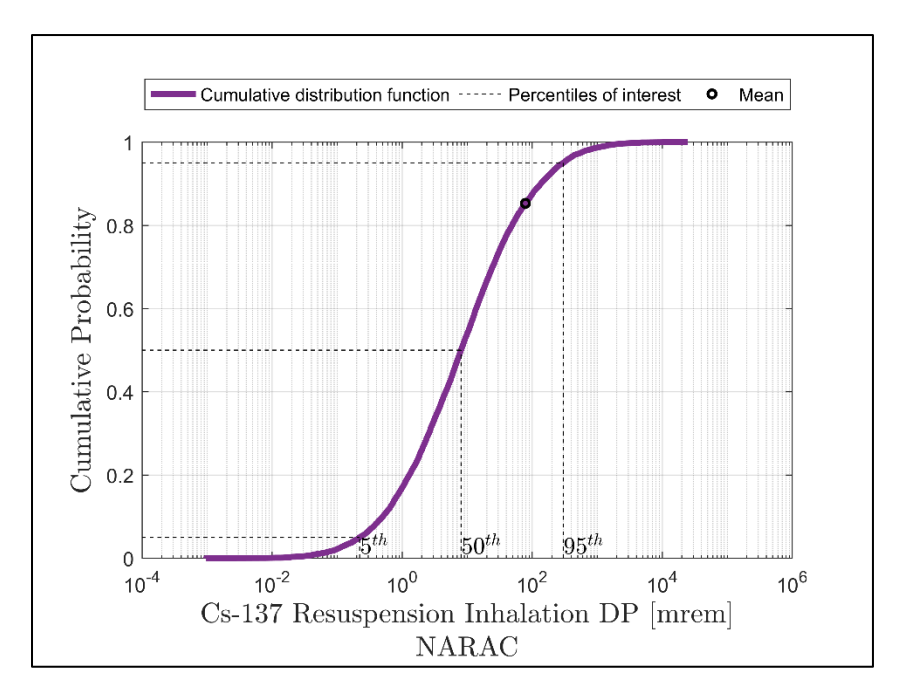


Figure 5.2-6. Cumulative probability with mean and percentiles of interest for the Cs-137 Resuspension Inhalation DP for NARAC.

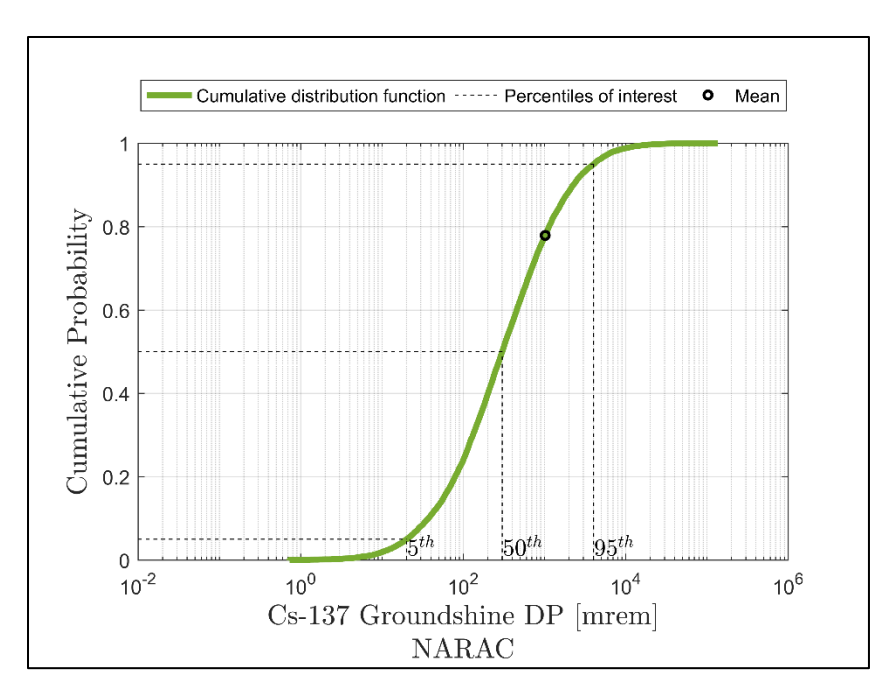


Figure 5.2-7. Cumulative probability with mean and percentiles of interest for the Cs-137 Groundshine DP for NARAC.

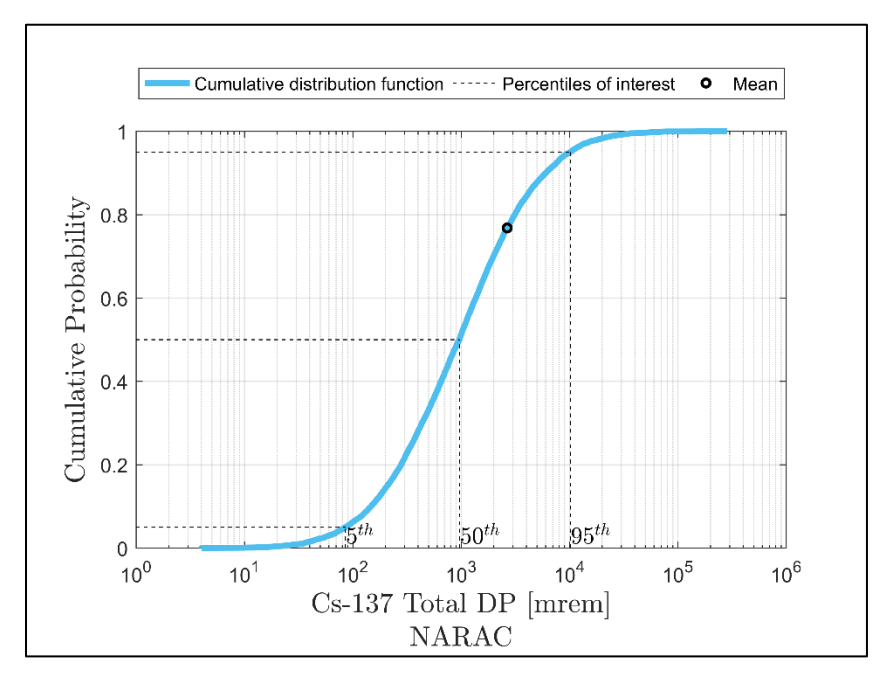


Figure 5.2-8. Cumulative probability with mean and percentiles of interest for the Cs-137 Total DP for NARAC.

The calculated values using the default inputs for each of the outputs shown in Table 5.2-1 and Table 5.2-2 lie between the 5<sup>th</sup> and 95<sup>th</sup> percentiles. This shows that the default values that are currently calculated and used to inform protective action decisions do not necessarily represent statistical outliers for this study scenario.

The DRL results for the NARAC simulations are nearly the same as the DRL results for the Laboratory Analysis simulations. The sole difference between these two simulations is that the mixture for the NARAC simulations was based on integrated air activity, while the mixture for the Laboratory Analysis simulations was based on activity per area. Although the distributions for these two concentrations are different, the difference is not reflected in the DRL results because these inputs are cancelled out in the DRL ratio. The difference is reflected in the DP results. The distribution for the air concentration multiplier is wider than the distribution for the Laboratory Analysis-based activity per area. This causes the difference in the 5<sup>th</sup> and 95<sup>th</sup> percentiles for the DPs to be much greater for the NARAC simulations than the Laboratory Analysis simulations. These results are graphically compared in Section 5.3.2.

## 5.2.2. Sensitivity Analysis Results

The sensitivity analysis results for the DRLs and DPs are provided in Sections 5.2.2.1 and 5.2.2.2, respectively. A description of the statistical interpretation of these tables and figures is given in Section 3.3.2. In each table, the inputs are listed in order of importance with the most important input variable on the first row of each table. In this context, importance means that the variable has the strongest relationship with the output of interest and explains the greatest amount of output variance.

The equations for the four pathway DP results do not include some of the uncertain input variables that were used for each simulation. However, these inputs were included in the regression model to ensure a complete coverage of the uncertain input space. The regression results show that these inputs are not important to the uncertainty in the outputs, as would be expected. Inputs that are not included in result equations are shown in italics in the sensitivity analysis result tables for these DP outputs.

Note that the use of linear rank regression to quantify the relationship between input and output uncertainty assumes a model to describe this relationship and numerically approximates the behavior of this relationship. Spurious numerical results are possible, meaning that inputs that are not expected to have an impact on the final output uncertainty could have small individual R<sup>2</sup> and SRRC values. The overall R<sup>2</sup> values for each output show that the linear rank regression model appropriately captures the majority of output variance and that the ranking of the most important parameters is valid.

#### 5.2.2.1. DRL Sensitivity Analysis Results

Table 5.2-3 through Table 5.2-5 include the sensitivity analysis results for the DRLs for the NARAC simulations. Figure 5.2-9 through Figure 5.2-11 include scatter plots which show the relationship between the most important inputs and the output for each DRL.

The DRLs for the NARAC simulations have essentially the same sensitivity results as the DRLs for the Laboratory Analysis simulations. The inputs for all three DRLs are ranked nearly the same, with deposition velocity contributing the most to each DRL. Inhalation dose coefficient multiplier uncertainty is the next important input to DRL uncertainty, followed by light-exercise breathing rate uncertainty, again due to their contribution to the Total DP through the Plume Inhalation DP. Similar to activity per area in the Laboratory Analysis simulations, the air concentration multiplier uncertainty does not contribute to DRL uncertainty because it is in both the numerator and denominator of the DRL equations and is thus cancelled out.

Table 5.2-3. Sensitivity analysis results for the Dose Rate DRL for NARAC.

Dose Rate DRL, R <sup>2</sup> = 0.934				
Variable Name	R <sup>2</sup> Individual	SRRC		
Deposition Velocity	0.576	0.759		
Inhalation Dose Coefficient Multiplier	0.186	-0.431		
Breathing Rate, Light Exercise, Adult Male	0.062	-0.247		
Deposition External Dose Coefficient Multiplier	0.059	0.243		
Weathering Coefficient Multiplier	0.038	0.194		
Ground Roughness Factor	0.011	0.104		
Resuspension Coefficient Multiplier	0.003	-0.059		
Breathing Rate, Activity Averaged, Adult Male	0.000	-0.014		
Air Concentration Multiplier	0.000	0.000		
Plume External Dose Coefficient Multiplier	0.000	0.000		

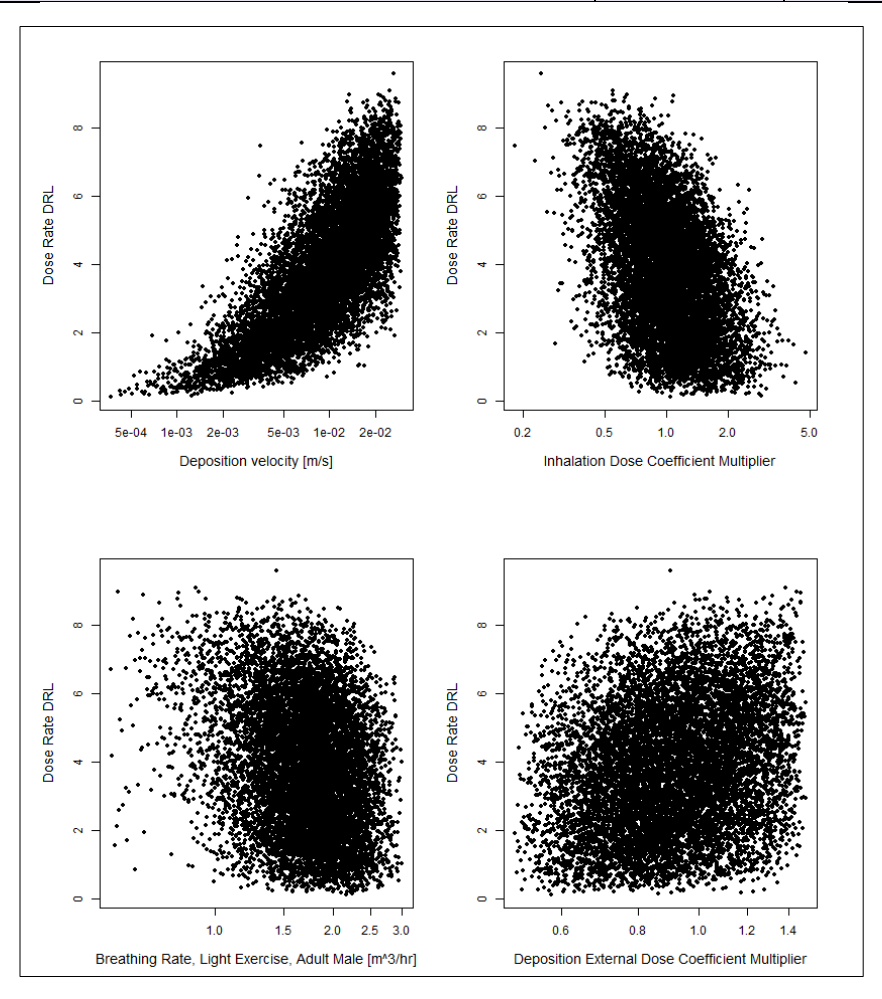


Figure 5.2-9. Scatter plots for the Dose Rate DRL for NARAC and the first four inputs shown in Table 5.2-3.

Table 5.2-4. Sensitivity analysis results for the Cs-137 Deposition DRL for NARAC.

Cs-137 Deposition DRL, R <sup>2</sup> = 0.924				
Variable Name	R <sup>2</sup> Individual	SRRC		
Deposition Velocity	0.601	0.777		
Inhalation Dose Coefficient Multiplier	0.185	-0.432		
Breathing Rate, Light Exercise, Adult Male	0.062	-0.250		
Weathering Coefficient Multiplier	0.038	0.195		
Deposition External Dose Coefficient Multiplier	0.029	-0.170		
Ground Roughness Factor	0.005	-0.072		
Resuspension Coefficient Multiplier	0.004	-0.059		
Breathing Rate, Activity Averaged, Adult Male	0.000	-0.012		
Air Concentration Multiplier	0.000	0.000		
Plume External Dose Coefficient Multiplier	0.000	0.000		

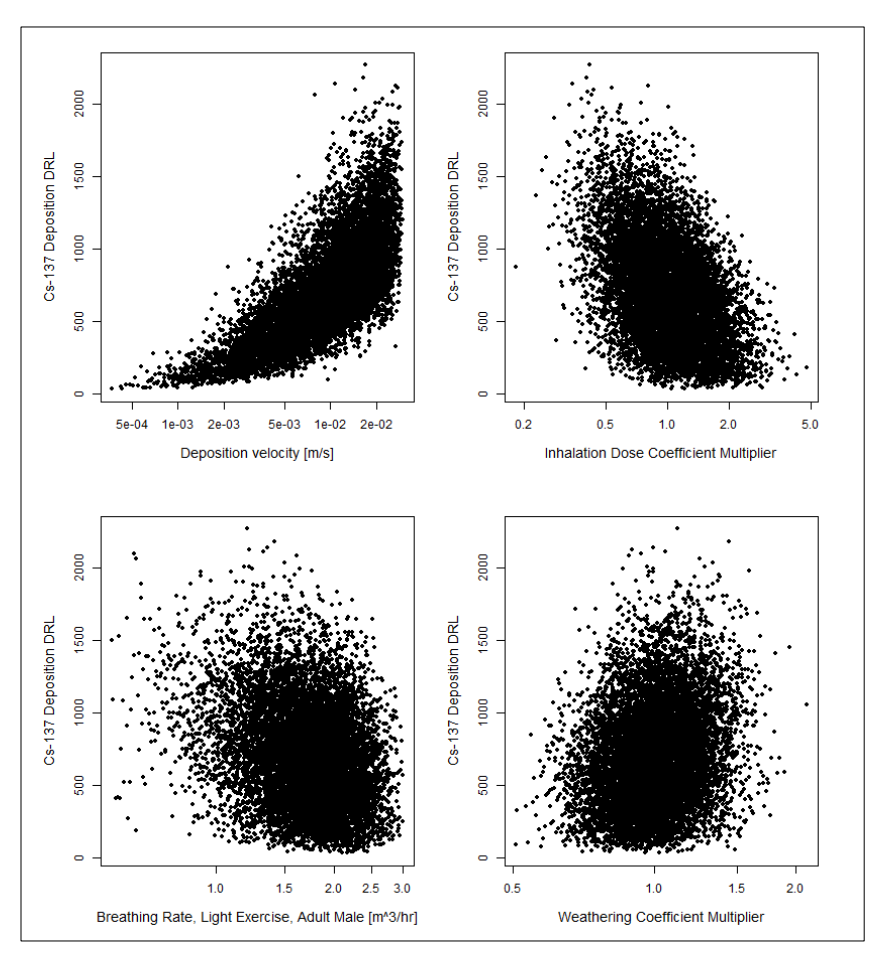


Figure 5.2-10. Scatter plots for the Cs-137 Deposition DRL for NARAC and the first four inputs shown in Table 5.2-4.

Table 5.2-5. Sensitivity analysis results for the Cs-137 Integrated Air DRL for NARAC.

Cs-137 Integrated Air DRL, R <sup>2</sup> = 0.904				
Variable Name	R <sup>2</sup> Individual	SRRC		
Deposition Velocity	0.381	-0.614		
Inhalation Dose Coefficient Multiplier	0.338	-0.583		
Breathing Rate, Light Exercise, Adult Male	0.111	-0.334		
Deposition External Dose Coefficient Multiplier	0.037	-0.193		
Weathering Coefficient Multiplier	0.026	-0.160		
Ground Roughness Factor	0.007	-0.081		
Resuspension Coefficient Multiplier	0.005	-0.068		
Air Concentration Multiplier	0.000	0.000		
Plume External Dose Coefficient Multiplier	0.000	0.000		
Breathing Rate, Activity Averaged, Adult Male	0.000	-0.009		

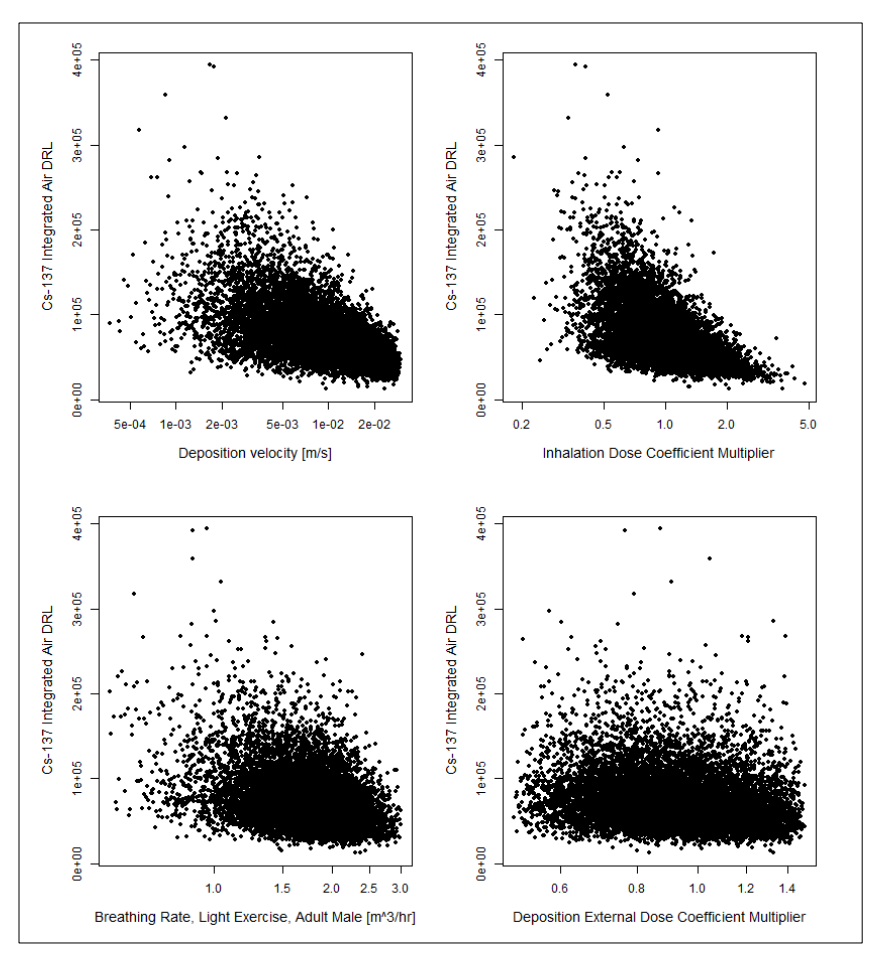


Figure 5.2-11. Scatter plots for the Cs-137 Integrated Air DRL for NARAC and the first four inputs shown in Table 5.2-5.

## 5.2.2.2. DP Sensitivity Analysis Results

Table 5.1-6 through Table 5.2-10 include the sensitivity analysis results for the DPs for the NARAC simulations. Figure 5.2-12 through Figure 5.2-16 include scatter plots which show the relationship between the most important inputs and the output for each DP.

For the NARAC simulations, the mean DP is greater than default DP for all of the DPs, as shown in Table 5.2-2. The air concentration multiplier is an important input for all of the DPs for the NARAC simulations. This input is lognormally distributed such that the mean is about 1.5 times greater than the default, as shown in Figure 4.3-2. In particular, the mean is much greater than the default for the Resuspension Inhalation DP for the NARAC distributions because the uncertainty in this parameter is driven by both the air concentration multiplier and the lognormally-distributed resuspension coefficient multiplier. The spread between the 5<sup>th</sup> and 95<sup>th</sup> percentiles is largest for the Resuspension Inhalation DP, as was also the case for the Laboratory Analysis simulations.

The air concentration multiplier contributes most to uncertainty for all of the DPs except Resuspension Inhalation, for which the resuspension coefficient multiplier uncertainty dominates, closely followed by the air concentration multiplier. The strong positive relationship between the air concentration multiplier and the Plume Inhalation DP and Plume Submersion DP can be seen in the upper left scatter plots in Figure 5.2-12 and Figure 5.2-13, respectively. Deposition velocity is also an important contributor to the ground pathway uncertainty because deposition velocity is used to deposit material from the air onto the ground. The SRRCs are positive for all of the important DP inputs for the NARAC simulations. The Total DP uncertainty is driven primarily by the air concentration multiplier, which is most important in the plume pathways, followed by deposition velocity, which is important in the ground pathways.

Table 5.2-6. Sensitivity analysis results for the Cs-137 Plume Inhalation DP for NARAC.

Cs-137 Plume Inhalation DP, R <sup>2</sup> = 0.980			
Variable Name	R <sup>2</sup> Individual	SRRC	
Air Concentration Multiplier	0.884	0.940	
Inhalation Dose Coefficient Multiplier	0.070	0.266	
Breathing Rate, Light Exercise, Adult Male	0.026	0.160	
Ground Roughness Factor	0.000	0.002	
Deposition External Dose Coefficient Multiplier	0.000	0.002	
Resuspension Coefficient Multiplier	0.000	0.000	
Weathering Coefficient Multiplier	0.000	0.000	
Deposition Velocity	0.000	0.000	
Breathing Rate, Activity Averaged, Adult Male	0.000	0.000	
Plume External Dose Coefficient Multiplier	0.000	0.000	

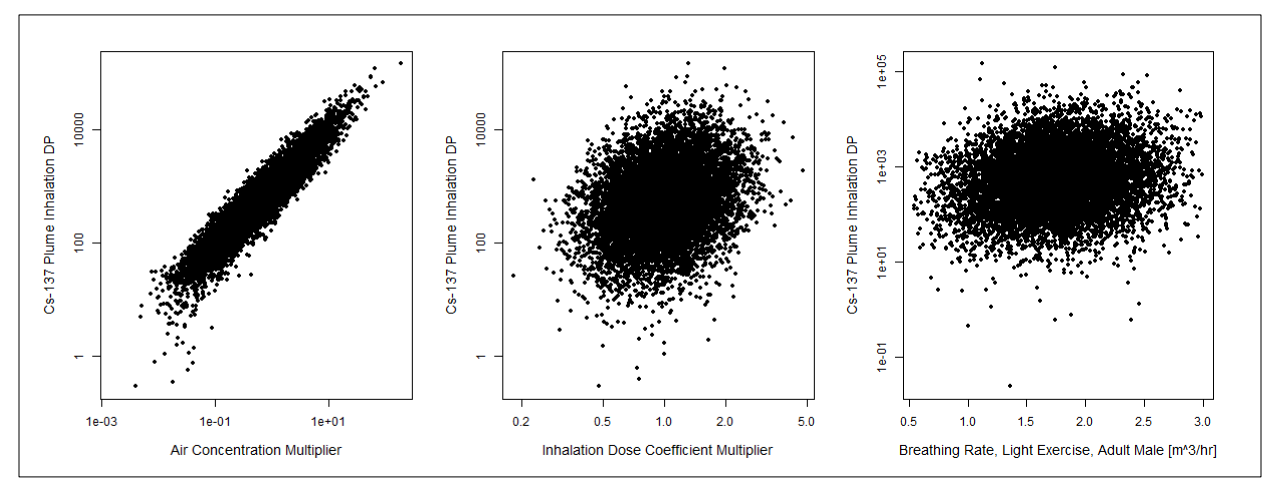


Figure 5.2-12. Scatter plots for the Cs-137 Plume Inhalation DP for NARAC and the first three inputs shown in Table 5.1-6.

Table 5.2-7. Sensitivity analysis results for the Cs-137 Plume Submersion DP for NARAC.

Cs-137 Plume Submersion DP, R <sup>2</sup> = 0.996			
Variable Name	R <sup>2</sup> Individual	SRRC	
Air Concentration Multiplier	0.972	0.985	
Plume External Dose Coefficient Multiplier	0.024	0.156	
Breathing Rate, Light Exercise, Adult Male	0.000	0.000	
Ground Roughness Factor	0.000	0.000	
Inhalation Dose Coefficient Multiplier	0.000	0.000	
Weathering Coefficient Multiplier	0.000	0.000	
Deposition velocity	0.000	0.000	
Breathing Rate, Activity Averaged, Adult Male	0.000	0.000	
Deposition External Dose Coefficient Multiplier	0.000	0.000	
Resuspension Coefficient Multiplier	0.000	-0.001	

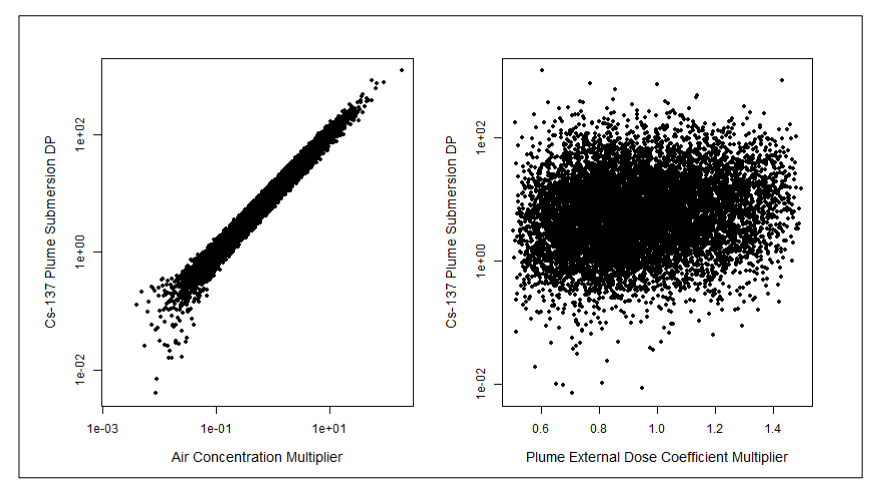


Figure 5.2-13. Scatter plots for the Cs-137 Plume Submersion DP for NARAC and the first two inputs shown in Table 5.2-7.

Table 5.2-8. Sensitivity analysis results for the Cs-137 Resuspension Inhalation DP for NARAC.

Cs-137 Resuspension Inhalation DP, R <sup>2</sup> = 0.939				
Variable Name	R <sup>2</sup> Individual	SRRC		
Resuspension Coefficient Multiplier	0.408	0.640		
Air Concentration Multiplier	0.384	0.621		
Deposition Velocity	0.106	0.325		
Inhalation Dose Coefficient Multiplier	0.033	0.182		
Breathing Rate, Activity Averaged, Adult Male	0.008	0.090		
Ground Roughness Factor	0.000	-0.005		
Deposition External Dose Coefficient Multiplier	0.000	0.005		
Breathing Rate, Light Exercise, Adult Male	0.000	0.000		
Weathering Coefficient Multiplier	0.000	0.000		
Plume External Dose Coefficient Multiplier	0.000	0.000		

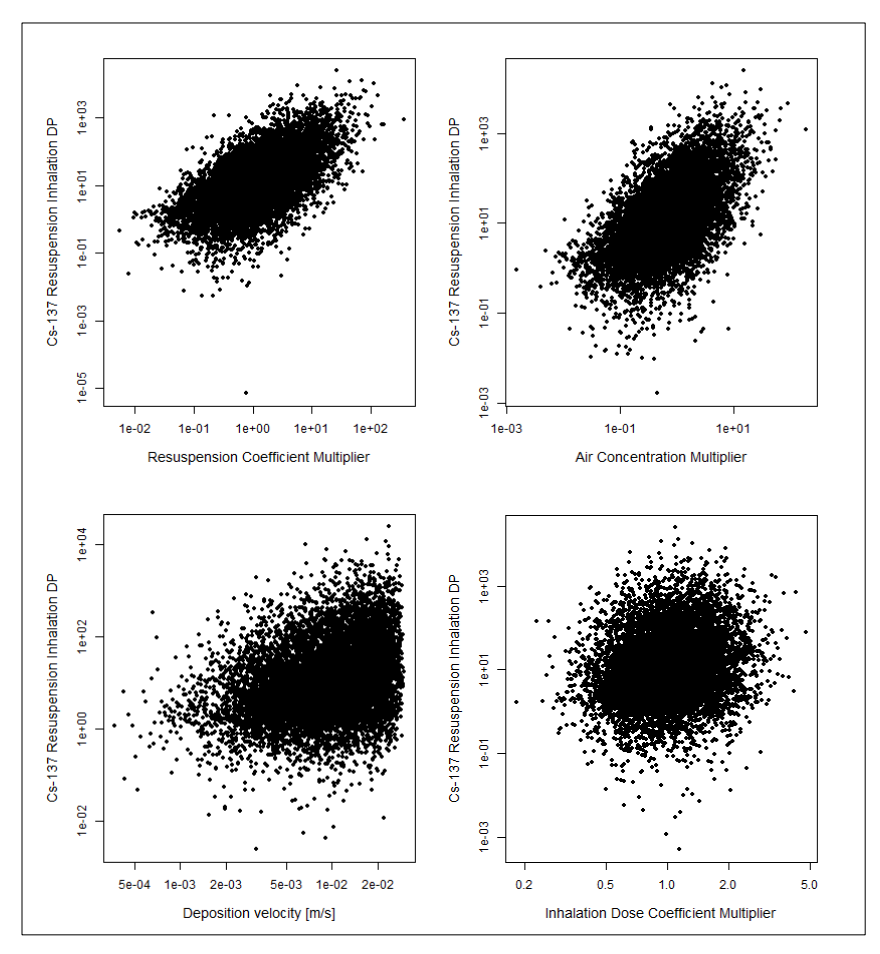


Figure 5.2-14. Scatter plots for the Cs-137 Resuspension Inhalation DP for NARAC and the first four inputs shown in Table 5.2-8.

Table 5.2-9. Sensitivity analysis results for the Cs-137 Groundshine DP for NARAC.

Cs-137 Groundshine DP, R <sup>2</sup> = 0.961				
Variable Name	R <sup>2</sup> Individual	SRRC		
Air Concentration Multiplier	0.730	0.856		
Deposition Velocity	0.196	0.442		
Deposition External Dose Coefficient Multiplier	0.020	0.141		
Weathering Coefficient Multiplier	0.012	0.110		
Ground Roughness Factor	0.003	0.057		
Breathing Rate, Light Exercise, Adult Male	0.000	0.000		
Inhalation Dose Coefficient Multiplier	0.000	0.000		
Resuspension Coefficient Multiplier	0.000	0.000		
Breathing Rate, Activity Averaged, Adult Male	0.000	0.000		
Plume External Dose Coefficient Multiplier	0.000	0.000		

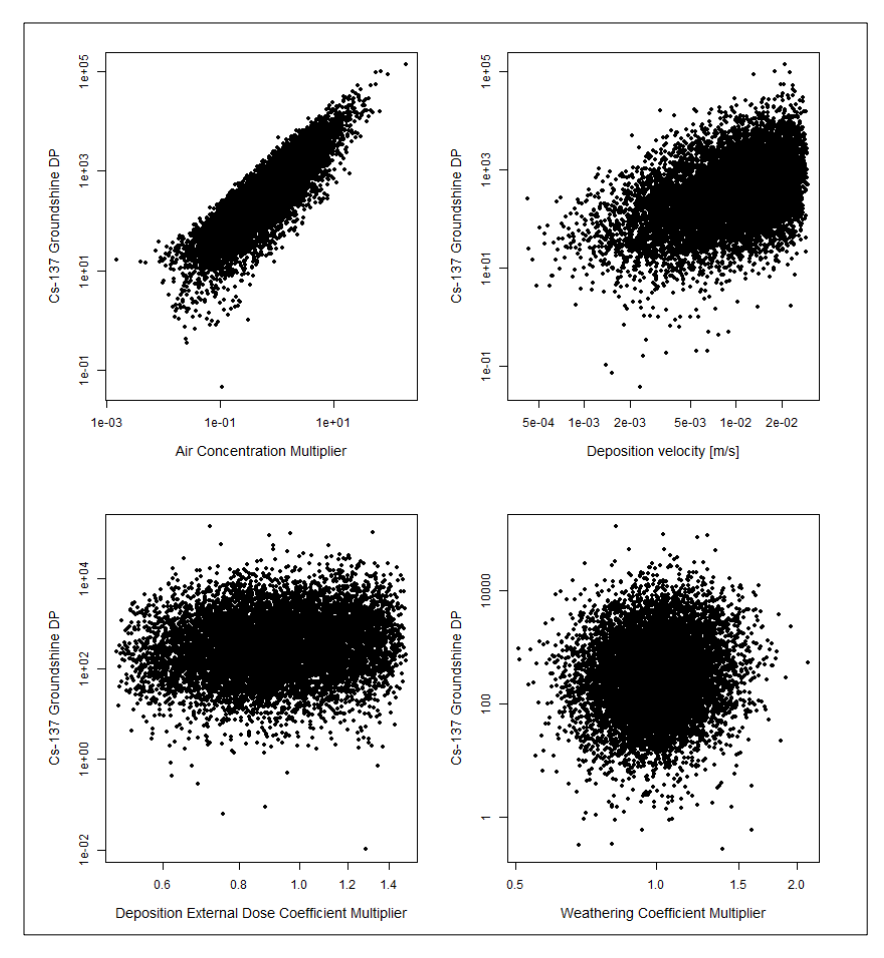


Figure 5.2-15. Scatter plots for the Cs-137 Groundshine DP for NARAC and the first four inputs shown in Table 5.2-9.

Table 5.2-10. Sensitivity analysis results for the Cs-137 Total DP for NARAC.

Cs-137 Total DP, R <sup>2</sup> = 0.981			
Variable Name	R <sup>2</sup> Individual	SRRC	
Air Concentration Multiplier	0.907	0.953	
Deposition Velocity	0.031	0.174	
Inhalation Dose Coefficient Multiplier	0.028	0.168	
Breathing Rate, Light Exercise, Adult Male	0.009	0.096	
Deposition External Dose Coefficient Multiplier	0.003	0.056	
Weathering Coefficient Multiplier	0.002	0.045	
Ground Roughness Factor	0.000	0.024	
Resuspension Coefficient Multiplier	0.000	0.020	
Breathing Rate, Activity Averaged, Adult Male	0.000	0.002	
Plume External Dose Coefficient Multiplier	0.000	0.000	

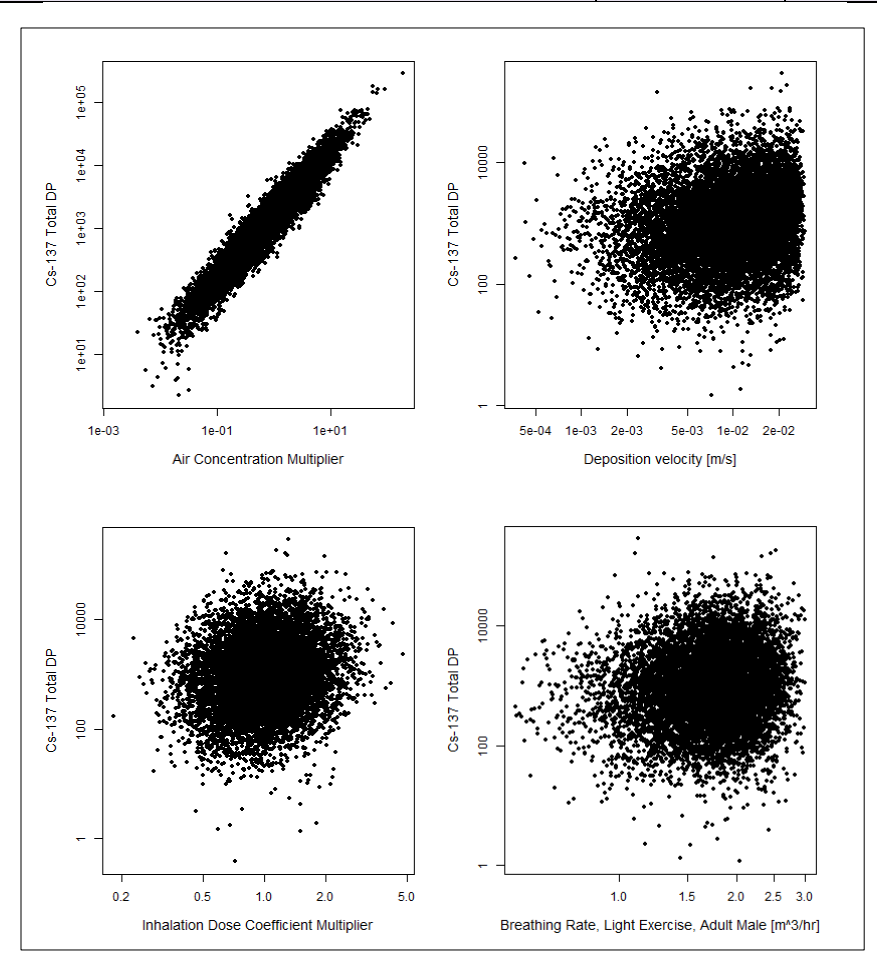


Figure 5.2-16. Scatter plots for the Cs-137 Total DP for NARAC and the first four inputs shown in Table 5.2-10.

# 5.2.3. Sampling Confidence Intervals

The table below shows the sampling CIs calculated about the mean for each output of interest. The sample mean is also shown for reference for each output. The steps used to calculate the CIs are described in Section 3.3.3. These 95% CIs are interpreted as follows: 'there is a 95% confidence that the true value of the mean falls within this interval.' The results given in Table 5.2-11 show that the estimate of the mean is well characterized by the 10,000 LHS samples used to quantify the uncertainty in each of the outputs of interest.

Table 5.2-11. Sampling confidence intervals for NARAC simulations.

Output Name	Lower Bound of 95% CI	Mean	Upper Bound of 95% CI
Dose Rate DRL [mrem/hr]	3.83	3.87	3.90
Cs-137 Deposition DRL [μCi/m²]	706	713	719
Cs-137 Integrated Air DRL [µCi-s/m³]	75200	75900	76600
Cs-137 Plume Inhalation DP [mrem]	1470	1550	1630
Cs-137 Plume Submersion DP [mrem]	14.0	14.7	15.3
Cs-137 Resuspension Inhalation DP [mrem]	70.4	78.8	87.5
Cs-137 Groundshine DP [mrem]	966	1020	1090
Cs-137 Total DP [mrem]	2530	2660	2810

# 5.3. Comparison of Uncertainty Analysis Results

The figures provided in the following sections show the comparison of the cumulative probabilities for each output of interest for all four activity sources (NARAC, Laboratory Analysis, In Situ Deposition, AMS) for both the DRL results (Section 5.3.1) and for the DP results (Section 5.3.2).

#### 5.3.1. DRL Result Comparisons

The DRL distributions shown in Figure 5.3-1 through Figure 5.3-3 are indistinguishable although they are not numerically exactly the same. A slight numerical difference can be seen in the NARAC-based DRL results relative to the other deposition-based DRL results due to the aggregated uncertainty in the Total DP, which is different between the air concentration-based NARAC simulations and the other three deposition-based simulations. This difference in the Total DP distribution is distinguishable and can be seen in Figure 5.3-8. However, the DRL results are essentially the same for all four of the activity sources because the only input distribution that distinguishes the four sets of simulations from each other is the activity per area or air concentration multiplier distributions, and the contribution to uncertainty from these distributions is effectively cancelled out in the DRL ratio because the mixture consists of a single radionuclide.

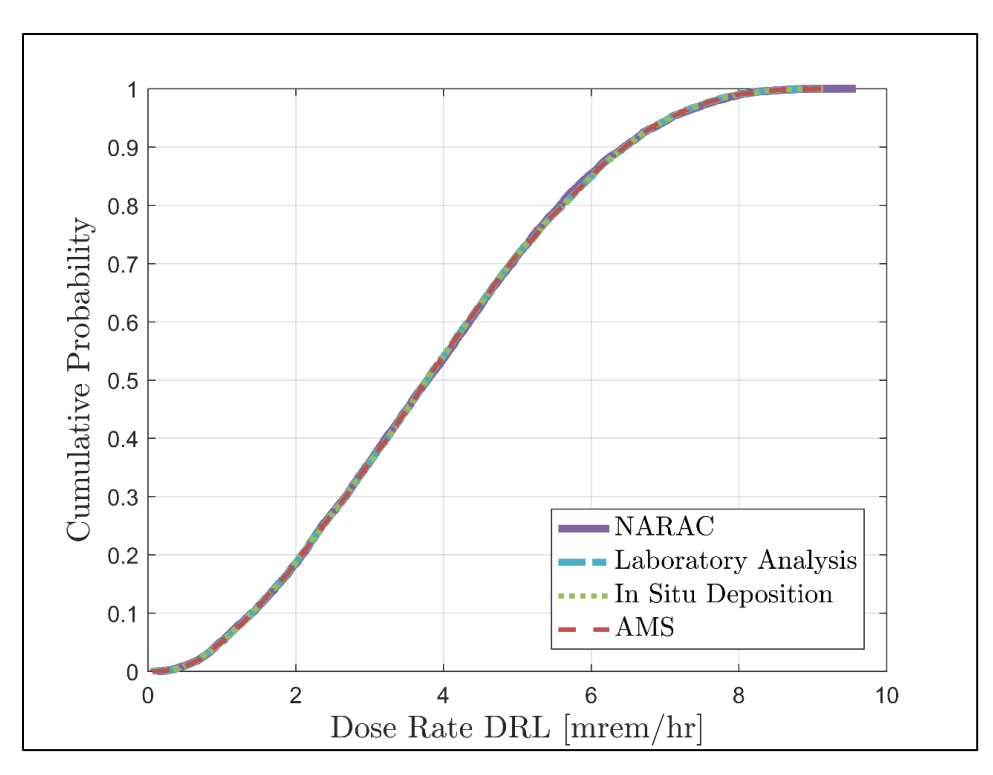


Figure 5.3-1. Comparison of cumulative probabilities for the Dose Rate DRL for NARAC, Laboratory Analysis, In Situ Deposition, and AMS.

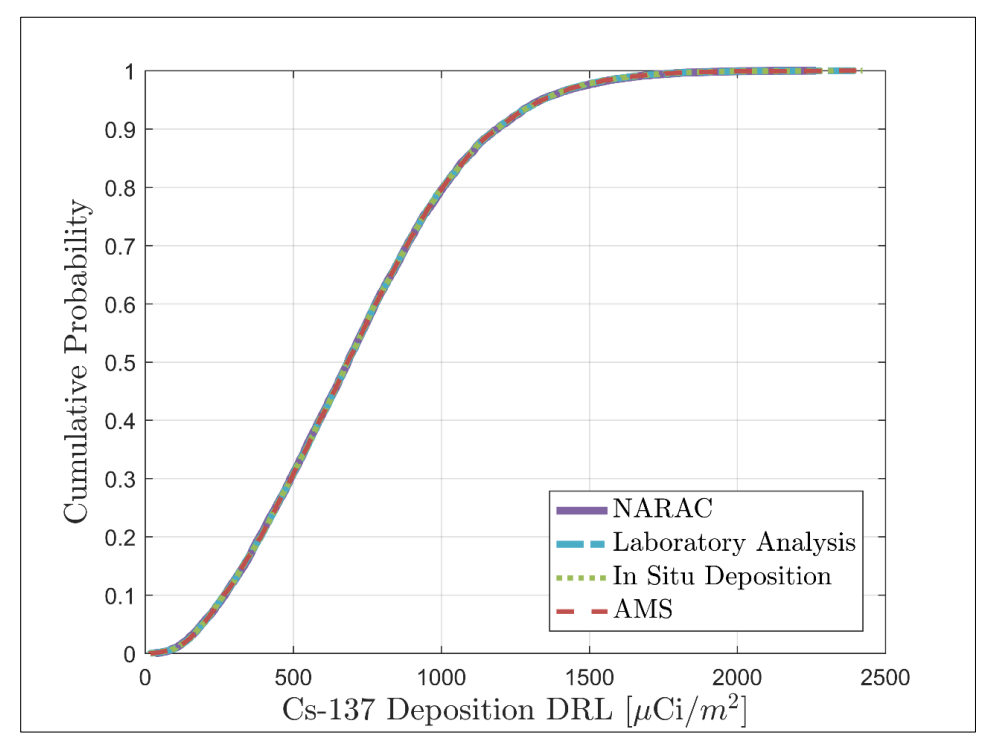


Figure 5.3-2. Comparison of cumulative probabilities for the Cs-137 Deposition DRL for NARAC, Laboratory Analysis, In Situ Deposition, and AMS.

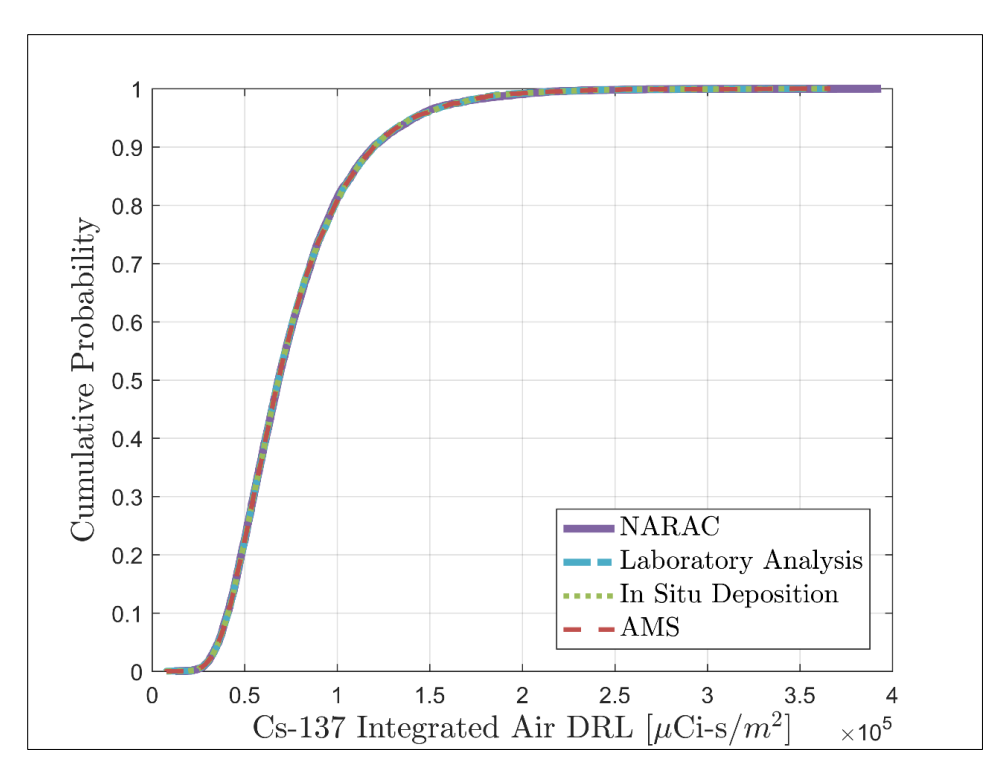


Figure 5.3-3. Comparison of cumulative probabilities for the Cs-137 Integrated Air DRL for NARAC, Laboratory Analysis, In Situ Deposition, and AMS.

## 5.3.2. DP Result Comparisons

Figure 5.3-4 through Figure 5.3-8 show a comparison of the DP results for all four activity sources. The DP results are essentially the same for Laboratory Analysis, In Situ Deposition, and AMS because the only difference between these simulations is the SD on the distribution for activity per area, and activity per area is not an important contributor to DP uncertainty.

Unlike the DRLs, the NARAC DP distributions are notably distinguishable from the other three deposition-based DP distributions. The NARAC DP results show a greater distribution spread than the other simulations because the distribution for the air concentration multiplier is wider than the distribution for activity per area. Additionally, the air concentration multiplier is a significant contributor to uncertainty for all of the NARAC DPs.

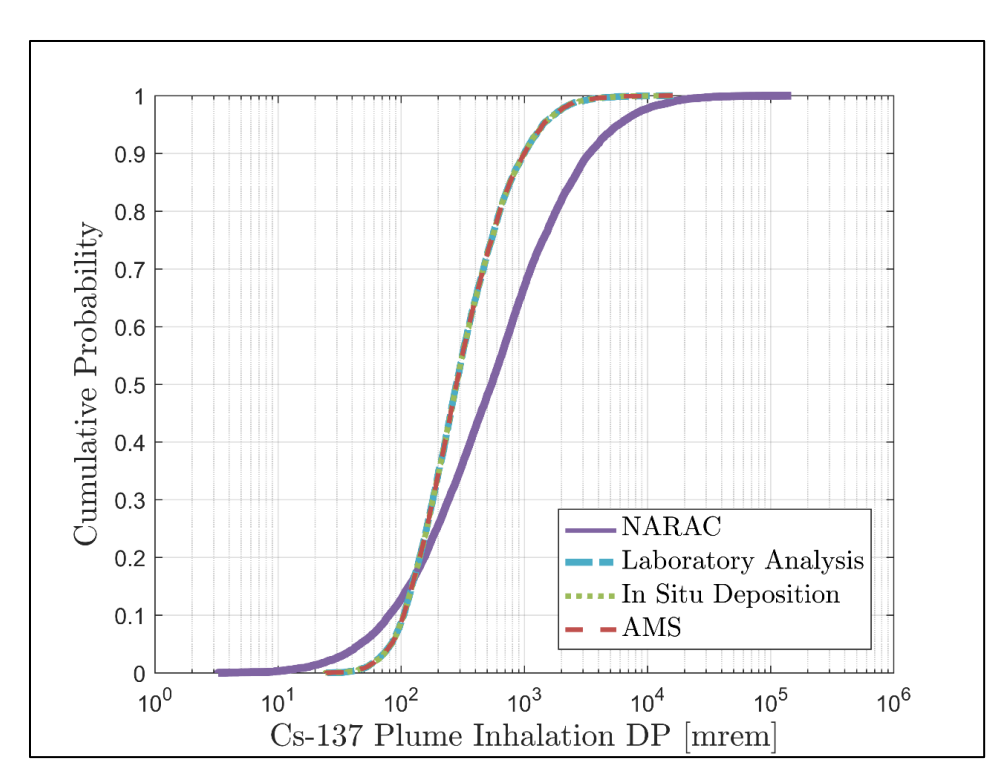


Figure 5.3-4. Comparison of cumulative probabilities for the Cs-137 Plume Inhalation DP for NARAC, Laboratory Analysis, In Situ Deposition, and AMS.

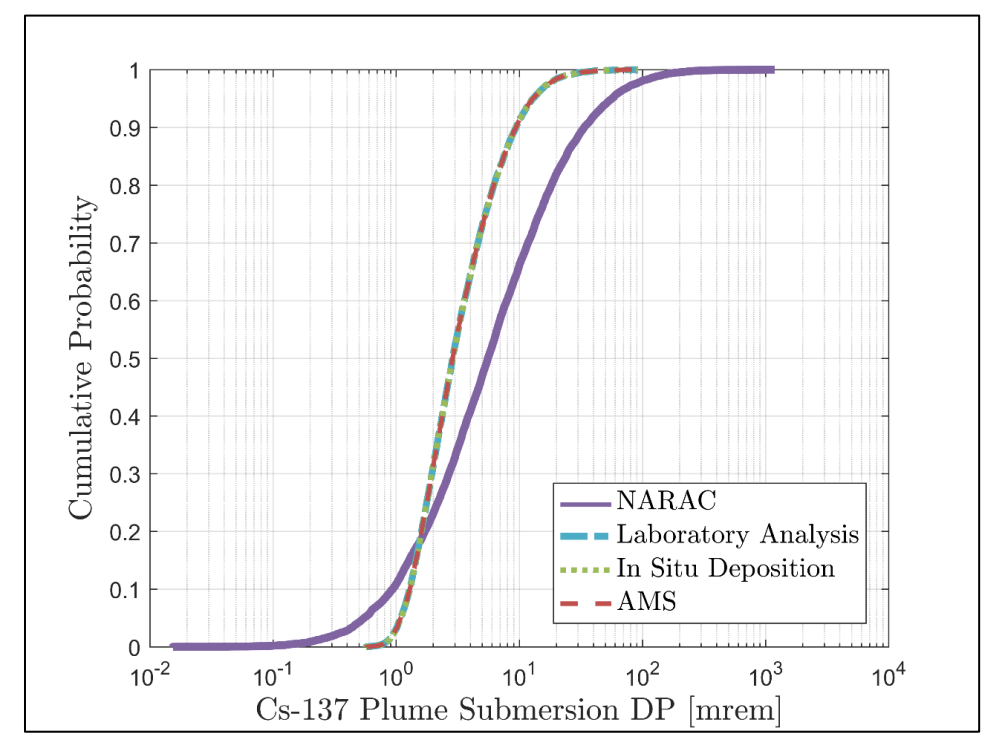


Figure 5.3-5. Comparison of cumulative probabilities for the Cs-137 Plume Submersion DP for NARAC, Laboratory Analysis, In Situ Deposition, and AMS.

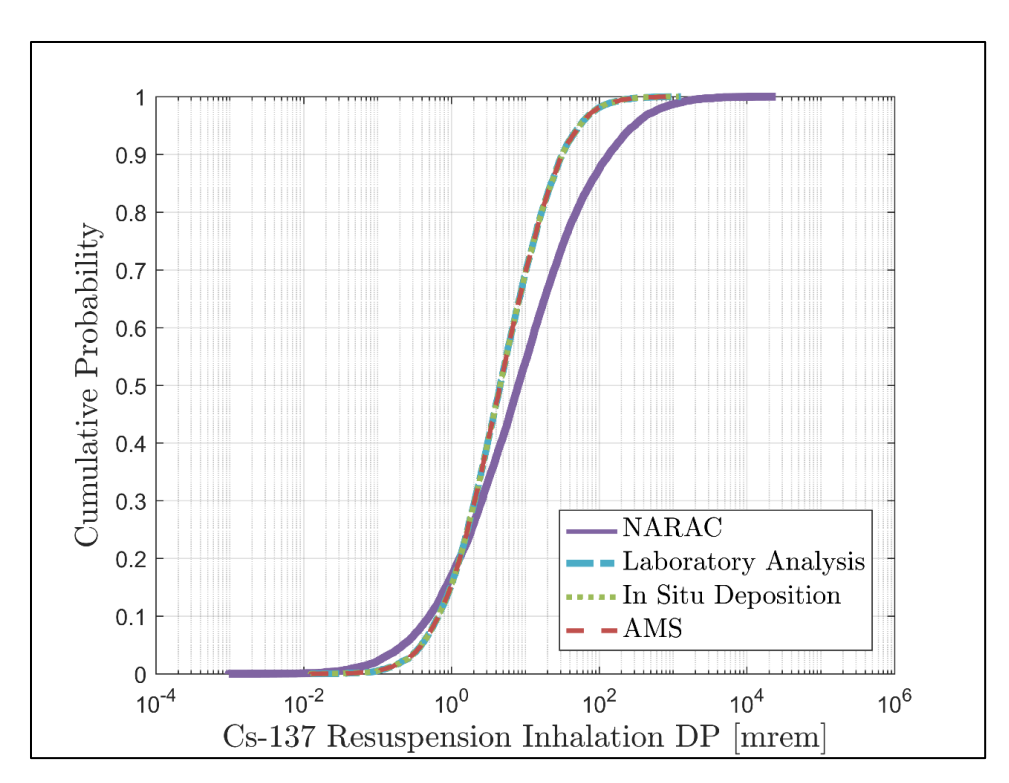


Figure 5.3-6. Comparison of cumulative probabilities for the Cs-137 Resuspension Inhalation DP for NARAC, Laboratory Analysis, In Situ Deposition, and AMS.

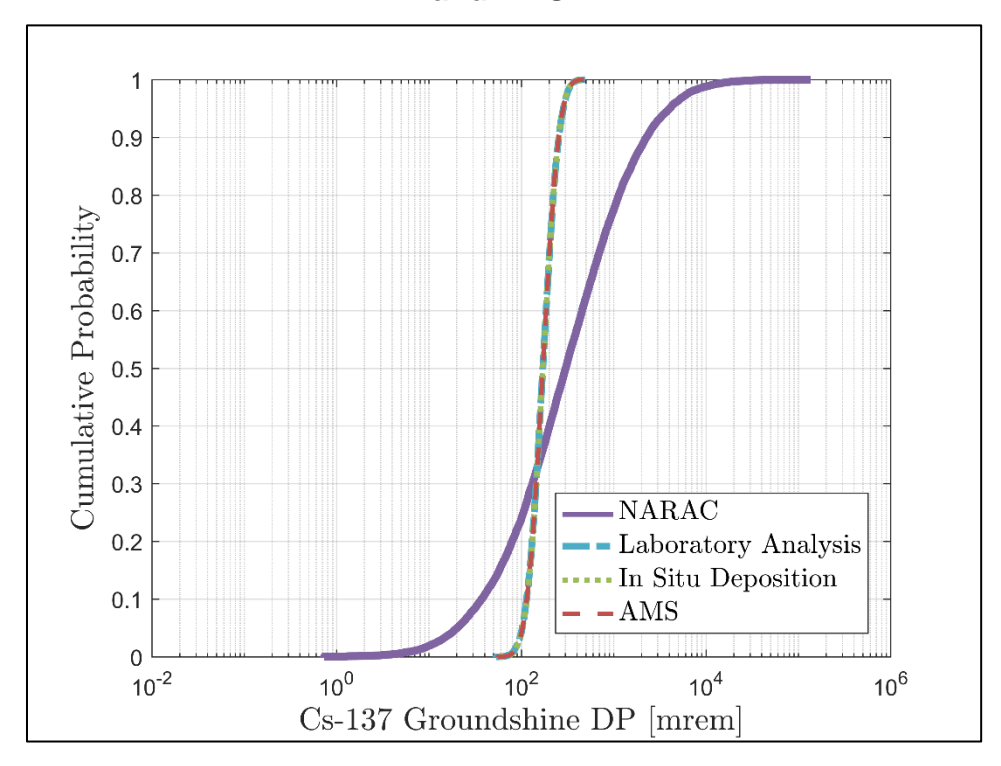


Figure 5.3-7. Comparison of cumulative probabilities for the Cs-137 Groundshine DP for NARAC, Laboratory Analysis, In Situ Deposition, and AMS.

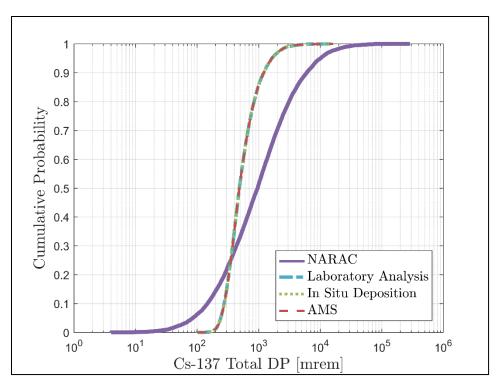


Figure 5.3-8. Comparison of cumulative probabilities for the Cs-137 Total DP for NARAC, Laboratory Analysis, In Situ Deposition, and AMS.

#### 6. SUMMARY

## 6.1. Summary of Overall Uncertainty Results

The results presented in this report show that the implementation of a probabilistic framework that can be used to characterize the uncertainty in CM data products was completed successfully. Following the selection of a study scenario, inputs were assigned probability distributions that were based on data and/or expert opinion. These input distributions represent an attempt to broadly characterize input uncertainty and could be refined if needed using additional data or further expert input. The coupled use of Dakota and Turbo FRMAC<sup>©</sup> allowed for automatic execution of simulations for each input sample, thus propagating input uncertainty through the model to the outputs. Finally, statistical post-processing methods were developed and used to characterize the uncertainty in the simulation results and to determine the sensitivity of uncertainty in simulation outputs to the uncertainty in the inputs.

The sensitivity analysis showed that the uncertainty in the NARAC-modeled air concentration is the most important contributor to DP uncertainty when the dose projection uses integrated air activity to define the radionuclide mixture. The uncertainty in deposition velocity is the most important contributor to DP uncertainty when the dose projection uses activity per area data to define the radionuclide mixture. These results can be used to motivate additional studies to better characterize these inputs and in turn reduce the overall uncertainty in the DP and DRL results.

It is important to note that the mixture for this analysis consisted of a single radionuclide at a concentration equal to the DRL. A radionuclide with different decay characteristics (e.g., half-life, radiations emitted) will likely yield different results, as will a mixture of multiple radionuclides. Also, an analysis using only the ground pathways (resuspension inhalation and groundshine) will likely yield very different results from this analysis, in which the inputs to the plume DPs dominated the overall uncertainty.

#### 6.2. Incorporating Uncertainty Results in Data Products

Two data products were generated using the uncertainty information for the Cs-137 Deposition DRL from the NARAC simulations and the simulation conditions noted in Section 0. The first map, shown in Figure 6.2-1, shows the distribution on the DRL as represented by the 5<sup>th</sup> and 95<sup>th</sup> percentiles along with the mean. The second map, shown in Figure 6.2-2, shows the default Cs-137 Deposition DRL that results from a single Turbo FRMAC<sup>©</sup> simulation using FRMAC Assessment default values for the inputs (i.e., what is currently used for data products), along with the mean Cs-137 Deposition DRL from the simulations and the calculated 95% CI about the mean.

Figure 6.2-1 can be interpreted as follows. Looking at the red contour for the 5<sup>th</sup> percentile, 95% of the simulation results have a Cs-137 Deposition DRL that is greater than 191  $\mu$ Ci/m². This means that 95% of the time, the contour could be drawn inside of the red shaded area if the contour was based on the DRL value calculated for a single simulation selected from the 10,000 samples. Further, 5% of the simulation results have a Cs-137 Deposition DRL that is less than 191  $\mu$ Ci/m². This means that 5% of the time the contour could be drawn outside the red shaded area if the contour was based on the DRL value calculated for a single simulation selected from the 10,000 samples.

Figure 6.2-2 shows the 95% CI about mean for the Cs-137 Deposition DRL. The width of this 95% CI is about 2% of the mean  $(713\pm7~\mu\text{Ci/m}^2)$ . For the selected scenario, the CI contours are nearly indistinguishable from the mean contour. This demonstrates that the sampling method and sample size used for this analysis adequately capture the uncertainty in the mean. Additionally, the default DRL contour covers nearly three times the area that the mean DRL contour covers. This shows that the default DRL is very conservative in comparison to the "best" statistical result derived from this uncertainty analysis for this demonstration scenario. Protective action recommendations based on our default method would result in a significantly larger impacted population. For the hypothetical scenario used to generate these data products, the statistically-derived result would reduce the number affected individuals by over 12,000.

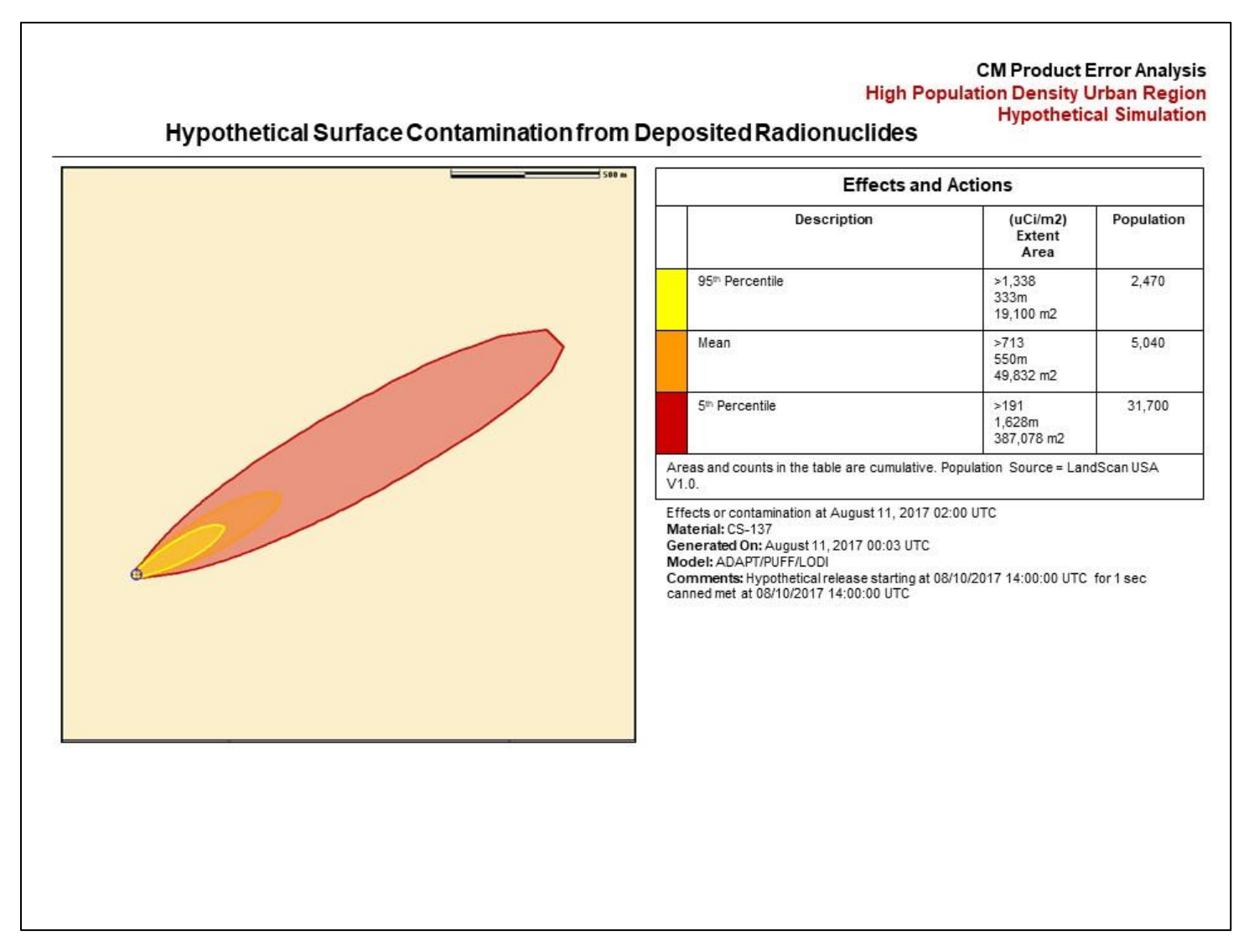


Figure 6.2-1. Data product displaying the Cs-137 Deposition DRL distribution from the NARAC simulations.

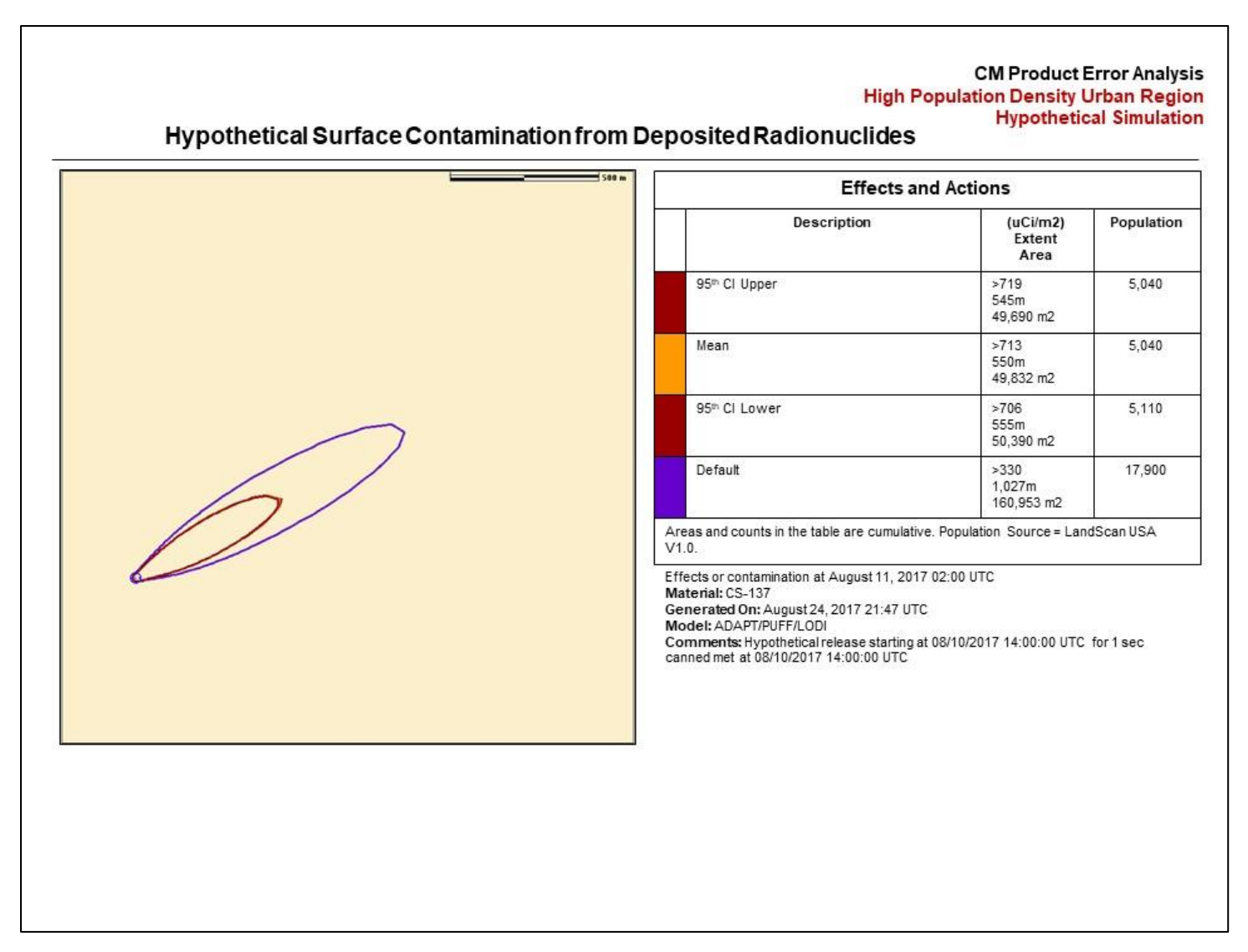


Figure 6.2-2. Data product displaying the Cs-137 Deposition DRL mean result from the NARAC simulations and the default DRL.

## 6.3. Implications & Future Work

The probabilistic framework developed for this project and described in this report was used to analyze an idealized single release scenario and served as a proof of concept that can be applied to additional release scenarios and their subsequent data products in the future. As the scope of the project is focused on the development of methods for characterizing uncertainty in CM data products, the explanations provided that link uncertainty analysis results to the physics of the problem could be further expanded in future work. An extension of this project will include this expanded application; additional scenarios and data products with increasingly complex calculations will be analyzed using the steps outlined in this report.

The statistical methods and tools used to both generate simulation inputs and to perform uncertainty and sensitivity analysis may need to be adapted to adequately analyze the results of increasingly complex scenarios and data products. Additional sampling techniques, such as importance sampling, may be useful if more information is needed in portions of the input space or output space (i.e., extreme high or low percentiles of input or output distributions). As the uncertainties in the inputs and the relationships between these uncertainties and the uncertainties in the outputs become more complex, additional regression techniques that capture additional types of input/output relationships, as well as conjoint relationships between inputs, may need to be added to the suite of tools used to complete the sensitivity analysis portion of the post-processing. Finally, as additional uncertainties are added to the simulations and scenarios under evaluation, comprehensive convergence studies that test the convergence in the percentiles of interest (i.e., 5<sup>th</sup>, 50<sup>th</sup>, 95<sup>th</sup>) in addition to the mean as the sample size increases may be necessary to confirm that the final set of samples characterizes the uncertainty in the results up to an acceptable level of precision.

The potential for implementation of uncertainty quantification calculations in a real-world response must be studied further. The current implementation of these calculations in Turbo FRMAC® executes the simulation for each sample one after the other; parallelization of these calculations would help to increase the calculation speed for a probabilistic analysis of a given scenario. However, the bulk of the effort required to run a comprehensive probabilistic analysis is in the definition of the input distributions that will be used to generate input samples. These input distributions may need to be changed based on the release scenario, information and data collected in the field as a response is happening, etc. As additional scenarios are analyzed using the probabilistic framework described in this report, it may be possible to streamline the definition of input distributions by generating a database of distributions for the most likely scenarios. This may make uncertainty quantification for real-world responses more feasible in the future. The ultimate use of and audience for uncertainty analysis results in a real-world response will require further discussion. This will require further development of map products and a consideration of how such products might be interpreted by decision makers.

#### 7. REFERENCES

- [1] PAG Manual: Protective Action Guides and Planning Guidance for Radiological Incidents, EPA-400/R-17/001, U.S. Environmental Protection Agency, Washington, DC, January 2017.
- [2] Fulton, J., et al., "Turbo FRMAC<sup>©</sup> Assessment Software Package," Sandia National Laboratories, Albuquerque, NM, 2017.
- [3] Federal Radiological Monitoring and Assessment Center (FRMAC) Assessment Manual, Volume 1 Overview and Methods, SAND2015-2884 R, Sandia National Laboratories, Albuquerque, NM, 2015.
- [4] Metropolis, N., and S. M. Ulam, "The Monte Carlo Method," *Journal of the American Statistical Association*, Vol. 44, pp. 335-341, 1949.
- [5] Helton, J.C, Johnson, J.D., Sallaberry, C.J., and Storlie, C.B. "Survey of Sampling-Based Methods for Uncertainty and Sensitivity Analysis." Sandia Report, SAND2006-2901, 2006.
- [6] McKay, M.D., R.J. Beckman, and W.J. Conover. "A Comparison of Three Methods for Selecting Values of Input Variables in the Analysis of Output from a Computer Code," *Technometrics*. Vol. 21, no. 2, pp. 239-245, 1979.
- [7] Helton, J.C. and F.J. Davis. "Latin Hypercube Sampling and the Propagation of Uncertainty in Analyses of Complex Systems," *Reliability Engineering and System Safety*. Vol. 81, no. 1, pp. 23-69, 2003.
- [8] Iman, R.L., Davenport, J.M., and Ziegler, D.K. "Latin Hypercube Sampling (Program User's Guide)," Technical Report SAND79-1473, Sandia National Laboratories, Albuquerque, NM, 1980.
- [9] Iman, R.L., and Conover, W.J. "A Distribution-Free Approach to Inducing Rank Correlation Among Input Variables," *Communications in Statistics*, B11(3), 311-334, 1982.
- [10] Swiler, L. P. and G. D. Wyss. "A User's Guide to Sandia's Latin Hypercube Sampling Software: LHS Unix Library/Standalone Version." Technical Report SAND2004-2439. Sandia National Laboratories, Albuquerque NM, 2004.
- [11] Adams, B.M., Bauman, L.E., Bohnhoff, W.J., Dalbey, K.R., Eddy, J.P., Ebeida, M.S., Eldred, M.S., Hough, P.D., Hu, K.T., Jakeman, J.D., Swiler, L.P., Stephens, J.A., Vigil, D.M., and Wildey, T.M, "DAKOTA, A Multilevel Parallel Object-Oriented Framework for Design Optimization, Parameter Estimation, Uncertainty Quantification, and Sensitivity Analysis: Version 6.0 User's Manual," Sandia Technical Report SAND2014-4633, May 2014.
- [12] R Core Team. "R: A Language and Environment for Statistical Computing." R Foundation for Statistical Computing. Vienna, Austria. URL http://www.R-project.org/. 2017.
- [13] Iman, R., and Conover, W. "The use of rank transformation in regression," *Technometrics*, Vol. 21, No. 4, pp. 499-509, 1979.
- [14] Storlie, C.B, Swiler, L.P., Helton, J.C., and Sallaberry, C.J. "Implementation and Evaluation of Nonparametric Regression Procedures for Sensitivity Analysis of Computationally

- Demanding Models." *Reliability Engineering & System Safety*. Vol. 94, No. 11, pp. 1735-1763, 2009.
- [15] Efron, B., and Tibshirani, R. J. An Introduction to the Bootstrap. CRC Press, 1994.
- [16] Evaluation of Severe Accident Risks: Quantification of Major Input Parameters, NUREG/CR-4551, Vol. 2, Rev. 1, Part 7, U.S. Nuclear Regulatory Commission, Washington, DC, 1990.
- [17] Severe Accident Risks: An Assessment for Five U.S. Nuclear Power Plants, NUREG-1150, U.S. Nuclear Regulatory Commission, Washington, DC, 1990.
- [18] *Human Respiratory Tract Model for Radiological Protection*, ICRP Publication 66, International Commission on Radiological Protection, Ottawa, Ontario, Canada, 1994.
- [19] Development of Probabilistic RESRAD 6.0 and RESRAD-BUILD 3.0 Computer Codes, NUREG/CR-6697, ANL/EAD/TM-98, Argonne National Laboratory, Argonne, IL, 2000.
- [20] Exposure Factors Handbook, EPA/600/R-090/052F, U.S. Environmental Protection Agency, Washington, DC, September 2011.
- [21] Eckerman, K., Radiation Dose and Health Risk Estimation: Technical Basis for the State-ofthe-Art Reactor Consequence Analysis Project, Oak Ridge National Laboratory, Oak Ridge, TN, 2012.
- [22] State-of-the-Art Reactor Consequence Analysis (SOARCA) Project, Sequoyah Integrated Deterministic and Uncertainty Analysis Draft Report, ML16096A374, Sandia National Laboratories, Albuquerque, NM, 2017.
- [23] Anspaugh, L. R., et al., "Movement of Radionuclides in Terrestrial Ecosystems by Physical Processes" in *Health Physics*, Vol. 82, pp. 670-679, April 2002.
- [24] Likhtarev, I.A., Kovgan, L.N., Jacob, P., Anspaugh, L.R., "Chernobyl Accident: Retrospective and Prospective Estimates of External Dose of the Population of Ukraine" in *Health Physics*, Vol. 82, pp. 290-303, 2002.
- [25] Beck, H.L., Exposure Rate Conversion Factors for Radionuclides Deposited on the Ground, EML-378, U.S. Department of Energy Environmental Measurements Laboratory, New York, NY, 1980.
- [26] MELCOR Accident Consequence Code System (MACCS) User's Guide and Reference Manual Draft Report, Sandia National Laboratories, Albuquerque, NM, 2017.
- [27] Maxwell, R. and Anspaugh, L., "An Improved Model for Prediction of Resuspension" in *Health Physics*, Vol. 101, pp. 722-730, December 2011.
- [28] Golikov, V.Y., Balonov, M.I., Jacob, P., "External Exposure of the Population Living in Areas of Russia Contaminated Due to the Chernobyl Accident" in *Radiat Environ Biophys*, Vol. 41, pp. 185-193, 2002.
- [29] Taylor, B. N., & E., K. C., "Guidelines for Evaluating and Expressing the Uncertainty of NIST Measurement Results", Technical Note 1297, National Institute of Standards and Technology, 1994.

- [30] Barad, M.L., "Project Prairie Grass, a field program in diffusion" in *Geophys. Res. Pap.* 59. Air Force Cambridge Centre, 1958.
- [31] Thuillier, R.H., "Evaluation of a Puff Dispersion Model in Complex Terrain" in *Journal of the Air & Waste Management Association*, 42:3, 290-297, 1992.
- [32] Foster, K.T., G. Sugiyama, J.S. Nasstrom, J.M. Leone, Jr., S.T. Chan, and B.M. Bowen, "The use of an operational model evaluation system for model intercomparison" in *Int. J. Environment and Pollution*, 14, 77-88, 2000.

# APPENDIX A: PROBABILISTIC ANALYSIS RESULTS FOR IN SITU DEPOSITION AND AMS

The probabilistic analysis results for In Situ Deposition (Section A.1) and AMS (Section A.2) are presented in this Appendix. The results for the Laboratory Analysis, In Situ, and AMS simulations are nearly the same, although slight differences can be seen in the DP outputs for these varying sources of deposition data. This is expected because the only difference between these simulations is the SD on the distribution for activity per area. For the sake of brevity, Laboratory Analysis was chosen to represent the results for this group because the results are similar enough that the same conclusions can be drawn for each deposition data source. The Laboratory Analysis results are given in greater detail in Section 5.1 because the activity per area distribution for Laboratory Analysis has the largest SD of the three. The scatter plots shown in Section 5.1 show the same trends as those for In Situ Deposition and AMS and were thus not included in this Appendix.

## A.1. In Situ Deposition

## A.1.1. Uncertainty Analysis Results

Table A.1- 1. DRL uncertainty results for In Situ Deposition simulations.

Output Name	Default	Mean	5th	50th	95th
Dose Rate DRL [mrem/hr]	1.98	3.869	0.989	3.779	7.066
Cs-137 Deposition DRL [μCi/m²]	3.31E2	712.550	194.564	683.833	1342.506
Cs-137 Integrated Air DRL [μCi-s/m³]	1.10E5	75856.595	35836.703	68270.251	140970.833

Table A.1- 2. DP uncertainty results for In Situ Deposition simulations.

Output Name	Default	Mean	5th	50th	95th
Cs-137 Plume Inhalation DP [mrem]	7.93E2	468.806	83.610	282.376	1425.926
Cs-137 Plume Submersion DP [mrem]	10.4	4.500	1.089	2.882	12.835
Cs-137 Resuspension Inhalation DP [mrem]	4.42	14.115	0.390	4.579	54.584
Cs-137 Groundshine DP [mrem]	1.89E2	179.445	103.348	171.416	283.873
Cs-137 Total DP [mrem]	9.97E2	666.867	243.768	487.823	1640.139

# A.1.2. Sensitivity Analysis Results

## A.1.2.1. DRL Sensitivity Analysis Results

Table A.1- 3. Sensitivity analysis results for the Dose Rate DRL for In Situ Deposition.

Dose Rate DRL, R <sup>2</sup> = 0.936			
Variable Name	R <sup>2</sup> Individual	SRRC	
Deposition Velocity	0.574	0.758	
Inhalation Dose Coefficient Multiplier	0.186	-0.429	
Breathing Rate, Light Exercise, Adult Male	0.063	-0.249	
Deposition External Dose Coefficient Multiplier	0.061	0.249	
Weathering Coefficient Multiplier	0.037	0.192	
Ground Roughness Factor	0.011	0.105	
Resuspension Coefficient Multiplier	0.004	-0.062	
Activity per Area	0.000	0.000	
Plume External Dose Coefficient Multiplier	0.000	0.000	
Breathing Rate, Activity Averaged, Adult Male	0.000	-0.010	

Table A.1- 4. Sensitivity analysis results for the Cs-137 Deposition for In Situ Deposition.

Cs-137 Deposition DRL, R <sup>2</sup> = 0.924				
Variable Name	R <sup>2</sup> Individual	SRRC		
Deposition Velocity	0.603	0.777		
Inhalation Dose Coefficient Multiplier	0.187	-0.430		
Breathing Rate, Light Exercise, Adult Male	0.062	-0.250		
Weathering Coefficient Multiplier	0.036	0.189		
Deposition External Dose Coefficient Multiplier	0.027	-0.166		
Ground Roughness Factor	0.005	-0.069		
Resuspension Coefficient Multiplier	0.004	-0.059		
Activity per Area	0.000	0.000		
Plume External Dose Coefficient Multiplier	0.000	0.000		
Breathing Rate, Activity Averaged, Adult Male	0.000	-0.008		

Table A.1- 5. Sensitivity analysis results for the Cs-137 Integrated Air DRL for In Situ Deposition.

Cs-137 Integrated Air DRL, R <sup>2</sup> = 0.905				
Variable Name	R <sup>2</sup> Individual	SRRC		
Deposition Velocity	0.379	-0.616		
Inhalation Dose Coefficient Multiplier	0.339	-0.580		
Breathing Rate, Light Exercise, Adult Male	0.113	-0.337		
Deposition External Dose Coefficient Multiplier	0.039	-0.198		
Weathering Coefficient Multiplier	0.026	-0.160		
Ground Roughness Factor	0.006	-0.078		
Resuspension Coefficient Multiplier	0.004	-0.064		
Activity per Area	0.000	0.000		
Plume External Dose Coefficient Multiplier	0.000	0.000		
Breathing Rate, Activity Averaged, Adult Male	0.000	-0.005		

# A.1.2.2. DP Sensitivity Analysis Results

Table A.1- 6. Sensitivity analysis results for the Cs-137 Plume Inhalation DP for In Situ Deposition.

Cs-137 Plume Inhalation DP, R <sup>2</sup> = 0.953				
Variable Name	R <sup>2</sup> Individual	SRRC		
Deposition Velocity	0.675	-0.821		
Inhalation Dose Coefficient Multiplier	0.204	0.450		
Breathing Rate, Light Exercise, Adult Male	0.074	0.272		
Activity per Area	0.000	0.014		
Ground Roughness Factor	0.000	0.000		
Resuspension Coefficient Multiplier	0.000	0.000		
Weathering Coefficient Multiplier	0.000	0.000		
Breathing Rate, Activity Averaged, Adult Male	0.000	0.000		
Deposition External Dose Coefficient Multiplier	0.000	0.000		
Plume External Dose Coefficient Multiplier	0.000	0.000		

Table A.1- 7. Sensitivity analysis results for the Cs-137 Plume Submersion DP for In Situ Deposition.

Cs-137 Plume Submersion DP, R <sup>2</sup> = 0.987			
Variable Name	R <sup>2</sup> Individual	SRRC	
Deposition Velocity	0.899	-0.947	
Plume External Dose Coefficient Multiplier	0.088	0.297	
Activity per Area	0.000	0.014	
Breathing Rate, Light Exercise, Adult Male	0.000	0.000	
Ground Roughness Factor	0.000	0.000	
Inhalation Dose Coefficient Multiplier	0.000	0.000	
Resuspension Coefficient Multiplier	0.000	0.000	
Weathering Coefficient Multiplier	0.000	0.000	
Breathing Rate, Activity Averaged, Adult Male	0.000	0.000	
Deposition External Dose Coefficient Multiplier	0.000	-0.002	

Table A.1- 8. Sensitivity analysis results for the Cs-137 Resuspension Inhalation DP for In Situ Deposition.

Cs-137 Resuspension Inhalation DP, R <sup>2</sup> = 0.985			
Variable Name	R <sup>2</sup> Individual	SRRC	
Resuspension Coefficient Multiplier	0.901	0.948	
Inhalation Dose Coefficient Multiplier	0.067	0.258	
Breathing Rate, Activity Averaged, Adult Male	0.017	0.131	
Activity per Area	0.000	0.006	
Plume External Dose Coefficient Multiplier	0.000	-0.002	
Breathing Rate, Light Exercise, Adult Male	0.000	0.000	
Ground Roughness Factor	0.000	0.000	
Weathering Coefficient Multiplier	0.000	0.000	
Deposition Velocity	0.000	0.000	
Deposition External Dose Coefficient Multiplier	0.000	0.000	

Table A.1- 9. Sensitivity analysis results for the Cs-137 Groundshine DP for In Situ Deposition.

Cs-137 Groundshine DP, R <sup>2</sup> = 0.954			
Variable Name	R <sup>2</sup> Individual	SRRC	
Deposition External Dose Coefficient Multiplier	0.536	0.736	
Weathering Coefficient Multiplier	0.327	0.570	
Ground Roughness Factor	0.089	0.299	
Activity per Area	0.001	0.033	
Breathing Rate, Light Exercise, Adult Male	0.000	0.000	
Inhalation Dose Coefficient Multiplier	0.000	0.000	
Resuspension Coefficient Multiplier	0.000	0.000	
Deposition Velocity	0.000	0.000	
Breathing Rate, Activity Averaged, Adult Male	0.000	0.000	
Plume External Dose Coefficient Multiplier	0.000	-0.007	

Table A.1- 10. Sensitivity analysis results for the Cs-137 Total DP for In Situ Deposition.

Cs-137 Total DP, R <sup>2</sup> = 0.920			
Variable Name	R <sup>2</sup> Individual	SRRC	
Deposition Velocity	0.618	-0.786	
Inhalation Dose Coefficient Multiplier	0.186	0.430	
Breathing Rate, Light Exercise, Adult Male	0.062	0.250	
Deposition External Dose Coefficient Multiplier	0.027	0.165	
Weathering Coefficient Multiplier	0.019	0.135	
Ground Roughness Factor	0.005	0.068	
Resuspension Coefficient Multiplier	0.003	0.059	
Activity per Area	0.001	0.023	
Plume External Dose Coefficient Multiplier	0.000	0.000	
Breathing Rate, Activity Averaged, Adult Male	0.000	0.006	

# A.1.3. Sampling Confidence Intervals

Table A.1-11. Sampling confidence intervals for In Situ Deposition simulations.

Output Name	Lower Bound of 95% CI	Mean	Upper Bound of 95% CI
Dose Rate DRL [mrem/hr]	3.83	3.87	3.90
Cs-137 Deposition DRL [μCi/m²]	705	713	719
Cs-137 Integrated Air DRL [μCi-s/m³]	75200	75900	76600
Cs-137 Plume Inhalation DP [mrem]	456	469	481
Cs-137 Plume Submersion DP [mrem]	4.40	4.50	4.61
Cs-137 Resuspension Inhalation DP [mrem]	13.4	14.1	14.9
Cs-137 Groundshine DP [mrem]	178	179	181
Cs-137 Total DP [mrem]	653	667	680

## A.2. AMS

## A.2.1. Uncertainty Analysis Results

Table A.2- 1. DRL uncertainty results for AMS simulations.

Output Name	Default	Mean	5th	50th	95th
Dose Rate DRL [mrem/hr]	1.98	3.869	0.989	3.779	7.066
Cs-137 Deposition DRL [μCi/m²]	3.31E2	712.550	194.564	683.833	1342.506
Cs-137 Integrated Air DRL [μCi-s/m³]	1.10E5	75856.595	35836.703	68270.251	140970.833

Table A.2- 2. DP uncertainty results for AMS simulations.

Output Name	Default	Mean	5th	50th	95th
Cs-137 Plume Inhalation DP [mrem]	7.93E2	468.808	83.290	281.461	1422.200
Cs-137 Plume Submersion DP [mrem] 10.4		4.501	1.090	2.875	12.876
Cs-137 Resuspension Inhalation DP [mrem]	4.42	14.121	0.390	4.564	55.155
Cs-137 Groundshine DP [mrem]	1.89E2	179.446	103.242	171.303	284.542
Cs-137 Total DP [mrem]	9.97E2	666.875	243.048	487.461	1635.934

# A.2.2. Sensitivity Analysis Results

## A.2.2.1. DRL Sensitivity Analysis Results

Table A.2- 3. Sensitivity analysis results for the Dose Rate DRL for AMS.

Dose Rate DRL, R <sup>2</sup> = 0.936				
Variable Name	R <sup>2</sup> Individual	SRRC		
Deposition Velocity	0.574	0.758		
Inhalation Dose Coefficient Multiplier	0.186	-0.429		
Breathing Rate, Light Exercise, Adult Male	0.063	-0.249		
Deposition External Dose Coefficient Multiplier	0.061	0.249		
Weathering Coefficient Multiplier	0.037	0.192		
Ground Roughness Factor	0.011	0.105		
Resuspension Coefficient Multiplier	0.004	-0.062		
Activity per Area	0.000	0.000		
Plume External Dose Coefficient Multiplier	0.000	0.000		
Breathing Rate, Activity Averaged, Adult Male	0.000	-0.010		

Table A.2- 4. Sensitivity analysis results for the Cs-137 Deposition DRL for AMS.

Cs-137 Deposition DRL, R <sup>2</sup> = 0.924				
Variable Name	R <sup>2</sup> Individual	SRRC		
Deposition Velocity	0.603	0.777		
Inhalation Dose Coefficient Multiplier	0.187	-0.430		
Breathing Rate, Light Exercise, Adult Male	0.062	-0.250		
Weathering Coefficient Multiplier	0.036	0.189		
Deposition External Dose Coefficient Multiplier	0.027	-0.166		
Ground Roughness Factor	0.005	-0.069		
Resuspension Coefficient Multiplier	0.004	-0.059		
Activity per Area	0.000	0.000		
Plume External Dose Coefficient Multiplier	0.000	0.000		
Breathing Rate, Activity Averaged, Adult Male	0.000	-0.008		

Table A.2- 5. Sensitivity analysis results for the Cs-137 Integrated Air DRL for AMS.

Cs-137 Integrated Air DRL, R <sup>2</sup> = 0.905				
Variable Name	R <sup>2</sup> Individual	SRRC		
Deposition Velocity	0.379	-0.616		
Inhalation Dose Coefficient Multiplier	0.339	-0.580		
Breathing Rate, Light Exercise, Adult Male	0.113	-0.337		
Deposition External Dose Coefficient Multiplier	0.039	-0.198		
Weathering Coefficient Multiplier	0.026	-0.160		
Ground Roughness Factor	0.006	-0.078		
Resuspension Coefficient Multiplier	0.004	-0.064		
Activity per Area	0.000	0.000		
Plume External Dose Coefficient Multiplier	0.000	0.000		
Breathing Rate, Activity Averaged, Adult Male	0.000	-0.005		

# A.2.2.2. DP Sensitivity Analysis Results

Table A.2- 6. Sensitivity analysis results for the Cs-137 Plume Inhalation DP for AMS.

Cs-137 Plume Inhalation DP, R <sup>2</sup> = 0.953				
Variable Name	R <sup>2</sup> Individual	SRRC		
Deposition Velocity	0.675	-0.821		
Inhalation Dose Coefficient Multiplier	0.204	0.450		
Breathing Rate, Light Exercise, Adult Male	0.074	0.272		
Activity per Area	0.001	0.033		
Ground Roughness Factor	0.000	0.000		
Resuspension Coefficient Multiplier	0.000	0.000		
Weathering Coefficient Multiplier	0.000	0.000		
Breathing Rate, Activity Averaged, Adult Male	0.000	0.000		
Deposition External Dose Coefficient Multiplier	0.000	0.000		
Plume External Dose Coefficient Multiplier	0.000	0.000		

Table A.2- 7. Sensitivity analysis results for the Cs-137 Plume Submersion DP for AMS.

Cs-137 Plume Submersion DP, R <sup>2</sup> = 0.987				
Variable Name	R <sup>2</sup> Individual	SRRC		
Deposition Velocity	0.898	-0.946		
Plume External Dose Coefficient Multiplier	0.088	0.297		
Activity per Area	0.001	0.036		
Breathing Rate, Light Exercise, Adult Male	0.000	0.000		
Ground Roughness Factor	0.000	0.000		
Inhalation Dose Coefficient Multiplier	0.000	0.000		
Resuspension Coefficient Multiplier	0.000	0.000		
Weathering Coefficient Multiplier	0.000	0.000		
Breathing Rate, Activity Averaged, Adult Male	0.000	0.000		
Deposition External Dose Coefficient Multiplier	0.000	0.000		

Table A.2- 8. Sensitivity analysis results for the Cs-137 Resuspension Inhalation DP for AMS.

Cs-137 Resuspension Inhalation DP, R <sup>2</sup> = 0.985				
Variable Name	R <sup>2</sup> Individual	SRRC		
Resuspension Coefficient Multiplier	0.901	0.948		
Inhalation Dose Coefficient Multiplier	0.067	0.258		
Breathing Rate, Activity Averaged, Adult Male	0.017	0.131		
Activity per Area	0.000	0.017		
Plume External Dose Coefficient Multiplier	0.000	-0.002		
Breathing Rate, Light Exercise, Adult Male	0.000	0.000		
Ground Roughness Factor	0.000	0.000		
Weathering Coefficient Multiplier	0.000	0.000		
Deposition Velocity	0.000	0.000		
Deposition External Dose Coefficient Multiplier	0.000	0.000		

Table A.2- 9. Sensitivity analysis results for the Cs-137 Groundshine DP for AMS.

Cs-137 Groundshine DP, $R^2 = 0.953$			
Variable Name	R <sup>2</sup> Individual	SRRC	
Deposition External Dose Coefficient Multiplier	0.533	0.733	
Weathering Coefficient Multiplier	0.325	0.568	
Ground Roughness Factor	0.089	0.298	
Activity per Area	0.007	0.085	
Breathing Rate, Light Exercise, Adult Male	0.000	0.000	
Inhalation Dose Coefficient Multiplier	0.000	0.000	
Resuspension Coefficient Multiplier	0.000	0.000	
Deposition Velocity	0.000	0.000	
Breathing Rate, Activity Averaged, Adult Male	0.000	0.000	
Plume External Dose Coefficient Multiplier	0.000	-0.007	

Table A.2- 10. Sensitivity analysis results for the Cs-137 Total DP for AMS.

Cs-137 Total DP, R <sup>2</sup> = 0.920				
Variable Name	R <sup>2</sup> Individual	SRRC		
Deposition Velocity	0.617	-0.785		
Inhalation Dose Coefficient Multiplier	0.186	0.430		
Breathing Rate, Light Exercise, Adult Male	0.062	0.250		
Deposition External Dose Coefficient Multiplier	0.027	0.165		
Weathering Coefficient Multiplier	0.019	0.135		
Ground Roughness Factor	0.004	0.068		
Resuspension Coefficient Multiplier	0.004	0.059		
Activity per Area	0.003	0.053		
Breathing Rate, Activity Averaged, Adult Male	0.000	0.006		
Plume External Dose Coefficient Multiplier	0.000	0.000		

# A.2.3. Sampling Confidence Intervals

Table A.2- 11. Sampling confidence intervals for AMS simulations.

Output Name	Lower Bound of 95% CI	Mean	Upper Bound of 95% CI
Dose Rate DRL [mrem/hr]	3.83	3.87	3.91
Cs-137 Deposition DRL [μCi/m²]	705	713	719
Cs-137 Integrated Air DRL [μCi-s/m³]	75200	75900	76600
Cs-137 Plume Inhalation DP [mrem]	456	469	481
Cs-137 Plume Submersion DP [mrem]	4.40	4.50	4.60
Cs-137 Resuspension Inhalation DP [mrem]	13.4	14.1	14.9
Cs-137 Groundshine DP [mrem]	178	179	180
Cs-137 Total DP [mrem]	655	667	680

#### **DISTRIBUTION**

1 Lawrence Livermore National Laboratory

Attn: Matthew Simpson P.O. Box 808, L-103 Livermore, CA 94551

Remote Sensing Laboratory – Nellis

Attn: Colin Okada (1), Avery Bingham (1), and RaJah Mena (1)

Nellis AFB, Bldg. 2211

4600 North Hollywood Blvd

Las Vegas, NV 89191

1	MS0744	Aubrey Eckert-Gallup	8853
1	MS0744	Patrick Mattie	8853
1	MS0748	Douglas Osborn	8852
1	MS0791	Lainy Cochran	6631
1	MS0791	Brian Hunt	6631
1	MS0791	Terry Kraus	6631
1	MS0791	Art Shanks	6631
1	MS0899	Technical Library	9536 (electronic copy)

